

Tel Aviv University  
The Raymond and Beverly Sackler  
Faculty of Exact Sciences

**Comparison of Local  
Absorbing Radiation Conditions  
for Scattering about Elliptical Body**

Thesis submitted in partial fulfillment of the requirements  
for the M. Sc. Degree at Tel-Aviv University

Department of Applied Mathematics

by

**Michael Medvinsky**

This work was prepared under the supervision of Professor Eli Turkel

August 29, 2007



To Janna

I would like to thank Eli Turkel, my supervisor, for his constant involvement and support during this work. I am also thankful to Yakov Olshansky for the Matlab routine for the exact solution about an ellipse and for being my "knowledge base" of Mathieu functions.

Of course, I am grateful to my family for their patience and *love*. Without them this work would never have come into existence (literally).



# Abstract

We present a comparison of various methods of local absorbing boundary conditions (ABC) for numerical solutions of the Helmholtz equation exterior to an ellipse. We also introduce a new boundary condition based on a modal expansion in Mathieu functions. We compare this new ABC for an outer ellipse with the other boundary conditions.

Elliptic equations in exterior regions usually require a boundary condition at infinity to ensure the well-posedness of the problem. One of the practical applications is the Helmholtz equation. For computational reasons one needs to truncate the unbounded domain. Typically, truncation is implemented by the introduction of an artificial outer domain, together with absorbing boundary conditions along this domain, that reduce wave reflections into the physical domain. Bayliss with Turkel [3] and later with Gunzburger [2] presented a sequence of boundary conditions in polar and spherical coordinates. These boundary conditions were generalized by several authors when the artificial surface is not a circle or sphere.

In this paper we consider scattering about an ellipse (for which the exact solution is known). We compare local boundary conditions that link only nearby neighbors of a boundary point. We consider the 2D Helmholtz equation in frequency space. We consider On Surface Radiation Conditions (OSRC) and also exterior problems solved by finite difference algorithm.



# Contents

<b>1</b>	<b>Introduction</b>	<b>15</b>
1.1	Elliptical Coordinates . . . . .	16
1.2	Helmholtz equation . . . . .	17
1.3	Mathieu functions . . . . .	19
<b>2</b>	<b>Previous work</b>	<b>21</b>
2.1	Various Generalizations of BGT . . . . .	22
2.1.1	Grote and Keller . . . . .	22
2.1.2	Reiner et al. . . . .	23
2.1.3	Kriegsmann et al. . . . .	24
2.1.4	Jones . . . . .	24
2.1.5	Kallivokas et al. . . . .	25
2.1.6	Antoine et al. . . . .	25
2.1.7	Meade et al. . . . .	26
<b>3</b>	<b>New Absorbing Boundary Condition</b>	<b>31</b>
<b>4</b>	<b>Numerical Implementation</b>	<b>35</b>
4.1	ABC on Elliptical Artificial Body . . . . .	35
4.1.1	Discretization of Various ABCs . . . . .	37
4.2	On Surface Radiation Condition . . . . .	45
4.2.1	Discretization of Various ABCs . . . . .	46

<b>5 Numerical Results</b>	<b>49</b>
5.1 On Surface Radiation Condition . . . . .	50
5.1.1 Dirichlet Condition . . . . .	50
5.1.2 Neumann Condition . . . . .	60
5.2 Absorbing Boundary Condition . . . . .	69
5.2.1 Dirichlet condition . . . . .	69
5.2.2 Neumann Condition . . . . .	88
<b>6 Conclusion</b>	<b>97</b>
<b>Bibliography</b>	<b>99</b>
<b>Appendix</b>	<b>102</b>
<b>A</b>	<b>103</b>
A.1 . . . . .	103
A.2 . . . . .	103
A.3 . . . . .	103

# List of Tables

5.1	OSRC Dirichlet boundary condition ( $\theta = 0^\circ$ ) $L_2$ error . . . . .	54
5.2	OSRC Dirichlet boundary condition ( $\theta = 5^\circ$ ) $L_2$ error . . . . .	59
5.3	OSRC Neumann boundary condition ( $\theta = 0^\circ$ ) $L_2$ error . . . . .	64
5.4	OSRC Neumann boundary condition ( $\theta = 5^\circ$ ) $L_2$ error . . . . .	68
5.5	ABC Dirichlet boundary condition ( $\theta = 0^\circ, a_{ext} = 1.1$ ) $L_2$ error . . .	72
5.6	ABC Dirichlet boundary condition ( $\theta = 0^\circ, a_{ext} = 1.5$ ) $L_2$ error . . .	75
5.7	ABC Dirichlet boundary condition ( $\theta = 0^\circ, a_{ext} = 2$ ) $L_2$ error . . .	78
5.8	ABC Dirichlet boundary condition ( $\theta = 5^\circ, a_{ext} = 1.1$ ) $L_2$ error . . .	81
5.9	ABC Dirichlet boundary condition ( $\theta = 5^\circ, a_{ext} = 1.5$ ) $L_2$ error . . .	84
5.10	ABC Dirichlet boundary condition ( $\theta = 5^\circ, a_{ext} = 2$ ) $L_2$ error . . .	87
5.11	ABC Neumann boundary condition ( $\theta = 0^\circ$ ) $L_2$ error . . . . .	91
5.12	ABC Neumann boundary condition ( $\theta = 5^\circ$ ) $L_2$ error . . . . .	95



# List of Figures

1.1	Elliptical Coordinates . . . . .	16
1.2	Scattering . . . . .	18
5.1	OSRC Dirichlet bc, $k = 1, 2$ , AR=10 and $\theta = 0^\circ$ . . . . .	50
5.2	OSRC Dirichlet bc, $k = 3, 4$ , AR=10 and $\theta = 0^\circ$ . . . . .	51
5.3	OSRC Dirichlet bc, $k = 1, 2$ , AR=3.3 and $\theta = 0^\circ$ . . . . .	51
5.4	OSRC Dirichlet bc, $k = 3, 4$ , AR=3.3 and $\theta = 0^\circ$ . . . . .	51
5.5	OSRC Dirichlet bc, $k = 1, 2$ , AR=2 and $\theta = 0^\circ$ . . . . .	52
5.6	OSRC Dirichlet bc, $k = 3, 4$ , AR=2 and $\theta = 0^\circ$ . . . . .	52
5.7	OSRC Dirichlet bc, $k = 1, 2$ , AR=1.4 and $\theta = 0^\circ$ . . . . .	52
5.8	OSRC Dirichlet bc, $k = 3, 4$ , AR=1.4 and $\theta = 0^\circ$ . . . . .	53
5.9	OSRC Dirichlet bc, $k = 1, 2$ , AR=1.1 and $\theta = 0^\circ$ . . . . .	53
5.10	OSRC Dirichlet bc, $k = 3, 4$ , AR=1.1 and $\theta = 0^\circ$ . . . . .	53
5.11	OSRC Dirichlet bc, $k = 1, 2$ , AR=10 and $\theta = 5^\circ$ . . . . .	56
5.12	OSRC Dirichlet bc, $k = 3, 4$ , AR=10 and $\theta = 5^\circ$ . . . . .	56
5.13	OSRC Dirichlet bc, $k = 1, 2$ , AR=3.3 and $\theta = 5^\circ$ . . . . .	56
5.14	OSRC Dirichlet bc, $k = 3, 4$ , AR=3.3 and $\theta = 5^\circ$ . . . . .	57
5.15	OSRC Dirichlet bc, $k = 1, 2$ , AR=2 and $\theta = 5^\circ$ . . . . .	57
5.16	OSRC Dirichlet bc, $k = 3, 4$ , AR=2 and $\theta = 5^\circ$ . . . . .	57
5.17	OSRC Dirichlet bc, $k = 1, 2$ , AR=1.4 and $\theta = 5^\circ$ . . . . .	58
5.18	OSRC Dirichlet bc, $k = 3, 4$ , AR=1.4 and $\theta = 5^\circ$ . . . . .	58
5.19	OSRC Dirichlet bc, $k = 1, 2$ , AR=1.1 and $\theta = 5^\circ$ . . . . .	58

5.20 OSRC Dirichlet bc, $k = 3, 4$ , AR=1.1 and $\theta = 5^\circ$ . . . . .	60
5.21 OSRC Neumann bc $k = 0.5, 1$ , AR=3.3 and $\theta = 0^\circ$ . . . . .	61
5.22 OSRC Neumann bc $k = 2, 4$ , AR=3.3 and $\theta = 0^\circ$ . . . . .	61
5.23 OSRC Neumann bc $k = 0.5, 1$ , AR=2 and $\theta = 0^\circ$ . . . . .	61
5.24 OSRC Neumann bc $k = 2, 4$ , AR=2 and $\theta = 0^\circ$ . . . . .	62
5.25 OSRC Neumann bc $k = 0.5, 1$ , AR=1.4 and $\theta = 0^\circ$ . . . . .	62
5.26 OSRC Neumann bc $k = 2, 4$ , AR=1.4 and $\theta = 0^\circ$ . . . . .	62
5.27 OSRC Neumann bc $k = 0.5, 1$ , AR=1.1 and $\theta = 0^\circ$ . . . . .	63
5.28 OSRC Neumann bc $k = 2, 4$ , AR=1.1 and $\theta = 0^\circ$ . . . . .	63
5.29 OSRC Neumann bc $k = 0.5, 1$ , AR=3.3 and $\theta = 5^\circ$ . . . . .	65
5.30 OSRC Neumann bc $k = 2, 4$ , AR=3.3 and $\theta = 5^\circ$ . . . . .	65
5.31 OSRC Neumann bc $k = 0.5, 1$ , AR=2 and $\theta = 5^\circ$ . . . . .	66
5.32 OSRC Neumann bc $k = 2, 4$ , AR=2 and $\theta = 5^\circ$ . . . . .	66
5.33 OSRC Neumann bc $k = 0.5, 1$ , AR=1.4 and $\theta = 5^\circ$ . . . . .	66
5.34 OSRC Neumann bc $k = 2, 4$ , AR=1.4 and $\theta = 5^\circ$ . . . . .	67
5.35 OSRC Neumann bc $k = 0.5, 1$ , AR=1.1 and $\theta = 5^\circ$ . . . . .	67
5.36 OSRC Neumann bc $k = 2, 4$ , AR=1.1 and $\theta = 5^\circ$ . . . . .	67
5.37 ABC Dirichlet bc, $a_{ext} = 1.1$ $k = 0.5, 1$ , AR=10 and $\theta = 0^\circ$ . . . . .	70
5.38 ABC Dirichlet bc, $a_{ext} = 1.1$ $k = 2, 4$ , AR=10 and $\theta = 0^\circ$ . . . . .	70
5.39 ABC Dirichlet bc, $a_{ext} = 1.1$ $k = 0.5, 1$ , AR=2 and $\theta = 0^\circ$ . . . . .	71
5.40 ABC Dirichlet bc, $a_{ext} = 1.1$ $k = 2, 4$ , AR=2 and $\theta = 0^\circ$ . . . . .	71
5.41 ABC Dirichlet bc, $a_{ext} = 1.1$ $k = 0.5, 1$ , AR=1.4 and $\theta = 0^\circ$ . . . . .	71
5.42 ABC Dirichlet bc, $a_{ext} = 1.1$ $k = 2, 4$ , AR=1.4 and $\theta = 0^\circ$ . . . . .	72
5.43 ABC Dirichlet bc, $a_{ext} = 1.5$ $k = 0.5, 1$ , AR=10 and $\theta = 0^\circ$ . . . . .	73
5.44 ABC Dirichlet bc, $a_{ext} = 1.5$ $k = 2, 4$ , AR=10 and $\theta = 0^\circ$ . . . . .	73
5.45 ABC Dirichlet bc, $a_{ext} = 1.5$ $k = 0.5, 1$ , AR=2 and $\theta = 0^\circ$ . . . . .	74
5.46 ABC Dirichlet bc, $a_{ext} = 1.5$ $k = 2, 4$ , AR=2 and $\theta = 0^\circ$ . . . . .	74
5.47 ABC Dirichlet bc, $a_{ext} = 1.5$ $k = 0.5, 1$ , AR=1.4 and $\theta = 0^\circ$ . . . . .	74

5.48	ABC Dirichlet bc, $a_{ext} = 1.5$ $k = 2, 4$ , AR=1.4 and $\theta = 0^\circ$ . . . . .	75
5.49	ABC Dirichlet bc, $a_{ext} = 2$ $k = 0.5, 1$ , AR=10 and $\theta = 0^\circ$ . . . . .	76
5.50	ABC Dirichlet bc, $a_{ext} = 2$ $k = 2, 4$ , AR=10 and $\theta = 0^\circ$ . . . . .	76
5.51	ABC Dirichlet bc, $a_{ext} = 2$ $k = 0.5, 1$ , AR=2 and $\theta = 0^\circ$ . . . . .	76
5.52	ABC Dirichlet bc, $a_{ext} = 2$ $k = 2, 4$ , AR=2 and $\theta = 0^\circ$ . . . . .	77
5.53	ABC Dirichlet bc, $a_{ext} = 2$ $k = 0.5, 1$ , AR=1.4 and $\theta = 0^\circ$ . . . . .	77
5.54	ABC Dirichlet bc, $a_{ext} = 2$ $k = 2, 4$ , AR=1.4 and $\theta = 0^\circ$ . . . . .	77
5.55	ABC Dirichlet bc $a_{ext} = 1.1$ $k = 0.5, 1$ , AR=10 and $\theta = 5^\circ$ . . . . .	79
5.56	ABC Dirichlet bc $a_{ext} = 1.1$ $k = 2, 4$ , AR=10 and $\theta = 5^\circ$ . . . . .	79
5.57	ABC Dirichlet bc $a_{ext} = 1.1$ $k = 0.5, 1$ , AR=2 and $\theta = 5^\circ$ . . . . .	80
5.58	ABC Dirichlet bc $a_{ext} = 1.1$ $k = 2, 4$ , AR=2 and $\theta = 5^\circ$ . . . . .	80
5.59	ABC Dirichlet bc $a_{ext} = 1.1$ $k = 0.5, 1$ , AR=1.4 and $\theta = 5^\circ$ . . . . .	80
5.60	ABC Dirichlet bc $a_{ext} = 1.1$ $k = 2, 4$ , AR=1.4 and $\theta = 5^\circ$ . . . . .	81
5.61	ABC Dirichlet bc $a_{ext} = 1.5$ $k = 0.5, 1$ , AR=10 and $\theta = 5^\circ$ . . . . .	82
5.62	ABC Dirichlet bc $a_{ext} = 1.5$ $k = 2, 4$ , AR=10 and $\theta = 5^\circ$ . . . . .	82
5.63	ABC Dirichlet bc $a_{ext} = 1.5$ $k = 0.5, 1$ , AR=2 and $\theta = 5^\circ$ . . . . .	82
5.64	ABC Dirichlet bc $a_{ext} = 1.5$ $k = 2, 4$ , AR=2 and $\theta = 5^\circ$ . . . . .	83
5.65	ABC Dirichlet bc $a_{ext} = 1.5$ $k = 0.5, 1$ , AR=1.4 and $\theta = 5^\circ$ . . . . .	83
5.66	ABC Dirichlet bc $a_{ext} = 1.5$ $k = 2, 4$ , AR=1.4 and $\theta = 5^\circ$ . . . . .	83
5.67	ABC Dirichlet bc $a_{ext} = 2$ $k = 0.5, 1$ , AR=10 and $\theta = 5^\circ$ . . . . .	85
5.68	ABC Dirichlet bc $a_{ext} = 2$ $k = 2, 4$ , AR=10 and $\theta = 5^\circ$ . . . . .	85
5.69	ABC Dirichlet bc $a_{ext} = 2$ $k = 0.5, 1$ , AR=2 and $\theta = 5^\circ$ . . . . .	86
5.70	ABC Dirichlet bc $a_{ext} = 2$ $k = 2, 4$ , AR=2 and $\theta = 5^\circ$ . . . . .	86
5.71	ABC Dirichlet bc $a_{ext} = 2$ $k = 0.5, 1$ , AR=1.4 and $\theta = 5^\circ$ . . . . .	86
5.72	ABC Dirichlet bc $a_{ext} = 2$ $k = 2, 4$ , AR=1.4 and $\theta = 5^\circ$ . . . . .	87
5.73	ABC Neumann bc, $a_{ext} = 2$ $k = 0.5, 1$ , AR=10 and $\theta = 0^\circ$ . . . . .	88
5.74	ABC Neumann bc, $a_{ext} = 2$ $k = 2, 4$ , AR=10 and $\theta = 0^\circ$ . . . . .	89
5.75	ABC Neumann bc, $a_{ext} = 2$ $k = 0.5, 1$ , AR=3.3 and $\theta = 0^\circ$ . . . . .	89

5.76	ABC Neumann bc, $a_{ext} = 2$ $k = 2, 4$ , AR=3.3 and $\theta = 0^\circ$ . . . . .	89
5.77	ABC Neumann bc, $a_{ext} = 2$ $k = 0.5, 1$ , AR=2 and $\theta = 0^\circ$ . . . . .	90
5.78	ABC Neumann bc, $a_{ext} = 2$ $k = 2, 4$ , AR=2 and $\theta = 0^\circ$ . . . . .	90
5.79	ABC Neumann bc, $a_{ext} = 2$ $k = 0.5, 1$ , AR=1.4 and $\theta = 0^\circ$ . . . . .	90
5.80	ABC Neumann bc, $a_{ext} = 2$ $k = 2, 4$ , AR=1.4 and $\theta = 0^\circ$ . . . . .	92
5.81	ABC Neumann bc, $a_{ext} = 2$ $k = 0.5, 1$ , AR=10 and $\theta = 5^\circ$ . . . . .	92
5.82	ABC Neumann bc, $a_{ext} = 2$ $k = 2, 4$ , AR=10 and $\theta = 5^\circ$ . . . . .	93
5.83	ABC Neumann bc, $a_{ext} = 2$ $k = 0.5, 1$ , AR=3.3 and $\theta = 5^\circ$ . . . . .	93
5.84	ABC Neumann bc, $a_{ext} = 2$ $k = 2, 4$ , AR=3.3 and $\theta = 5^\circ$ . . . . .	93
5.85	ABC Neumann bc, $a_{ext} = 2$ $k = 0.5, 1$ , AR=2 and $\theta = 5^\circ$ . . . . .	94
5.86	ABC Neumann bc, $a_{ext} = 2$ $k = 2, 4$ , AR=2 and $\theta = 5^\circ$ . . . . .	94
5.87	ABC Neumann bc, $a_{ext} = 2$ $k = 0.5, 1$ , AR=1.4 and $\theta = 5^\circ$ . . . . .	94
5.88	ABC Neumann bc, $a_{ext} = 2$ $k = 2, 4$ , AR=1.4 and $\theta = 5^\circ$ . . . . .	96

# Chapter 1

## Introduction

Technologies such as ultrasound, sonar, radar or geophysical exploration deal with recognition of objects or their properties. It is done by means of the shooting of an acoustic or electromagnetic wave toward the objects and then investigating the reflected wave. This is an ill-posed inverse scattering problem that is difficult to solve, especially from a numerical and computational viewpoint. Usually, to solve inverse problems one needs an effective method to solve a direct problem. In this instance, we focus on a direct frequency domain problem.

For example, consider the wave equation

$$\frac{1}{c^2} \frac{\partial^2 v}{\partial t^2} - \Delta v = 0$$

When we apply the Fourier transform in time, assuming  $v = e^{-i\omega t}u$ , the wave equation becomes a Helmholtz equation:

$$\Delta u + \frac{\omega^2}{c^2}u = \Delta u + k^2u = 0$$

Our discussion here concerns the numerical solution of a Helmholtz equation exterior to an ellipse in elliptical coordinates. In Section 1.1 we introduce the elliptical coordinates, in section Section 1.2 we describe the problem and the Helmholtz equation, followed by a brief introduction of Mathieu functions in Section 1.3. In Chapter 2 we present various generalizations of the Bayliss-Gunzburger-Turkel (BGT) boundary condition followed by the new boundary condition in Chapter 3. In Chapter 4 we present details of our implementation, with numerical results of comparison in Chapter 5, followed by our conclusion in Chapter 6.

## 1.1 Elliptical Coordinates

In this section we introduce elliptic coordinates (see Figure 1.1 on page 16). Consider an ellipse in the  $(x, y)$  plane that is given by  $\left(\frac{x}{a}\right)^2 + \left(\frac{y}{b}\right)^2 = 1$  where  $a, b$  are the major and minor semi-axes of the scatterer, respectively.

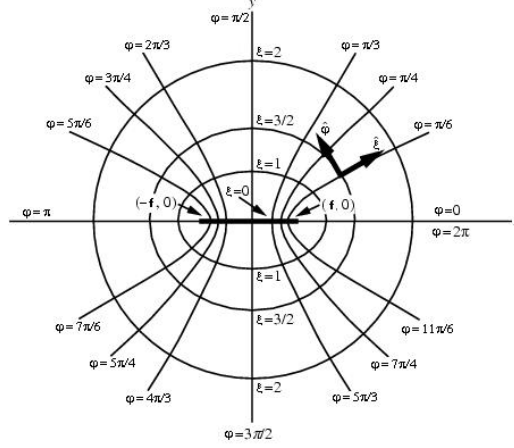


Figure 1.1: Elliptical Coordinates

The eccentricity of the ellipse is given by  $e = \frac{f}{a} = \sqrt{1 - \frac{b^2}{a^2}} \in [0, 1]$ , where  $f = \sqrt{a^2 - b^2}$  is the semi-focal distance (the distance from the center to either focus). The ellipse can be defined by any pair from  $\{a, b, f, e\}$ . The most common definition of elliptic coordinates  $(\xi, \varphi)$ , which comes from the real and imaginary parts of  $(x + iy) = f \cosh(\xi + i\varphi)$ , is given by:

$$\begin{cases} x = f \cosh \xi \cos \varphi \\ y = f \sinh \xi \sin \varphi \end{cases} \quad (1.1)$$

where  $\xi \geq 0$  and  $\varphi \in [0, 2\pi)$ . The parametric representation of the ellipse is given by  $(a \cos \varphi, b \sin \varphi)$ . Thus, when we fix  $\xi$  ( $\xi = \xi_j$ ) the semi axes are  $a = f \cosh \xi_j$  and  $b = f \sinh \xi_j$ . Fixing  $\varphi = \varphi_n$  then gives us  $\frac{x}{\cos \varphi_n} - \frac{y}{\sin \varphi_n} = \cosh \xi - \sinh \xi = 1$  and the appropriate surface is reduced to a hyperbola.

The following definitions will be used later in this paper. The scale factors, or metrics, are given by

$$h_\xi = h_\varphi = f \sqrt{\sinh^2 \xi + \sin^2 \varphi} = f \sqrt{0.5(\cosh 2\xi - \cos 2\varphi)}$$

Along the fixed ellipse  $\xi_j$  it becomes

$$h_\xi = h_\varphi = \frac{\partial s}{\partial \varphi} = \sqrt{a^2 \sin^2 \varphi + b^2 \cos^2 \varphi} \quad (1.2)$$

We can now define curvature  $\zeta = \frac{ab}{h_\xi^3}$  and the normal ( $n$ ) and tangential ( $s$ ) derivatives:

$$\begin{aligned} \frac{\partial u}{\partial n} &= \frac{1}{h_\xi} \frac{\partial u}{\partial \xi} \\ \frac{\partial u}{\partial s} &= \frac{1}{h_\varphi} \frac{\partial u}{\partial \varphi} \end{aligned}$$

## 1.2 Helmholtz equation

The Helmholtz equation, named for Hermann von Helmholtz, is the elliptic partial differential equation  $\Delta u + k^2 u = 0$  where  $\Delta = \nabla^2$  is the Laplacian and  $k = \frac{2\pi}{\lambda}$  is the wave number. Helmholtz equations are used to model a variety of important physical systems, ranging from heat distribution to the transmission of sound. In this paper we consider an acoustical scattering problem.

The Helmholtz equation exterior to some body represents wave scattering about the body at a given frequency. We consider a plane wave propagating through a homogeneous media and impacting the body. To determine a unique solution to the scattering problem we choose the Sommerfeld radiation condition (1.5) at infinity. Physically, this represents the demand that scattered waves cannot enter the domain from infinity. Formally, the problem for the scattered 2D wave  $u$  is described by

$$\Delta u + k^2 u = 0 \quad \text{in } \Omega \quad (1.3)$$

$$\begin{cases} u = -u_{inc} & \text{on } \partial\Omega \\ \text{or } \frac{\partial u}{\partial n} = -\frac{\partial u_{inc}}{\partial n} & \text{on } \partial\Omega \end{cases} \quad (1.4)$$

$$\lim_{r \rightarrow \infty} r^{\frac{1}{2}} \left( \frac{\partial u}{\partial r} - iku \right) = 0 \quad (1.5)$$

where  $u_{inc} = e^{-ik(x\cos\theta + y\sin\theta)}$  is the incoming plane wave and  $\theta$  is the incident angle.

When computing wave scattering about a body either in the time domain or the frequency domain one needs to truncate the unbounded domain and introduce an artificial surface with an absorbing boundary condition to prevent reflections of outgoing waves into the domain. We consider local absorbing boundary conditions (ABCs) that link only nearby neighbors of a boundary point. We shall consider the

Helmholtz equation in frequency space. Then these boundary conditions are of the form  $0 = Bu = \left(\frac{\partial u}{\partial n} - iku\right) + \text{low order correction terms}$ .

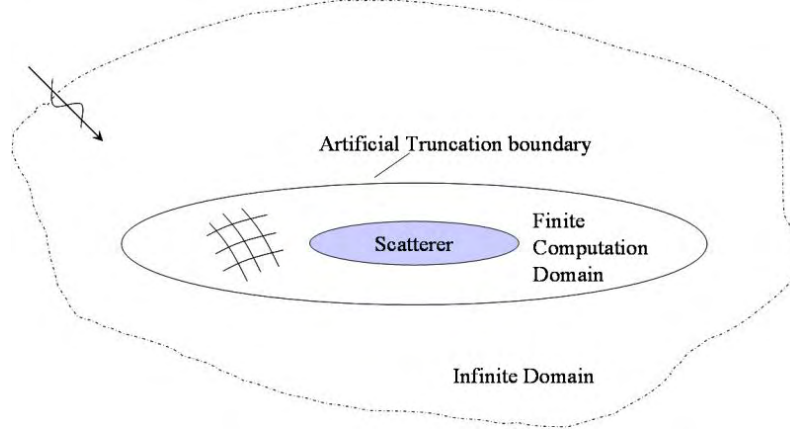


Figure 1.2: Scattering

The general curvilinear form of the Laplacian is

$$\Delta u = \frac{1}{h_1 h_2 h_3} \left[ \frac{\partial}{\partial u_1} \left( \frac{h_2 h_3}{h_1} \frac{\partial}{\partial u_1} \right) + \frac{\partial}{\partial u_2} \left( \frac{h_1 h_3}{h_2} \frac{\partial}{\partial u_2} \right) + \frac{\partial}{\partial u_3} \left( \frac{h_1 h_2}{h_3} \frac{\partial}{\partial u_3} \right) \right] u$$

where the  $h_i$  are the metrics of the coordinate system. Since in 2D elliptical coordinates we have identical metrics in both directions we have the following form of Helmholtz equation:

$$\frac{1}{h_\xi^2} \left[ \frac{\partial^2}{\partial \xi^2} + \frac{\partial^2}{\partial \varphi^2} \right] u + k^2 u = 0$$

Let us show that the Helmholtz equation is separable in elliptical coordinates. First, rewrite the Helmholtz equation in a more convenient way :

$$\left[ \frac{\partial^2}{\partial \xi^2} + \frac{\partial^2}{\partial \varphi^2} \right] u + h_\xi^2 k^2 u = 0 \quad (1.6)$$

Attempting a separation of variables by writing  $u(\xi, \varphi) = \Psi(\xi)\Phi(\varphi)$  equation 1.6 becomes

$$\Phi \frac{\partial^2 \Psi}{\partial \xi^2} + \Psi \frac{\partial^2 \Phi}{\partial \varphi^2} + h_\xi^2 k^2 \Psi \Phi = 0$$

Divide by  $\Psi\Phi$  to get

$$\frac{1}{\Psi} \frac{\partial^2 \Psi}{\partial \xi^2} + \frac{1}{\Phi} \frac{\partial^2 \Phi}{\partial \varphi^2} + h_\xi^2 k^2 = 0$$

Expanding the  $h_\xi$  term

$$\frac{1}{\Psi} \frac{\partial^2 \Psi}{\partial \xi^2} + \frac{1}{\Phi} \frac{\partial^2 \Phi}{\partial \varphi^2} + \frac{f^2 k^2}{2} (\cosh 2\xi - \cos 2\varphi) = 0$$

allows us to rewrite it in the following form

$$\left( \frac{1}{\Psi} \frac{\partial^2 \Psi}{\partial \xi^2} + \frac{f^2 k^2}{2} \cosh 2\xi \right) + \left( \frac{1}{\Phi} \frac{\partial^2 \Phi}{\partial \varphi^2} - \frac{f^2 k^2}{2} \cos 2\varphi \right) = 0$$

Now we can get the following system

$$\begin{aligned} \frac{1}{\Psi} \frac{\partial^2 \Psi}{\partial \xi^2} + \frac{f^2 k^2}{2} \cosh 2\xi &= a \\ a + \frac{1}{\Phi} \frac{\partial^2 \Phi}{\partial \varphi^2} - \frac{f^2 k^2}{2} \cos 2\varphi &= 0 \end{aligned}$$

where  $a$  is the separation variable. Let us define  $q = \frac{f^2 k^2}{4}$  to get the most known form of this system of equations:

$$\frac{\partial^2 \Psi}{\partial \xi^2} - (a - 2q \cosh 2\xi) \Psi = 0 \quad (1.7)$$

$$\frac{\partial^2 \Phi}{\partial \varphi^2} + (a - 2q \cos 2\varphi) \Phi = 0 \quad (1.8)$$

The equations (1.7) and (1.8) are known as the radial and angular Mathieu equations (RME, AME), respectively. Their solutions are the radial and angular Mathieu functions (RMFs, AMFs). In the mathematics literature equations (1.7) and (1.8) are often called modified and ordinary Mathieu equations. The transformation  $\varphi \mapsto i\xi$  "modifies" AME to RME and vice versa. The introduction of the Mathieu functions is given in the next section.

### 1.3 Mathieu functions

The Mathieu functions were introduced by Emile Mathieu in 1868 [17] when he was analyzing the movements of membranes of elliptical shape. As was shown in the previous section, Mathieu equations appear in the solution of Helmholtz equations in elliptical coordinates. The forms of equations (1.7) and (1.8) were introduced by Ince [9] and often called the canonical form of the radial (i.e. Modified) and the angular (i.e. ordinary) Mathieu equations.

Physical considerations are usually such that AME (equation (1.8)) has periodic solutions with period  $\pi$  or  $2\pi$ . The values of  $a$  which satisfy this condition are known as characteristic values (eigenvalues), and they generate an infinite set of real values which have the property  $a_m < a_{m+n} : m, n \in \mathbb{N}^1$ . When the solutions  $\Phi(\varphi)$  are even with respect to  $\varphi = 0$ , the characteristic values are denoted as  $a_m(q)$ , whereas for odd solutions they are represented as  $b_m(q)$ .

Since AME (1.8) is a second-order differential equation, there are two families of independent solutions denoted as the first and the second kind. The even and odd solutions of the first kind are usually denoted  $ce$  and  $se$ , as first suggested by Whittaker and Watson [23], from their relation to the cosine-elliptic and sine-elliptic respectively. The solutions of the second kind are non periodic.

The Radial Mathieu equation (1.7) plays in elliptic coordinates a similar role as the Bessel equation in circular coordinates. In this sense, for each Bessel function [J, N, I, and K] there exists a Radial Mathieu function; however the presence of even and odd versions in the elliptic case leads to eight RMFs. The solutions of the first kind are denoted as  $Ne, No$  where 'e' and 'o' denote even and odd respectively. The second kind is denoted in a similar way  $Je, Jo$ . Our case does not consist of  $q < 0$ , hence we will not deal with I,K, but there is a similar naming convention.

Analogous to Hankel functions  $H_m^{(1),(2)}$  occurring in Bessel equations and circular cylinder coordinates, there also exist the Mathieu-Hankel functions ( $Me, Mo$ ) of the first and second kind, that are also called the third and fourth kind of solution.

Now we can write the solution to the Helmholtz equation in the following way:

$$u(\xi, \varphi) = \sum_{n=0}^{\infty} \alpha_n Me_n^{(1)}(\xi, q) ce_n(\xi, q) + \beta_n Mo_n^{(1)}(\xi, q) se_n(\xi, q) \quad (1.9)$$

where  $\alpha_n, \beta_n$  are functions of  $q$ , incident angle  $\theta$  and artificial ellipse  $\xi_0$ .

---

<sup>1</sup> $\mathbb{N}$  denote set of natural numbers (non-negative integers)

## Chapter 2

# Previous work

Bayliss and Turkel (1980) [3] introduced a sequence of boundary conditions for the Helmholtz equation. They considered an expansion (2.1) of spherical (cylindrical in 2D) waves that asymptotically converge in the reciprocal of the distance.

$$u \sim \sqrt{\frac{2}{\pi kr}} e^{i(kr - \frac{\pi}{2})} \sum_{j=0}^{\infty} \frac{f_j(\theta)}{k^j r^j} \quad (2.1)$$

Then they designed a sequence of boundary conditions that match higher order terms in the portion that corresponds to waves leaving the domain. Together with Gunzburger [2] this was generalized to the frequency domain. Since the series consist of spherical and cylindrical waves, the terms that appear include the distance from the origin and also the derivatives in spherical and polar coordinates.

$$BGT : B_m u = \left[ \prod_{j=1}^m \left( \frac{\partial}{\partial r} - ik + \frac{2j - \frac{3}{2}}{r} \right) \right] u \quad (2.2)$$

In this work we will be focused on the most popular boundary conditions  $B_1, B_2$ . Particularly we will write these cases implicitly.

$$\begin{aligned} BGT_1 : \frac{\partial u}{\partial r} &= \left( ik - \frac{1}{2r} \right) u & (2.3) \\ BGT_2 : 0 &= \left( \frac{\partial}{\partial r} - ik + \frac{5}{2r} \right) \left( \frac{\partial}{\partial r} - ik + \frac{1}{2r} \right) u \\ &= \frac{\partial^2 u}{\partial r^2} + \left( -2ik + \frac{3}{r} \right) \frac{\partial u}{\partial r} + \left( \frac{3}{4r^2} - k^2 + \frac{3ik}{r} \right) u \end{aligned}$$

Using the Helmholtz equation in polar coordinates to eliminate  $\frac{\partial^2 u}{\partial r^2}$  we get

$$\begin{aligned}
\frac{\partial u}{\partial r} &= \frac{1}{2\left(ik - \frac{1}{r}\right)} \left( \frac{3}{4r^2} - 2k^2 + \frac{3ik}{r} \right) u - \frac{1}{2r^2\left(ik - \frac{1}{r}\right)} \frac{\partial^2 u}{\partial \theta^2} \\
&= \left( ik - \frac{1}{2r} - \frac{1}{8r^2\left(ik - \frac{1}{r}\right)} \right) u - \frac{1}{2r^2\left(ik - \frac{1}{r}\right)} \frac{\partial^2 u}{\partial \theta^2}
\end{aligned} \tag{2.4}$$

An alternative method was introduced in 1993 by Li and Cendes [15]. They considered a modal expansion

$$u \sim \sum_{n=0}^{\infty} A_n(\theta) H_n(kr) \tag{2.5}$$

where  $H_n$  is an  $n^{\text{th}}$  order Hankel function of the second kind. Another modal expansion was used by Givoli and Keller [5]:

$$u = H_0(kr) \sum_{j=0}^{\infty} \frac{f_j(\theta)}{r^j} + H_1(kr) \sum_{j=0}^{\infty} \frac{g_j(\theta)}{r^j} \tag{2.6}$$

Both approaches yield the following boundary condition

$$\frac{\partial u}{\partial r} = k \frac{H'_0(kr)}{H_0(kr)} u \tag{2.7}$$

$$\frac{\partial u}{\partial r} = k \left[ \frac{H'_0(kr)}{H_0(kr)} + \left( \frac{H'_0(kr)}{H_0(kr)} - \frac{H'_1(kr)}{H_1(kr)} \right) \frac{\partial^2 u}{\partial \theta^2} \right] u \tag{2.8}$$

To reach this boundary condition put  $\sigma = r$  and  $\psi_i(k\sigma) = H_i(kr)$  in Chapter 3 equation (3.4) and then reduce it using the Hankel equation. The significant difference between (2.3),(2.4) and (2.7),(2.8) is the accuracy when  $k$  is small.

## 2.1 Various Generalizations of BGT

In this section we present a brief survey of various generalizations of BGT (2.2) about an ellipse. These generalizations will later be compared with the exact solution and with the new one. For now we will call  $a, b$  the semi-axes of the artificial elliptical boundary.

### 2.1.1 Grote and Keller

In 1995 Grote and Keller [7, 6] considered an approach similar to the original BGT paper [2]. They based their work on an expansion in elliptical waves (2.9) instead

of the cylindrical expansion (2.1) used by Bayliss et al.

$$u \sim \sqrt{\frac{2}{\pi k f \cosh \xi}} e^{i(kf \cosh \xi - \frac{\pi}{4})} \sum_{j=0}^{\infty} \frac{g_j(\theta, k)}{(kf \cosh \xi)^j} \quad (2.9)$$

They found that replacing  $r \rightarrow f \cosh \xi$  is the main difference between (2.1) and (2.9). They then applied this transformation on (2.2) to get

$$B_m u = \left[ \prod_{j=1}^m \left( \frac{1}{f \sinh \xi} \frac{\partial}{\partial \xi} - ik + \frac{2j - \frac{3}{2}}{f \cosh \xi} \right) \right] u \quad (2.10)$$

$$BGT_1 : \frac{\partial u}{\partial \xi} = \frac{b}{a} \left( ika - \frac{1}{2} \right) u \quad (2.11)$$

$$\begin{aligned} BGT_2 : 0 &= \left( \frac{1}{f \sinh \xi} \frac{\partial}{\partial \xi} - ik + \frac{1}{2f \cosh \xi} \right) \left( \frac{1}{f \sinh \xi} \frac{\partial}{\partial \xi} - ik + \frac{5}{2f \cosh \xi} \right) u \\ &= \frac{1}{b^2} \frac{\partial^2 u}{\partial \xi^2} - \frac{1}{b^2} \frac{a}{b} \frac{\partial u}{\partial \xi} + \left( -2ik + \frac{3}{a} \right) \frac{1}{b} \frac{\partial u}{\partial \xi} + \left( \frac{3}{4a^2} - k^2 - \frac{3ik}{a} \right) u \\ &= \frac{\partial^2 u}{\partial \xi^2} + \left( -2ikb + 3\frac{b}{a} - \frac{a}{b} \right) \frac{\partial u}{\partial \xi} + \left( \frac{b^2}{a^2} \frac{3}{4} - k^2 b^2 - \frac{3ikb^2}{a} \right) u \end{aligned}$$

Using Helmholtz equation (1.6) to eliminate  $\frac{\partial^2 u}{\partial \xi^2}$  we get

$$\frac{\partial u}{\partial \xi} = \frac{1}{(-2ikb + 3\frac{b}{a} - \frac{a}{b})} \left( \frac{\partial^2 u}{\partial \varphi^2} + \left( h_\xi^2 k^2 - \frac{b^2}{a^2} \frac{3}{4} + k^2 b^2 + \frac{3ikb^2}{a} \right) u \right) \quad (2.12)$$

### 2.1.2 Reiner et al.

The simplest method was presented in 2005 by Reiner, Djellouli and Harari [20]. They replace  $r \rightarrow f \cosh \xi$  like Grote and Keller [7], but they present a different form in the case of  $m = 2$ . In particular, instead of

$$\frac{\partial^2 u}{\partial r^2} \rightarrow \frac{1}{b^2} \frac{\partial^2 u}{\partial \xi^2} - \frac{1}{b^2} \frac{a}{b} \frac{\partial u}{\partial \xi}$$

(see (2.12)) they eliminate  $\frac{\partial^2 u}{\partial r^2}$  using the Helmholtz equation in polar coordinates and then replace  $r \rightarrow f \cosh \xi$  and  $\theta \mapsto \varphi$ . Hence they get

$$\begin{aligned} 0 &= -\frac{1}{a^2} \frac{\partial^2 u}{\partial \varphi^2} - \frac{1}{a^2} \frac{\partial u}{\partial \xi} - k^2 u + \left(-2ik + \frac{3}{a}\right) \frac{1}{b} \frac{\partial u}{\partial \xi} + \left(\frac{3}{4a^2} - k^2 + \frac{3ik}{a}\right) u \\ &= -\frac{\partial^2 u}{\partial \varphi^2} - \frac{a}{b} 2(ika - 1) \frac{\partial^2 u}{\partial \xi^2} + a^2 \left(\frac{3}{4a^2} - 2k^2 + \frac{3ik}{a}\right) u \end{aligned}$$

Solving it for  $\frac{\partial u}{\partial \xi}$  one can get

$$\begin{aligned} \frac{\partial u}{\partial \xi} &= \frac{b}{a} \left( \frac{a^2}{2(ika - 1)} \left( \frac{3}{4a^2} - 2k^2 + \frac{3ik}{a} \right) u - \frac{1}{2(ika - 1)} \frac{\partial^2 u}{\partial \varphi^2} \right) \\ &= \frac{b}{a} \left( \left( ika - \frac{1}{2} - \frac{1}{8(ika - 1)} \right) u - \frac{1}{2(ika - 1)} \frac{\partial^2 u}{\partial \varphi^2} \right) \end{aligned} \quad (2.13)$$

### 2.1.3 Kriegsmann et al.

An interesting method was suggested in 1987 by Kriegsmann et al. [14]. They note that the metrics of polar(spherical) coordinate are  $h_r = 1, h_\theta = r$ , so  $\frac{\partial}{\partial n} \equiv \frac{\partial}{\partial r}$  and  $\frac{\partial}{\partial s} \equiv \frac{1}{r} \frac{\partial}{\partial \theta}$ . Furthermore, the curvature on an artificial circular boundary is  $\zeta(x, y) = \frac{x'y'' - x''y'}{(x'^2 + y'^2)^{3/2}} = \frac{(-r \sin \theta)^2 + (r \cos \theta)^2}{((r \sin \theta)^2 + (r \cos \theta)^2)^{3/2}} = \frac{1}{r}$ . Hence they get the boundary condition

$$BGT_1 : \frac{1}{h_\xi} \frac{\partial u}{\partial \xi} = \frac{\partial u}{\partial n} = \left( ik - \frac{\zeta}{2} \right) u \quad (2.14)$$

$$BGT_2 : \frac{\partial u}{\partial n} = \left( ik - \frac{\zeta}{2} - \frac{\zeta^2}{8(ik - \zeta)} \right) u - \frac{1}{2(ik - \zeta)} \frac{\partial^2 u}{\partial s^2} \quad (2.15)$$

### 2.1.4 Jones

Later, in 1989, Jin et al. [10] (see also [12]) used (2.15) to study the scattering of electromagnetic waves by impedance-loaded elliptical cylinders of varying eccentricities. With the radiation impacting in the  $\theta = 0$  direction, the accuracy of (2.15) reduced as  $\frac{b}{a}$  becomes small. Jones [11] (see also [12]) used derivatives of curvature to improve Kriegsmann's method, and got the following modifications

$$\begin{aligned} BGT_2 : \frac{\partial u}{\partial n} &= \left( ik - \frac{\zeta}{2} - \frac{\zeta^2}{8(ik - \zeta)} \right) u - \frac{1}{8ik(ik - \zeta)} \frac{\partial^2 \zeta}{\partial s^2} u - \\ &\quad - \frac{1}{2(ik - \zeta)} \frac{\partial^2 u}{\partial s^2} - \frac{1}{2ik(ik - \zeta)} \frac{\partial \zeta}{\partial s} \frac{\partial u}{\partial s} \end{aligned}$$

Thus

$$\frac{\partial u}{\partial n} = \left( ik - \frac{\zeta}{2} - \frac{1}{8(ik - \zeta)} \left( \zeta^2 + \frac{1}{ik} \frac{\partial^2 \zeta}{\partial s^2} \right) \right) u - \frac{1}{2(ik - \zeta)} \left( \frac{\partial^2 u}{\partial s^2} + \frac{1}{ik} \frac{\partial \zeta}{\partial s} \frac{\partial u}{\partial s} \right) \quad (2.16)$$

### 2.1.5 Kallivokas et al.

Kallivokas et al. [13] considered a geometric optics-type expansion

$$u = e^{-ik\chi} \sum \frac{f_j}{(ik + \gamma)^j}$$

where  $\gamma$  is an arbitrary function introduced for dissipation and hence stability. They defined a sequence of boundary conditions. One of them, the second order in Kallivokas terminology, when one chooses  $\gamma = -\zeta$ , is similar to Kriegsmann's  $BGT_2$  [see equation (2.15)]. The following third order condition in Kallivokas' terminology will be used for the comparisons.

$$\begin{aligned} \frac{\partial u}{\partial n} &= \left( ik - \frac{\zeta}{2} - \frac{1}{8(ik - \zeta)} \left( \zeta^2 + \frac{1}{(ik - \zeta)} \frac{\partial^2 \zeta}{\partial s^2} \right) \right) u - \\ &- \frac{1}{2(ik - \zeta)} \left( \frac{1}{(ik - \zeta)} \frac{\partial \zeta}{\partial s} \frac{\partial u}{\partial s} + \frac{\partial^2 u}{\partial s^2} \right) \end{aligned} \quad (2.17)$$

### 2.1.6 Antoine et al.

Antoine et al. used an asymptotic expansion in  $k$ . Their expansion was based on pseudo differential operators using a decomposition into incoming and outgoing waves as an extension of  $(\sqrt{\Delta}u - ku)(\sqrt{\Delta}u + ku) = \Delta u - (ik)^2 u$ . For the two terms that they calculated they recovered the BGT boundary condition for the circle and the sphere. For an ellipse, in the  $BGT_1$  case, the resultant boundary conditions were similar to Kriegsmann's (2.14). The elliptical  $BGT_2$ -like result was the following boundary condition:

$$\frac{\partial u}{\partial n} = \left( ik - \frac{\zeta}{2} - \frac{\zeta^2}{8(ik - \zeta)} + \frac{1}{8k^2} \frac{\partial^2 \zeta}{\partial s^2} \right) u - \frac{\partial}{\partial s} \left( \frac{1}{2(ik - \zeta)} \frac{\partial u}{\partial s} \right) \quad (2.18)$$

### 2.1.7 Meade et al.

Meade et al. [19, 18, 16] used the chain rule to translate the original BGT from polar coordinates to normal-tangential coordinates. We will show here the similar application of the chain rule directly to elliptical coordinates. Let us write (2.4) in general form

$$\frac{\partial u}{\partial r} = \alpha u + \beta \frac{\partial^2 u}{\partial \theta^2} \quad (2.19)$$

where

$$\alpha = ik - \frac{1}{2r} - \frac{1}{8r^2(ik - 1/r)}$$

and

$$\beta = -\frac{1}{2r^2(ik - 1/r)}$$

Applying the chain rule to  $\frac{\partial u}{\partial \xi}$  and then using (2.19) one can get

$$\frac{\partial u}{\partial \xi} = \frac{\partial u}{\partial r} \frac{\partial r}{\partial \xi} + \frac{\partial u}{\partial \theta} \frac{\partial \theta}{\partial \xi} = \left( \alpha u + \beta \frac{\partial^2 u}{\partial \theta^2} \right) \frac{\partial r}{\partial \xi} + \frac{\partial u}{\partial \theta} \frac{\partial \theta}{\partial \xi} \quad (2.20)$$

We now want to rewrite (2.20) without derivatives with respect to  $\theta$  but with derivatives of  $u$  in elliptical coordinates. Thus we use the chain rule again to express  $\frac{\partial}{\partial \theta}$

$$\begin{aligned} \frac{\partial^2 u}{\partial \theta^2} &= \frac{\partial}{\partial \theta} \left( \frac{\partial u}{\partial \xi} \frac{\partial \xi}{\partial \theta} + \frac{\partial u}{\partial \varphi} \frac{\partial \varphi}{\partial \theta} \right) \\ &= \frac{\partial^2 u}{\partial \xi^2} \left( \frac{\partial \xi}{\partial \theta} \right)^2 + 2 \frac{\partial^2 u}{\partial \varphi \partial \xi} \frac{\partial \xi}{\partial \theta} \frac{\partial \varphi}{\partial \theta} + \frac{\partial^2 u}{\partial \varphi^2} \left( \frac{\partial \varphi}{\partial \theta} \right)^2 + \frac{\partial^2 \xi}{\partial \theta^2} \frac{\partial u}{\partial \xi} + \frac{\partial^2 \varphi}{\partial \theta^2} \frac{\partial u}{\partial \varphi} \end{aligned}$$

Using the elliptical Helmholtz equation to eliminate the  $\frac{\partial^2 u}{\partial \xi^2}$  term one gets

$$\begin{aligned} \frac{\partial^2 u}{\partial \theta^2} &= \left( -\frac{\partial^2 u}{\partial \varphi^2} - k^2 h_\xi^2 u \right) \left( \frac{\partial \xi}{\partial \theta} \right)^2 + 2 \frac{\partial^2 u}{\partial \varphi \partial \xi} \frac{\partial \xi}{\partial \theta} \frac{\partial \varphi}{\partial \theta} + \\ &+ \frac{\partial^2 u}{\partial \varphi^2} \left( \frac{\partial \varphi}{\partial \theta} \right)^2 + \frac{\partial^2 \xi}{\partial \theta^2} \frac{\partial u}{\partial \xi} + \frac{\partial^2 \varphi}{\partial \theta^2} \frac{\partial u}{\partial \varphi} \\ &= -k^2 h_\xi^2 u \left( \frac{\partial \xi}{\partial \theta} \right)^2 + 2 \frac{\partial^2 u}{\partial \varphi \partial \xi} \frac{\partial \xi}{\partial \theta} \frac{\partial \varphi}{\partial \theta} + \frac{\partial^2 u}{\partial \varphi^2} \left( \left( \frac{\partial \varphi}{\partial \theta} \right)^2 - \left( \frac{\partial \xi}{\partial \theta} \right)^2 \right) + \\ &+ \frac{\partial^2 \xi}{\partial \theta^2} \frac{\partial u}{\partial \xi} + \frac{\partial^2 \varphi}{\partial \theta^2} \frac{\partial u}{\partial \varphi} \end{aligned}$$

We apply this result to (2.20)

$$\begin{aligned}
\frac{\partial u}{\partial \xi} &= \alpha \frac{\partial r}{\partial \xi} u + \frac{\partial \xi}{\partial \theta} \frac{\partial \theta}{\partial \xi} \frac{\partial u}{\partial \xi} + \frac{\partial \varphi}{\partial \theta} \frac{\partial \theta}{\partial \xi} \frac{\partial u}{\partial \varphi} + \beta \frac{\partial r}{\partial \xi} \frac{\partial^2 u}{\partial \theta^2} \\
&= \frac{\partial r}{\partial \xi} \left( \alpha - \beta h^2 k^2 \left( \frac{\partial \xi}{\partial \theta} \right)^2 \right) u + \left( \frac{\partial \varphi}{\partial \theta} \frac{\partial \theta}{\partial \xi} + \beta \frac{\partial r}{\partial \xi} \frac{\partial^2 \varphi}{\partial \theta^2} \right) \frac{\partial u}{\partial \varphi} + \\
&+ 2\beta \frac{\partial r}{\partial \xi} \frac{\partial \xi}{\partial \theta} \frac{\partial \varphi}{\partial \theta} \frac{\partial^2 u}{\partial \varphi \partial \xi} + \beta \frac{\partial r}{\partial \xi} \frac{\partial^2 u}{\partial \varphi^2} \left( \left( \frac{\partial \varphi}{\partial \theta} \right)^2 - \left( \frac{\partial \xi}{\partial \theta} \right)^2 \right) + \\
&+ \frac{\partial \xi}{\partial \theta} \frac{\partial \theta}{\partial \xi} \frac{\partial u}{\partial \xi} + \beta \frac{\partial r}{\partial \xi} \frac{\partial^2 \xi}{\partial \varphi^2} \frac{\partial u}{\partial \xi}
\end{aligned}$$

With simple algebraic manipulations one can write it as

$$\begin{aligned}
\Upsilon \frac{\partial u}{\partial \xi} &= \frac{\partial r}{\partial \xi} \left( \alpha - \beta h^2 k^2 \left( \frac{\partial \xi}{\partial \theta} \right)^2 \right) u + \left( \frac{\partial \varphi}{\partial \theta} \frac{\partial \theta}{\partial \xi} + \beta \frac{\partial r}{\partial \xi} \frac{\partial^2 \varphi}{\partial \theta^2} \right) \frac{\partial u}{\partial \varphi} + \\
&+ 2\beta \frac{\partial r}{\partial \xi} \frac{\partial \xi}{\partial \theta} \frac{\partial \varphi}{\partial \theta} \frac{\partial^2 u}{\partial \varphi \partial \xi} + \beta \frac{\partial r}{\partial \xi} \frac{\partial^2 u}{\partial \varphi^2} \left( \left( \frac{\partial \varphi}{\partial \theta} \right)^2 - \left( \frac{\partial \xi}{\partial \theta} \right)^2 \right)
\end{aligned}$$

where  $\Upsilon = \left( 1 - \frac{\partial \xi}{\partial \theta} \frac{\partial \theta}{\partial \xi} - \beta \frac{\partial r}{\partial \xi} \frac{\partial^2 \xi}{\partial \theta^2} \right)$ . Next we try to simplify it using the following identities

- $\frac{\partial r}{\partial \xi} \frac{\partial \xi}{\partial r} + \frac{\partial \theta}{\partial \xi} \frac{\partial \xi}{\partial \theta} = \frac{\frac{\partial r}{\partial \xi} \frac{\partial \theta}{\partial \varphi} - \frac{\partial \theta}{\partial \xi} \frac{\partial r}{\partial \varphi}}{\mathcal{J}} = 1$
- $\frac{\partial \varphi}{\partial r} \frac{\partial r}{\partial \xi} + \frac{\partial \varphi}{\partial \theta} \frac{\partial \theta}{\partial \xi} = \frac{-\frac{\partial \theta}{\partial \xi} \frac{\partial r}{\partial \xi} + \frac{\partial r}{\partial \xi} \frac{\partial \theta}{\partial \xi}}{\mathcal{J}} = 0$

where  $\mathcal{J}$  is the Jacobian.

Now we can write Meade's ABC for elliptical coordinates

$$\frac{\partial u}{\partial \xi} = \frac{1}{C} \left( Au + B \frac{\partial u}{\partial \varphi} + D \frac{\partial^2 u}{\partial \varphi^2} + E \frac{\partial^2 u}{\partial \varphi \partial \xi} \right) \quad (2.21)$$

where

$$\begin{aligned}
A &= \alpha - \beta h^2 k^2 \left( \frac{\partial \xi}{\partial \theta} \right)^2 \\
B &= -\frac{\partial \varphi}{\partial r} + \beta \frac{\partial^2 \varphi}{\partial \theta^2} \\
C &= \frac{\partial \xi}{\partial r} - \beta \frac{\partial^2 \xi}{\partial \theta^2} \\
D &= \beta \left( \left( \frac{\partial \varphi}{\partial \theta} \right)^2 - \left( \frac{\partial \xi}{\partial \theta} \right)^2 \right) \\
E &= 2\beta \frac{\partial \xi}{\partial \theta} \frac{\partial \varphi}{\partial \theta}
\end{aligned}$$

The equation (2.21) is more complicated than the previous ABCs, especially because of inconvenient mixed derivatives. It is impossible to express  $\frac{\partial^2 u}{\partial \varphi \partial \xi}$  in terms of other terms in (2.21). Meade et al. suggested a few ways to treat mixed derivatives. The simple one is to ignore the inconvenient term, while the interesting one is to derive  $BGT_1$ .

Let us develop the boundary condition that is obtained by this approach. After applying the chain rule  $BGT_1$  becomes

$$\begin{aligned}
\frac{\partial u}{\partial \xi} &= \frac{\partial u}{\partial r} \frac{\partial r}{\partial \xi} + \frac{\partial u}{\partial \theta} \frac{\partial \theta}{\partial \xi} \\
&= \frac{\partial r}{\partial \xi} \left( iku - \frac{u}{2r} \right) + \frac{\partial \theta}{\partial \xi} \left( \frac{\partial \xi}{\partial \theta} \frac{\partial u}{\partial \xi} + \frac{\partial \varphi}{\partial \theta} \frac{\partial u}{\partial \varphi} \right) \\
&= \frac{1}{\xi_r} \left( iku - \frac{u}{2r} - \frac{\partial \varphi}{\partial r} \frac{\partial u}{\partial \varphi} \right)
\end{aligned}$$

To achieve the last equality one can use the identities listed on the previous page, 27. Then, we derive it with respect to  $\varphi$  and reach

$$\begin{aligned}
\frac{\partial^2 u}{\partial \varphi \partial \xi} &= -\frac{1}{\xi_r^2} \frac{\partial^2 \xi}{\partial \varphi \partial r} \left( iku - \frac{u}{2r} - \frac{\partial \varphi}{\partial r} \frac{\partial u}{\partial \varphi} \right) \\
&+ \frac{1}{\xi_r} \left( \left( ik - \frac{1}{2r} - \frac{\partial \varphi}{\partial \varphi \partial r} \right) \frac{\partial u}{\partial \varphi} + \frac{1}{2r^2} \frac{\partial r}{\partial \varphi} u - \frac{\partial \varphi}{\partial r} \frac{\partial^2 u}{\partial \varphi^2} \right) \\
&= \frac{1}{\xi_r} \left( \left( ik - \frac{1}{2r} - \frac{\partial \varphi}{\partial \varphi \partial r} \right) \frac{\partial u}{\partial \varphi} + \frac{1}{2r^2} \frac{\partial r}{\partial \varphi} u - \frac{\partial \varphi}{\partial r} \frac{\partial^2 u}{\partial \varphi^2} - \frac{\partial^2 \xi}{\partial \varphi \partial r} \frac{\partial u}{\partial \xi} \right)
\end{aligned}$$

Substituting this in (2.21) gives us

$$\frac{\partial u}{\partial \xi} = \frac{1}{\tilde{C}} \left( \tilde{A}u + \tilde{B} \frac{\partial u}{\partial \varphi} + \tilde{D} \frac{\partial^2 u}{\partial \varphi^2} \right) \quad (2.22)$$

where

$$\begin{aligned} \tilde{A} &= A + E \frac{1}{\xi_r} \frac{1}{2r^2} \frac{\partial r}{\partial \varphi} \\ \tilde{B} &= B + E \frac{1}{\xi_r} \left( ik - \frac{1}{2r} - \frac{\partial \varphi}{\partial \varphi \partial r} \right) \\ \tilde{C} &= C + E \frac{1}{\xi_r} \frac{\partial^2 \xi}{\partial \varphi \partial r} \\ \tilde{D} &= D - E \frac{1}{\xi_r} \frac{\partial \varphi}{\partial r} \end{aligned}$$



## Chapter 3

# New Absorbing Boundary Condition

The original BGT boundary condition was developed from a series in  $\frac{1}{r}$ . For scattering about a circle, an alternative is to use a modal expansion in Hankel functions [15]. The resultant ABC has coefficients that involve  $H_j^{(1)}(kr)$ ,  $j = 0, 1$ . For large  $k$  this gives results similar to the BGT approach. However, for small wave numbers it is significantly better. For scattering about an ellipse we consider a modal expansion in Mathieu functions. The resultant ABC has the same structure as before, but now the coefficients involve Mathieu functions.

Assume an expansion in arbitrary functions [15]:

$$u = c_0\psi_0(k\sigma) + c_1\psi_1(k\sigma) \quad (3.1)$$

$$\frac{\partial u}{\partial \sigma} = kc_0\psi_0'(k\sigma) + kc_1\psi_1'(k\sigma) \quad (3.2)$$

$$\frac{\partial^2 u}{\partial \sigma^2} = k^2c_0\psi_0''(k\sigma) + k^2c_1\psi_1''(k\sigma) \quad (3.3)$$

Solving for  $c_0, c_1$  from the first two equations we get

$$c_0 = \frac{k\psi_1'u - \psi_1\frac{\partial u}{\partial \sigma}}{kD}$$
$$c_1 = \frac{k\psi_0'u - \psi_0\frac{\partial u}{\partial \sigma}}{kD}$$

where  $D = \psi_0\psi_1' - \psi_0'\psi_1$  Substituting it in (3.3) we get

$$\frac{\partial^2 u}{\partial \sigma^2} + k\frac{\psi_0''\psi_1 - \psi_0\psi_1''}{D}\frac{\partial u}{\partial \sigma} + k^2\frac{-\psi_0''\psi_1' + \psi_0'\psi_1''}{D}u \quad (3.4)$$

For elliptical coordinates,  $\sigma = \xi$  and  $\psi_j(k\sigma) = M_j(\xi)$  where  $M_j$  is a Mathieu-Hankel function of  $j$ th order [see (1.9)]. But, as stated in Section 1.3, there are even and odd Mathieu-Hankel functions, and hence it is not completely obvious which Mathieu functions to choose as the first two functions  $M_j(\xi)$ . However, the exact solution for scattering about an ellipse with a plane wave at zero angle does not contain any of the odd Mathieu functions (by symmetry). Also, for larger aspect ratios the first even and the first odd characteristic values are extremely close. Hence, we choose two even Mathieu-Hankel functions  $M_j(\xi) = Me_j(\xi)$ ,  $j = 0, 1$ , with the corresponding characteristic values  $a_0, a_1$ .

Now (3.4) becomes

$$0 = \frac{\partial^2 u}{\partial \xi^2} + \frac{M_1 M_0'' - M_0 M_1''}{D} \frac{\partial u}{\partial \xi} + \frac{-M_1' M_0'' + M_0' M_1''}{D} u$$

with  $D = M_0 M_1' - M_0' M_1$ .

One can reduce the  $M''$  term using the Mathieu equation

$$M_n'' = (a_n - 2q \cosh(2\xi)) M_n$$

Thus

$$\begin{aligned} M_1 M_0'' - M_0 M_1'' &= M_1 (a_0 - 2q \cosh(2\xi)) M_0 - M_0 (a_1 - 2q \cosh(2\xi)) M_1 \\ &= (a_0 - a_1) M_0 M_1 \end{aligned}$$

and

$$\begin{aligned} -M_1' M_0'' + M_0' M_1'' &= -M_1' (a_0 - 2q \cosh(2\xi)) M_0 + M_0' (a_1 - 2q \cosh(2\xi)) M_1 \\ &= -M_0 M_1' a_0 + M_0' M_1 a_1 + (M_0 M_1' - M_0' M_1) 2q \cosh(2\xi) \\ &= D a_0 - D a_0 - M_0 M_1' a_0 + M_0' M_1 a_1 + 2Dq \cosh(2\xi) \\ &= -D a_0 + M_0' M_1 (a_1 - a_0) + 2Dq \cosh(2\xi) \end{aligned}$$

to reach following formula

$$0 = \frac{\partial^2 u}{\partial \xi^2} + \frac{(a_0 - a_1) M_0 M_1}{D} \frac{\partial u}{\partial \xi} + \frac{-D a_0 + M_0' M_1 (a_1 - a_0) + 2Dq \cosh(2\xi)}{D} u$$

Now we remove  $\frac{\partial^2 u}{\partial \xi^2}$  term using Helmholtz equation (1.6) and get

$$0 = \frac{(a_0 - a_1) M_0 M_1}{D} \frac{\partial u}{\partial \xi} + \left( -a_0 + \frac{M'_0 M_1 (a_1 - a_0)}{D} + 2q \cos(2\varphi) \right) u - \frac{\partial^2 u}{\partial \varphi^2}$$

Solving it for  $\frac{\partial u}{\partial \xi}$  we reach the new boundary condition

$$\begin{aligned} \frac{\partial u}{\partial \xi} = & \\ & \frac{D}{(a_0 - a_1) M_0 M_1} \left( a_0 + \frac{M'_0 M_1 (a_0 - a_1)}{D} - 2q \cos(2\varphi) \right) u + \\ & + \frac{D}{(a_0 - a_1) M_0 M_1} \frac{\partial^2 u}{\partial \varphi^2} \end{aligned} \quad (3.5)$$



## Chapter 4

# Numerical Implementation

In this chapter we describe the discretization used for the comparison of our boundary condition with the approaches described in Chapter 2. One wishes that the outer artificial surface resemble the scatterer to prevent unnecessary interior nodes. Hence, for oval-like scatterers we consider an elliptical outer surface. In some cases these boundary conditions were imposed on the scatterer itself (OSRC).

We consider a comparison for both the Dirichlet and Neumann problems, when absorbing boundary conditions are imposed directly on the ellipse (OSRC) and exterior to the ellipse (ABC). In the next two sections we will explain the main points of our implementation.

### 4.1 ABC on Elliptical Artificial Body

For the boundary condition on the artificial body we consider a finite difference approximation. For the finite difference discretization we shall construct a linear system of equations  $Au = b$ . For the Neumann problem we compare the solution  $u$  on the internal boundary, while for the Dirichlet problem  $u$  is known. Hence, for the Dirichlet problem, we compare the normal derivative approximated by

$$\left(\frac{\partial u}{\partial n}\right)_{1,j} = \frac{-u_{3,j} + 4u_{2,j} - 3u_{1,j}}{2\delta_\xi h_\xi}$$

on the internal boundary. We will describe the numerical scheme for the Helmholtz equation with both Dirichlet and Neumann boundary conditions, followed by the discretization of various ABCs in Section 4.1.1.



so we have  $b_1 = -2\delta_\xi \frac{\partial u_{inc}}{\partial \xi}$ ,  $B_1 = 2I$  and  $A_1$  is similar to that from (4.2).

#### 4.1.1 Discretization of Various ABCs

Let us define  $B_2$  and  $A_n$  for ABCs from Chapter 2 and for the new condition. Particularly, one can see below that  $B_2 = 2I$ , so we will talk only about coefficients of

$$A_n = \begin{pmatrix} \hat{d}_{n,1} & \tilde{\alpha}_1 & 0 & \cdots & \hat{\alpha}_1 \\ \hat{\alpha}_2 & \hat{d}_{n,2} & \tilde{\alpha}_2 & 0 \cdots & 0 \\ 0 & & \ddots & & \vdots \\ \vdots & & \hat{\alpha}_{n-1} & \hat{d}_{n,n-1} & \tilde{\alpha}_{n-1} \\ \tilde{\alpha}_n & 0 & \cdots & \hat{\alpha}_n & \hat{d}_{n,n} \end{pmatrix} \quad (4.3)$$

#### Grote and Keller

- $BGT_1$  Recall equation (2.11)

$$\frac{\partial u}{\partial \xi} = \frac{b}{a} \left( ika - \frac{1}{2} \right) u$$

for which the central difference scheme it is given by

$$\frac{u_{n+1,j} - u_{n-1,j}}{2\delta_\xi} = \frac{b}{a} \left( ika - \frac{1}{2} \right) u_{n,j}$$

when the Helmholtz equation (4.1) is used to eliminate the  $u_{n+1,j}$  term, it becomes

$$0 = 2u_{n-1,j} + \alpha (u_{n,j+1} + u_{n,j-1}) + \left( 2\delta_\xi \frac{b}{a} \left( ika - \frac{1}{2} \right) + d_{n,j} \right) u_{n,j}$$

from which  $A_n$  members can be defined:

$$\begin{aligned} \tilde{\alpha}_j &= \hat{\alpha}_j \\ \hat{\alpha}_j &= \alpha \\ \hat{d}_{n,j} &= 2\delta_\xi \frac{b}{a} \left( ika - \frac{1}{2} \right) + d_{n,j} \end{aligned}$$

- $BGT_2$  Starting from equation (2.12)

$$\frac{\partial u}{\partial \xi} = \beta \left( \frac{\partial^2 u}{\partial \varphi^2} + \gamma u \right)$$

where

$$\beta = \left( -2ikb + 3\frac{b}{a} - \frac{a}{b} \right)^{-1}$$

and

$$\gamma = h_{n,j}^2 k^2 - \frac{b^2}{a^2} \frac{5}{4} + k^2 b^2 + \frac{3ikb^2}{a}$$

and writing its central difference scheme

$$\frac{u_{n+1,j} - u_{n-1,j}}{2\delta_\xi} = \beta \left( \frac{u_{n,j+1} - 2u_{n,j} + u_{n,j-1}}{\delta_\varphi^2} + \gamma u_{n,j} \right)$$

after eliminating the  $u_{n+1,j}$  term using the Helmholtz equation (4.1) to get

$$\begin{aligned} 0 &= \alpha \left( 2\beta \frac{1}{\delta_\xi} + 1 \right) (u_{n,j+1} + u_{n,j-1}) \\ &+ \left( 2\beta \delta_\xi \left( \gamma - \frac{2}{\delta_\varphi^2} \right) + d_{n,j} \right) u_{n,j} + 2u_{n-1,j} \end{aligned}$$

We reach

$$\begin{aligned} \tilde{\alpha}_j &= \hat{\alpha}_j \\ \hat{\alpha}_j &= \alpha \left( 2\beta \frac{1}{\delta_\xi} + 1 \right) \\ \hat{d}_{n,j} &= 2\beta \delta_\xi \left( \gamma - \frac{2}{\delta_\varphi^2} \right) + d_{n,j} \end{aligned}$$

**Reiner et al.**

- $BGT_2$  Rewrite equation (2.13)

$$\frac{\partial u}{\partial \xi} = \frac{b}{a} \left( \beta u - \frac{1}{2(ika-1)} \frac{\partial^2 u}{\partial \varphi^2} \right)$$

where  $\beta = ika - \frac{1}{2} - \frac{1}{8(ika-1)}$ . Using a central difference scheme

$$\frac{u_{n+1,j} - u_{n-1,j}}{2\delta_\xi} = \frac{b}{a} \left( \beta u_{n,j} - \frac{1}{2(ika-1)} \frac{u_{n,j+1} - 2u_{n,j} + u_{n,j-1}}{\delta_\varphi^2} \right)$$

and using the Helmholtz equation (4.1) again to eliminate  $u_{n+1,j}$  to obtain

$$\begin{aligned} 0 &= 2u_{n-1,j} + \left( \alpha - \frac{b}{a} \frac{1}{(ika-1)} \frac{\delta_\xi}{\delta_\varphi^2} \right) (u_{n,j+1} + u_{n,j-1}) + \\ &+ \left( 2\delta_\xi \frac{b}{a} \left( \beta + \frac{1}{(ika-1)} \frac{\delta_\xi}{\delta_\varphi^2} \right) + d_{n,j} \right) u_{n,j} \end{aligned}$$

one can define

$$\begin{aligned} \tilde{\alpha}_j &= \hat{\alpha}_j \\ \hat{\alpha}_j &= \alpha - \frac{b}{a} \frac{1}{(ika-1)} \frac{\delta_\xi}{\delta_\varphi^2} \\ \hat{d}_{n,j} &= 2\delta_\xi \frac{b}{a} \left( ika - \frac{1}{2} - \frac{1}{8(ika-1)} + \frac{1}{(ika-1)} \frac{\delta_\xi}{\delta_\varphi^2} \right) + d_{n,j} \end{aligned}$$

**Kriegsmann et al.**

- $BGT_1$  Kriegsmann  $BGT_1$  given by (2.14)

$$\frac{1}{h_\xi} \frac{\partial u}{\partial \xi} = \frac{\partial u}{\partial n} = \left( ik - \frac{\zeta}{2} \right) u$$

Its central difference scheme given by

$$\frac{u_{n+1,j} - u_{n-1,j}}{2\delta_\xi} = h_\xi \left( ik - \frac{\zeta}{2} \right) u_{n,j}$$

Applying it in the Helmholtz equation (4.1) to eliminate  $u_{n+1,j}$ :

$$0 = 2u_{n-1,j} + \alpha (u_{n,j+1} + u_{n,j-1}) + \left( 2\delta_\xi h_{n,j} \left( ik - \frac{\zeta}{2} \right) + d_{n,j} \right) u_{n,j}$$

we arrive at

$$\begin{aligned} \tilde{\alpha}_j &= \hat{\alpha}_j \\ \hat{\alpha}_j &= \alpha \\ \hat{d}_{n,j} &= 2\delta_\xi h_{n,j} \left( ik - \frac{\zeta}{2} \right) + d_{n,j} \end{aligned}$$

- $BGT_2$  Remember the equation (2.15)

$$\frac{\partial u}{\partial n} = \left( ik - \frac{\zeta}{2} - \frac{\zeta^2}{8(ik-\zeta)} \right) u - \frac{1}{2(ik-\zeta)} \frac{\partial^2 u}{\partial s^2}$$

One can use A.2 to abolish the  $\frac{\partial^2}{\partial s^2}$  term to reach the following form

$$\begin{aligned}\frac{\partial u}{\partial \xi} &= h_\xi \left( ik - \frac{\zeta}{2} - \frac{\zeta^2}{8(ik - \zeta)} \right) u - \frac{h_\xi}{2(ik - \zeta)} \left( \frac{1}{h_\xi^2} \frac{\partial^2 u}{\partial \varphi^2} - \frac{2\Psi}{h_\xi^2} \frac{\partial u}{\partial \varphi} \right) \\ &= h_\xi \left( ik - \frac{\zeta}{2} - \frac{\zeta^2}{8(ik - \zeta)} \right) u - \frac{1}{2h_\xi(ik - \zeta)} \left( \frac{\partial^2 u}{\partial \varphi^2} - 2\Psi \frac{\partial u}{\partial \varphi} \right)\end{aligned}$$

where  $\Psi = \frac{f^2 \sin(2\varphi)}{4h_{i,j}^2}$

Now let us write its central difference scheme

$$\begin{aligned}\frac{u_{n+1,j} - u_{n-1,j}}{2\delta_\xi} &= h_{n,j} \left( ik - \frac{\zeta}{2} - \frac{\zeta^2}{8(ik - \zeta)} \right) - \frac{1}{2h_{n,j}(ik - \zeta)} \times \\ &\times \left( \frac{u_{n,j+1} - 2u_{n,j} + u_{n,j-1}}{\delta_\varphi^2} - 2\Psi \frac{u_{n,j+1} - u_{n,j-1}}{2\delta_\varphi} \right) \\ &= h_{n,j} \left( ik - \frac{\zeta}{2} - \frac{\zeta^2}{8(ik - \zeta)} + \frac{1}{h_{n,j}^2 \delta_\varphi^2 (ik - \zeta)} \right) u_{n,j} - \\ &- \frac{1}{2h_{n,j}(ik - \zeta) \delta_\varphi} \left( \frac{1}{\delta_\varphi} - \Psi \right) u_{n,j+1} - \\ &- \frac{1}{2h_{n,j}(ik - \zeta) \delta_\varphi} \left( \frac{1}{\delta_\varphi} + \Psi \right) u_{n,j-1}\end{aligned}$$

We once more want to eliminate the term  $u_{n+1,j}$  that is still in the Helmholtz equation (4.1). One can then express the formula as

$$\begin{aligned}0 &= \left( \alpha - \frac{\sqrt{\alpha}}{h_{n,j}(ik - \zeta)} \left( \frac{1}{\delta_\varphi} - \Psi \right) \right) u_{n,j+1} + \\ &+ \left( \alpha - \frac{\sqrt{\alpha}}{h_{n,j}(ik - \zeta)} \left( \frac{1}{\delta_\varphi} + \Psi \right) \right) u_{n,j-1} + \\ &+ 2u_{n-1,j} + (2\delta_\xi h_{n,j} \beta + d_{n,j}) u_{n,j}\end{aligned}$$

where

$$\beta = \left( ik - \frac{\zeta}{2} - \frac{\zeta^2}{8(ik - \zeta)} + \frac{1}{h_{n,j}^2 \delta_\varphi^2 (ik - \zeta)} \right)$$

And we accomplish

$$\begin{aligned}\hat{\alpha}_j &= \alpha - \frac{\sqrt{\alpha}}{h_{n,j}(ik - \zeta)} \left( \frac{1}{\delta_\varphi} + \Psi \right) \\ \tilde{\alpha}_j &= \alpha - \frac{\sqrt{\alpha}}{h_{n,j}(ik - \zeta)} \left( \frac{1}{\delta_\varphi} - \Psi \right) \\ \hat{d}_{n,j} &= 2\delta_\xi h_{n,j} \left( ik - \frac{\zeta}{2} - \frac{\zeta^2}{8(ik - \zeta)} + \frac{1}{h_{n,j}^2 \delta_\varphi^2 (ik - \zeta)} \right) + d_{n,j}\end{aligned}$$

**Jones**

- $BGT_2$  Consider equation (2.16)

$$\frac{\partial u}{\partial n} = \gamma u - \frac{1}{2(ik - \zeta)} \left( \frac{\partial^2 u}{\partial s^2} + \frac{1}{ik} \frac{\partial \zeta}{\partial s} \frac{\partial u}{\partial s} \right)$$

where  $\gamma = ik - \frac{\zeta}{2} - \frac{1}{8(ik - \zeta)} \left( \zeta^2 + \frac{1}{ik} \frac{\partial^2 \zeta}{\partial s^2} \right)$ . As before, we remove the  $\frac{\partial^2}{\partial s^2}$  term with A.2 and write it as a central difference scheme

$$\begin{aligned}\frac{u_{n+1,j} - u_{n-1,j}}{2\delta_\xi} &= h_{n,j} \gamma u_{n,j} - \frac{1}{2(ik - \zeta)} \times \\ &\times \left( \frac{1}{h_{n,j}} \frac{u_{n,j+1} - 2u_{n,j} + u_{n,j-1}}{\delta_\varphi^2} + 2\beta \frac{u_{n,j+1} - u_{n,j-1}}{2\delta_\varphi} \right)\end{aligned}$$

where  $\beta = -\frac{f \sin(2\varphi)}{4h_\xi^3} + \frac{1}{2ik} \frac{\partial \zeta}{\partial s}$ .

When the Helmholtz equation (4.1) is used to reduce  $u_{n+1,j}$  one gets

$$\begin{aligned}0 &= \left( \alpha - \frac{\sqrt{\alpha}}{(ik - \zeta)} \left( \frac{1}{\delta_\varphi h_{n,j}} + \beta \right) \right) u_{n,j+1} \\ &+ \left( \alpha - \frac{\sqrt{\alpha}}{(ik - \zeta)} \left( \frac{1}{\delta_\varphi h_{n,j}} - \beta \right) \right) u_{n,j-1} \\ &+ \left( 2\delta_\xi h_{n,j} \gamma + \frac{1}{h_{n,j}} \frac{2\delta_\xi}{\delta_\varphi^2} \frac{1}{(ik - \zeta)} + d_{n,j} \right) u_{n,j} + 2u_{n-1,j}\end{aligned}$$

And we finish with

$$\begin{aligned}\hat{\alpha}_j &= \alpha - \frac{\sqrt{\alpha}}{(ik - \zeta)} \left( \frac{1}{\delta_\varphi h_{n,j}} - \beta \right) \\ \tilde{\alpha}_j &= \alpha - \frac{\sqrt{\alpha}}{(ik - \zeta)} \left( \frac{1}{\delta_\varphi h_{n,j}} + \beta \right) \\ \hat{d}_{n,j} &= 2\delta_\xi h_{n,j} \gamma + \frac{1}{h_{n,j}} \frac{2\delta_\xi}{\delta_\varphi^2} \frac{1}{(ik - \zeta)} + d_{n,j}\end{aligned}$$

**Kallivokas et al.**

- $BGT_2$  In similar way to work with (2.17)

$$\frac{\partial u}{\partial n} = \beta u - \frac{1}{2(ik - \zeta)} \left( \frac{1}{(ik - \zeta)} \frac{\partial \zeta}{\partial s} \frac{\partial u}{\partial s} + \frac{\partial^2 u}{\partial s^2} \right)$$

where  $\beta = ik - \frac{\zeta}{2} - \frac{1}{8(ik - \zeta)} \left( \zeta^2 + \frac{1}{(ik - \zeta)} \frac{\partial^2 \zeta}{\partial s^2} \right)$ . Next we eliminate the term  $\frac{\partial^2}{\partial s^2}$  using A.2 and reach the following central difference scheme

$$\begin{aligned} \frac{u_{n+1,j} - u_{n-1,j}}{2\delta_\xi} &= h_{n,j} \tilde{\beta} u_{n,j} - \frac{1}{2(ik - \zeta)} \frac{1}{h_{n,j} \delta_\varphi} \times \\ &\times \left( \left( \frac{1}{\delta_\varphi} + \gamma \frac{1}{2} \right) u_{n,j+1} + \left( \frac{1}{\delta_\varphi} - \gamma \frac{1}{2} \right) u_{n,j-1} \right) \end{aligned}$$

where  $\tilde{\beta} = \beta + \frac{1}{2(ik - \zeta)} \frac{1}{h_{n,j}^2} \frac{2u_j^i}{\delta_\varphi^2}$  and  $\gamma = \frac{1}{(ik - \zeta)} \frac{\partial \zeta}{\partial \varphi} + \frac{f^2 \sin(2\varphi)}{-2h_\xi^2}$

Once again we apply the Helmholtz equation (4.1) to eliminate  $u_{n+1,j}$  and reach

$$\begin{aligned} 0 &= (2\delta_\xi h_{n,j} \beta + d_{n,j}) u_{n,j} + \\ &+ \left( \alpha - \frac{\sqrt{\alpha}}{(ik - \zeta)} \frac{1}{h_{n,j}} \left( \frac{1}{\delta_\varphi} + \gamma \frac{1}{2} \right) \right) u_{n,j+1} + \\ &+ \left( \alpha - \frac{\sqrt{\alpha}}{(ik - \zeta)} \frac{1}{h_{n,j}} \left( \frac{1}{\delta_\varphi} - \gamma \frac{1}{2} \right) \right) u_{n,j-1} + 2u_{n-1,j} \end{aligned}$$

And we have

$$\begin{aligned} \hat{\alpha}_j &= \alpha - \frac{\sqrt{\alpha}}{(ik - \zeta)} \frac{1}{h_{n,j}} \left( \frac{1}{\delta_\varphi} - \gamma \frac{1}{2} \right) \\ \tilde{\alpha}_j &= \alpha - \frac{\sqrt{\alpha}}{(ik - \zeta)} \frac{1}{h_{n,j}} \left( \frac{1}{\delta_\varphi} + \gamma \frac{1}{2} \right) \\ \hat{d}_{n,j} &= 2\delta_\xi h_{n,j} \beta + d_{n,j} \end{aligned}$$

**Antoine et al.**

- $BGT_2$  When dealing with equation (2.18)

$$\frac{\partial u}{\partial \xi} = h_\xi \beta u - \frac{\partial}{\partial \varphi} \left( \frac{1}{2(ik - \zeta)} \frac{1}{h_\xi} \frac{\partial u}{\partial \varphi} \right)$$

where

$$\beta = ik - \frac{\zeta}{2} - \frac{\zeta^2}{8(ik - \zeta)} + \frac{1}{8k^2} \frac{\partial^2 \zeta}{\partial s^2}$$

we use A.3 to eliminate the  $\frac{\partial}{\partial \varphi} \left( \frac{1}{2(ik-\zeta)} \frac{1}{h_\xi} \frac{\partial u}{\partial \varphi} \right)$  term. And then we write the following central difference scheme

$$\begin{aligned} \frac{u_{n+1,j} - u_{n-1,j}}{2\delta_\xi} &= h_{n,j} \beta u_{n,j} - \frac{1}{2(ik-\zeta)} \times \\ &\times \left( 2\Upsilon \frac{u_{n,j+1} - u_{n,j-1}}{2\delta_\varphi} + \frac{1}{h_{n,j}} \frac{u_{n,j+1} - 2u_{n,j} + u_{n,j-1}}{\delta_\varphi^2} \right) \end{aligned}$$

where  $\Upsilon = \left( \frac{1}{2(ik-\zeta)} \frac{\partial \zeta}{\partial s} - \frac{f^2 \sin(2\varphi)}{4h_{i,j}^3} \right)$ . Now we use the Helmholtz equation (4.1) again to eliminate  $u_{n+1,j}$  and reach

$$\begin{aligned} 0 &= \left( \alpha - \frac{\sqrt{\alpha}}{(ik-\zeta)} \left( \Upsilon + \frac{1}{h_{n,j} \delta_\varphi} \right) \right) u_{n,j+1} + 2u_{n-1,j} + \\ &+ \left( \alpha + \frac{\sqrt{\alpha}}{(ik-\zeta)} \left( \Upsilon - \frac{1}{h_{n,j} \delta_\varphi} \right) \right) u_{n,j-1} + \\ &+ \left( 2\delta_\xi h_{n,j} \left( \beta + \frac{1}{ik-\zeta} \frac{1}{h_{n,j}^2} \frac{1}{\delta_\varphi^2} \right) + d_{n,j} \right) u_{n,j} \end{aligned}$$

Thus we have

$$\begin{aligned} \hat{\alpha}_j &= \alpha + \frac{\sqrt{\alpha}}{(ik-\zeta)} \left( \Upsilon - \frac{1}{h_{n,j} \delta_\varphi} \right) \\ \tilde{\alpha}_j &= \alpha - \frac{\sqrt{\alpha}}{(ik-\zeta)} \left( \Upsilon + \frac{1}{h_{n,j} \delta_\varphi} \right) \\ \hat{d}_{n,j} &= 2\delta_\xi h_{n,j} \left( ik - \frac{\zeta}{2} - \frac{\zeta^2}{8(ik-\zeta)} + \frac{1}{8k^2} \frac{\partial^2 \zeta}{\partial s^2} + \frac{1}{ik-\zeta} \frac{1}{h_{n,j}^2} \frac{1}{\delta_\varphi^2} \right) + d_{n,j} \end{aligned}$$

**Meade et al**

- *BGT*<sub>2</sub> We use (2.22)

$$\frac{\partial u}{\partial \xi} = \frac{1}{\tilde{C}} \left( \tilde{A}u + \tilde{B} \frac{\partial u}{\partial \varphi} + \tilde{D} \frac{\partial^2 u}{\partial \varphi^2} \right)$$

where the coefficients are defined on page 29 and the central difference scheme is given by

$$\frac{u_{i+1,j} - u_{i-1,j}}{2\delta_\xi} = \frac{1}{\tilde{C}} \left( \tilde{A}u_{i,j} + \tilde{B} \frac{u_{i,j+1} - u_{i,j-1}}{2\delta_\varphi} + \tilde{D} \frac{u_{i,j+1} - 2u_{i,j} + u_{i,j-1}}{\delta_\varphi^2} \right)$$

which can be rewritten as

$$\begin{aligned} \frac{u_{i+1,j} - u_{i-1,j}}{2\delta_\xi} &= \frac{1}{\tilde{C}} \left( \left( \tilde{A} - \frac{2\tilde{D}}{\delta_\varphi^2} \right) u_{i,j} + \frac{1}{\delta_\varphi} \left( \frac{\tilde{B}}{2} + \frac{\tilde{D}}{\delta_\varphi} \right) u_{i,j+1} + \right. \\ &\quad \left. + \frac{1}{\delta_\varphi} \left( \frac{\tilde{D}}{\delta_\varphi} - \frac{\tilde{B}}{2} \right) u_{i,j-1} \right) \end{aligned}$$

We use the Helmholtz equation (4.1) to eliminate  $u_{n+1,j}$  and get

$$\begin{aligned} 0 &= \left( 2\frac{\sqrt{\alpha}}{\tilde{C}} \left( \delta_\varphi \tilde{A} - \frac{2\tilde{D}}{\delta_\varphi} \right) + d_{n,j} \right) u_{i,j} + 2u_{i-1}^j + \\ &\quad + \left( 2\frac{\sqrt{\alpha}}{\tilde{C}} \left( \frac{\tilde{D}}{\delta_\varphi} + \frac{\tilde{B}}{2} \right) + \alpha \right) u_i^{j+1} + \left( 2\frac{\sqrt{\alpha}}{\tilde{C}} \left( \frac{\tilde{D}}{\delta_\varphi} - \frac{\tilde{B}}{2} \right) + \alpha \right) u_i^{j-1} \end{aligned}$$

and we reach

$$\begin{aligned} \hat{\alpha}_j &= 2\frac{\sqrt{\alpha}}{\tilde{C}} \left( \frac{\tilde{D}}{\delta_\varphi} - \frac{\tilde{B}}{2} \right) + \alpha \\ \tilde{\alpha}_j &= 2\frac{\sqrt{\alpha}}{\tilde{C}} \left( \frac{\tilde{D}}{\delta_\varphi} + \frac{\tilde{B}}{2} \right) + \alpha \\ \hat{d}_{n,j} &= 2\frac{\sqrt{\alpha}}{\tilde{C}} \left( \delta_\varphi \tilde{A} - \frac{2\tilde{D}}{\delta_\varphi} \right) + d_{n,j} \end{aligned}$$

### New ABC

Finally, for our method we define  $\mu = \frac{D}{(a_0 - a_1)M_0M_1}$  and  $\nu = \frac{M'_0M_1(a_0 - a_1)}{D}$ , so that equation (3.5) becomes

$$\frac{\partial u}{\partial \xi} = \mu (a_0 + \nu - 2q \cos(2\varphi)) u + \mu \frac{\partial^2 u}{\partial \varphi^2}$$

for which the finite difference scheme reads

$$\frac{u_{n+1,j} - u_{n-1,j}}{2\delta_\xi} = \mu (a_0 + \eta - 2q \cos(2v)) u_{i,j} + \mu \frac{u_{n,j+1} - 2u_{n,j} + u_{n,j-1}}{\delta_\varphi^2}$$

Once more we are using the Helmholtz equation (4.1) to eliminate  $u_{n+1,j}$ , so that the scheme is given by

$$\begin{aligned}
0 &= \left( \mu \frac{2\delta_\xi}{\delta_\varphi^2} + \alpha \right) (u_{n,j+1} + u_{n,j-1}) + \\
&+ \left( 2\delta_\xi \mu \left( a_0 + \eta - 2q \cos(2v) - \frac{2}{\delta_\varphi^2} \right) + d_{n,j} \right) u_{n,j} + 2u_{n-1,j}
\end{aligned}$$

and we finish with

$$\begin{aligned}
\hat{\alpha}_j &= \tilde{\alpha}_j \\
\tilde{\alpha}_j &= \mu \frac{2\delta_\xi}{\delta_\varphi^2} + \alpha \\
\hat{d}_{n,j} &= 2\delta_\xi \mu \left( a_0 + \eta - 2q \cos(2v) - \frac{2}{\delta_\varphi^2} \right) + d_{n,j}
\end{aligned}$$

## 4.2 On Surface Radiation Condition

From the Sommerfeld condition one can derive the physical demand that waves not enter the domain from infinity. On the scatterer body we specify  $Bu = -Bu_{inc}$  and also the ABC. This can be viewed [see [1]] as using a degenerate artificial boundary.

For a Dirichlet problem, the implementation of OSRC is straight forward. In particular, for  $BGT_1$ -like conditions we apply the operator directly on the incident (plane) wave. For  $BGT_2$ -like conditions, where a second derivative in  $\varphi$  appears (or, alternatively, derivatives with respect to arc-length), we use analytical derivatives of the plane wave for the computation.

For a Neumann problem,  $\frac{\partial u}{\partial \xi}$  is known, so to retrieve  $u$  we have to solve a second order ordinary differential equation (ODE) described by the boundary condition. The ODE appears only for  $BGT_2$ -like conditions, while for  $BGT_1$  we have to solve a simple equation. For this reason we omit here the  $BGT_1$  case. We solve the ODE by finite differences similarly to that used in the previous section. In particular, we solve the linear system  $Au = b$  where  $b = \frac{\partial u}{\partial \xi}$  and

$$A = \begin{pmatrix} d_1 & d_1^+ & 0 & \cdots & d_1^- \\ d_2^- & d_2 & d_2^+ & 0 \cdots & 0 \\ 0 & & \ddots & & \vdots \\ \vdots & & d_{n-1}^- & d_{n-1} & d_{n-1}^+ \\ d_n^+ & 0 & \cdots & d_n^- & d_n \end{pmatrix} \quad (4.4)$$

The scheme is similar to that used for the ABC, except that we do not have

the  $u_{n+1,j}$  term to eliminate since  $\frac{\partial u}{\partial \xi}$  is given. Following, we write the  $d, d^+, d^-$  for different methods.

#### 4.2.1 Discretization of Various ABCs

##### Grote and Keller

$$\begin{aligned} d_j^- &= \frac{\beta}{\delta_\phi^2} \\ d_j^+ &= \frac{\beta}{\delta_\phi^2} \\ d_j &= \gamma - \frac{2}{\delta_\phi^2} \end{aligned}$$

where  $\beta = (-2ikb + 3\frac{b}{a} - \frac{a}{b})^{-1}$  and  $\gamma = h_j^2 k^2 - \frac{b^2}{a^2} \frac{3}{4} + k^2 b^2 + \frac{3ikb^2}{a}$

##### Reiner et al.

$$\begin{aligned} d_j^- &= -\frac{b}{a} \frac{1}{2(ika-1)} \frac{1}{\delta_\phi^2} \\ d_j^+ &= -\frac{b}{a} \frac{1}{2(ika-1)} \frac{1}{\delta_\phi^2} \\ d_j &= \frac{b}{a} \left( ika - \frac{1}{2} - \frac{1}{8(ika-1)} + \frac{1}{(ika-1)} \frac{1}{\delta_\phi^2} \right) \end{aligned}$$

##### Kriegsmann et al.

$$\begin{aligned} d_j^- &= -\frac{1}{2h_j(ik-\zeta)\delta_\phi} \left( \frac{1}{\delta_\phi} + \frac{f^2 \sin(2\varphi)}{4h_j^2} \right) \\ d_j^+ &= -\frac{1}{2h_j(ik-\zeta)\delta_\phi} \left( \frac{1}{\delta_\phi} - \frac{f^2 \sin(2\varphi)}{4h_j^2} \right) \\ d_j &= h_j \left( ik - \frac{\zeta}{2} - \frac{\zeta^2}{8(ik-\zeta)} + \frac{1}{h_j^2 \delta_\phi^2 (ik-\zeta)} \right) \end{aligned}$$

**Jones**

$$\begin{aligned}
d_j^- &= -\frac{1}{2h_\xi(ik-\zeta)\delta_\varphi} \left( \frac{1}{\delta_\varphi} - \left( \frac{1}{2ik} \frac{\partial\zeta}{\partial\varphi} - \frac{f^2 \sin(2\varphi)}{4h_j^2} \right) \right) \\
d_j^+ &= -\frac{1}{2h_\xi(ik-\zeta)\delta_\varphi} \left( \frac{1}{\delta_\varphi} + \left( \frac{1}{2ik} \frac{\partial\zeta}{\partial\varphi} - \frac{f^2 \sin(2\varphi)}{4h_j^2} \right) \right) \\
d_j &= h_j \left( ik - \frac{\zeta}{2} - \frac{1}{8(ik-\zeta)} \left( \zeta^2 + \frac{1}{ik} \frac{\partial^2\zeta}{\partial s^2} \right) + \frac{1}{h_j(ik-\zeta)} \frac{1}{\delta_\varphi^2} \right)
\end{aligned}$$

**Kallivokas et al.**

$$\begin{aligned}
d_j^- &= -\frac{1}{2(ik-\zeta)} \frac{1}{h_{n,j}\delta_\varphi} \left( \frac{1}{\delta_\varphi} - \gamma \frac{1}{2} \right) \\
d_j^+ &= -\frac{1}{2(ik-\zeta)} \frac{1}{h_{n,j}\delta_\varphi} \left( \frac{1}{\delta_\varphi} + \gamma \frac{1}{2} \right) \\
d_j &= h_{n,j} \left( ik - \frac{\zeta}{2} - \frac{1}{8(ik-\zeta)} \left( \zeta^2 + \frac{1}{(ik-\zeta)} \frac{\partial^2\zeta}{\partial s^2} \right) + \frac{1}{2(ik-\zeta)} \frac{1}{h_{n,j}^2} \frac{2u_i^j}{\delta_\varphi^2} \right)
\end{aligned}$$

where  $\gamma = \frac{1}{(ik-\zeta)} \frac{\partial\zeta}{\partial\varphi} + \frac{f^2 \sin(2\varphi)}{-2h_\xi^2}$

**Antoine et al.**

$$\begin{aligned}
d_j^- &= \frac{1}{2(ik-\zeta)\delta_\varphi} \left( \left( \frac{1}{2(ik-\zeta)} \frac{\partial\zeta}{\partial s} - \frac{f^2 \sin(2\varphi)}{4h_j^3} \right) - \frac{1}{h_j\delta_\varphi} \right) \\
d_j^+ &= -\frac{1}{2(ik-\zeta)\delta_\varphi} \left( \left( \frac{1}{2(ik-\zeta)} \frac{\partial\zeta}{\partial s} - \frac{f^2 \sin(2\varphi)}{4h_j^3} \right) + \frac{1}{h_j\delta_\varphi} \right) \\
d_j &= h_j \left( ik - \frac{\zeta}{2} - \frac{\zeta^2}{8(ik-\zeta)} + \frac{1}{8k^2} \frac{\partial^2\zeta}{\partial s^2} + \frac{1}{2(ik-\zeta)} \frac{1}{h_j^2} \frac{2}{\delta_\varphi^2} \right)
\end{aligned}$$

Meade et al.

$$\begin{aligned} d_j^- &= \frac{1}{\tilde{C}} \left( \tilde{A} - \frac{2\tilde{D}}{\delta_\varphi^2} \right) \\ d_j^+ &= \frac{1}{\tilde{C}} \frac{1}{\delta_\varphi} \left( \frac{\tilde{D}}{\delta_\varphi} + \frac{\tilde{B}}{2} \right) \\ d_j &= \frac{1}{\tilde{C}} \frac{1}{\delta_\varphi} \left( \frac{\tilde{D}}{\delta_\varphi} - \frac{\tilde{B}}{2} \right) \end{aligned}$$

New ABC

$$\begin{aligned} d_i^- &= \frac{1}{\delta_\varphi^2} \\ d_i^+ &= \frac{1}{\delta_\varphi^2} \\ d_i &= \mu \left( a_0 + \eta - 2q \cos(2\varphi) - \mu \frac{2}{\delta_\varphi^2} \right) \end{aligned}$$

where  $\mu = \frac{D}{(a_0 - a_1)M_0M_1}$ ,  $\eta = \frac{M'_0M_1(a_0 - a_1)}{D}$ ,  $q = \frac{f^2k^2}{4}$

## Chapter 5

# Numerical Results

In the following discussion we present numerical results for the comparison of methods described in Chapter 2<sup>1</sup> and Chapter 3. One wishes that the outer artificial surface resemble the scatterer to prevent unnecessary interior nodes. Hence, for oval-like scatterers we consider an elliptical outer surface. In some cases these boundary conditions were imposed on the scatterer itself (OSRC).

Until now, we have referred to  $a, b$  as the semi-axes of the artificial elliptical boundary. Hereafter,  $a, b$  represents the semi-axes of the internal boundary ellipse.

In all cases the major axis is  $a = 1$  and we vary the minor axis  $b$ . All figures below present the solution at  $180^\circ$  or  $185^\circ$  [i.e. behind the ellipse in (or near) the shadow region, in other words the incident angle  $\theta = 0^\circ$  or  $\theta = 5^\circ$  respectively]. The specific incident angle ( $\theta$ ) and aspect ratio ( $AR = \frac{a}{b}$ ) appears in the capture of each figure. We compute the  $L_2$ -error on the scatterer between the approximate solutions and the exact one. For the Dirichlet problem the solution on the scatterer is given by the incoming wave, and so we compare the normal derivative there, while for the Neumann problem the normal derivative on the scatterer is known and we compare the solution itself.

In Section 5.1 we present a comparison of the approximate solution for the On Surface Radiation Condition, followed by a comparison of the Absorbing Boundary Condition in Section 5.2.

---

<sup>1</sup>Here and later in this chapter we omit Meade's method, because we had very poor results and it was not clear if this problem was due to our implementation, some numerical problem or the problem of the method itself. Thus we cannot develop an objective discussion about these results.

## 5.1 On Surface Radiation Condition

In this section we consider various absorbing boundary conditions described in Chapter 2 imposed directly on the scattering ellipse (OSRC). The next two subsections present the results for Dirichlet and Neumann conditions on an elliptical scatterer.

### 5.1.1 Dirichlet Condition

Let us start with the Dirichlet problem with an incident angle  $\theta = 0$ . In Figures 5.1 and 5.2 on page 50 we compare several methods with the exact solution for various wave numbers ( $k = 1, 2, 3, 4$ ) and an aspect ratio  $(\frac{a}{b}) = 10$ . The  $L_2$  error between the approximate normal derivative of the solutions and the exact one is given in the legend. The errors of all the OSRC results for  $\theta = 0$  also can be found in Table 5.1 on page 54. In Figures 5.3 and 5.4 on page 51 we consider the same wave numbers but with an aspect ratio 3.3, in Figures 5.5 and 5.6 on page 52 the aspect ratio is 2, in Figures 5.7 and 5.8 on page 52 the aspect ratio is 1.4, and in Figures 5.9 and 5.10 on page 53 the aspect ratio is 1.1.

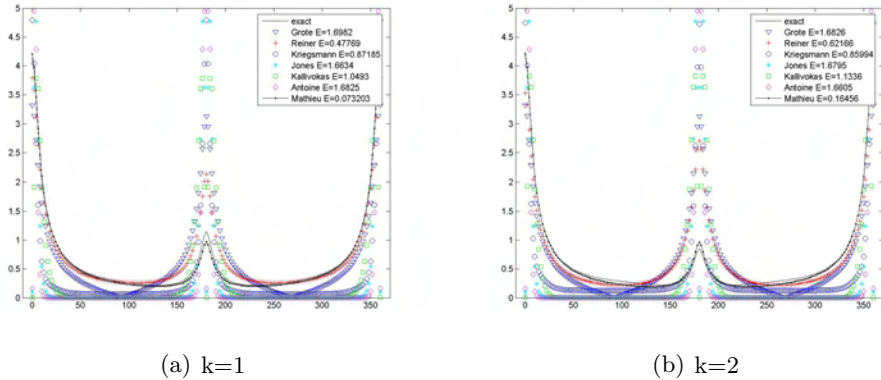


Figure 5.1: OSRC Dirichlet bc,  $k = 1, 2$ , AR=10 and  $\theta = 0^\circ$

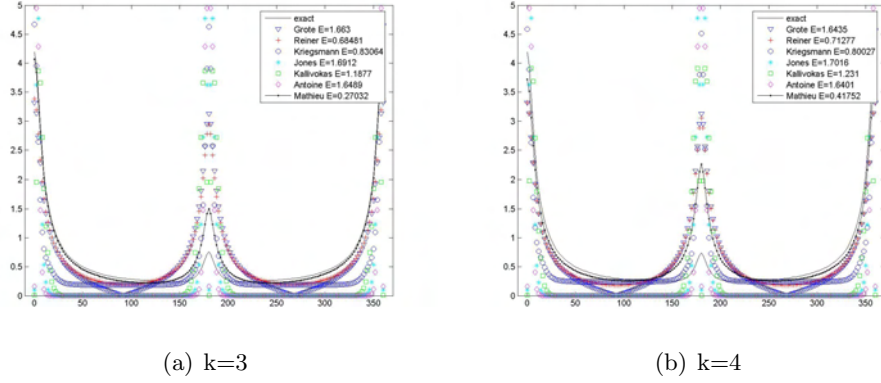


Figure 5.2: OSRC Dirichlet bc,  $k = 3, 4$ , AR=10 and  $\theta = 0^\circ$

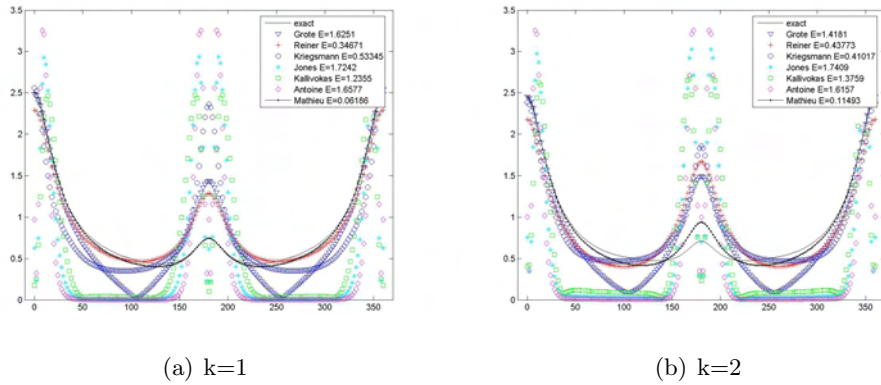


Figure 5.3: OSRC Dirichlet bc,  $k = 1, 2$ , AR=3.3 and  $\theta = 0^\circ$

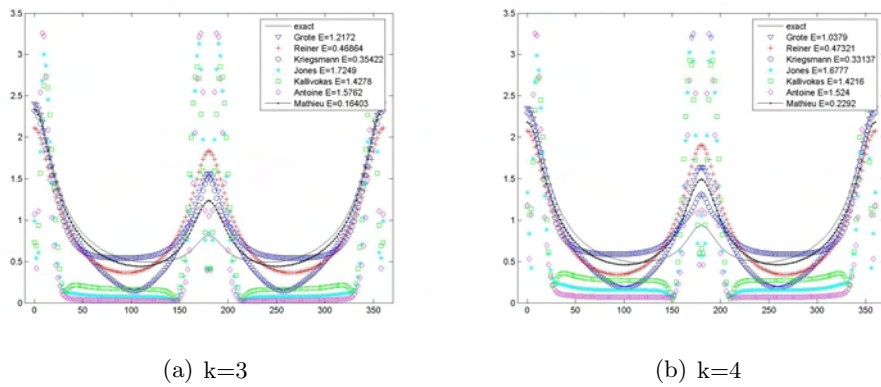
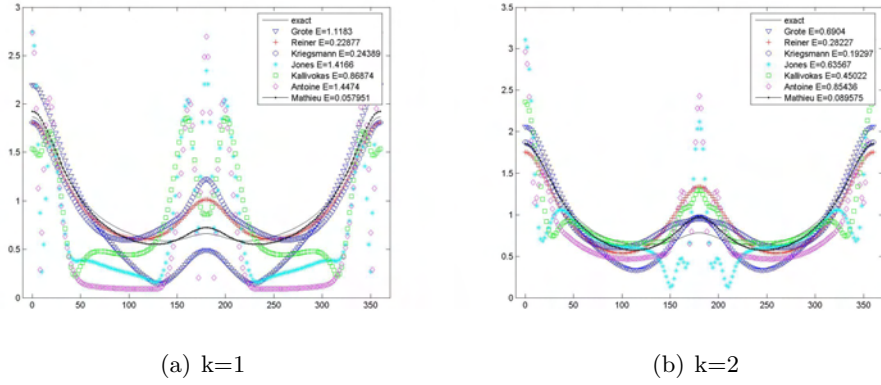
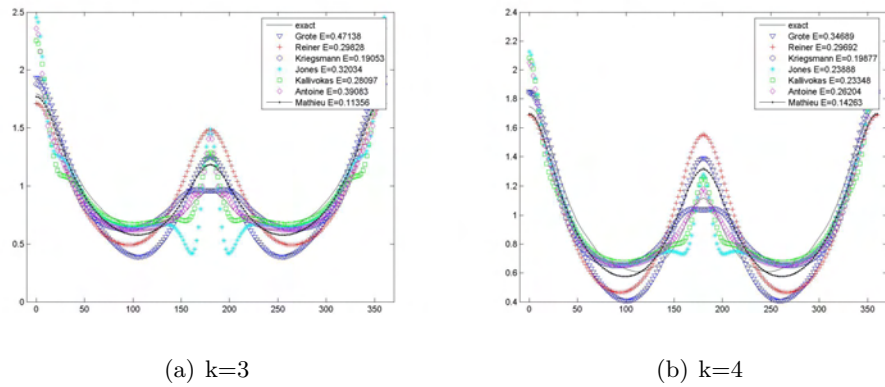
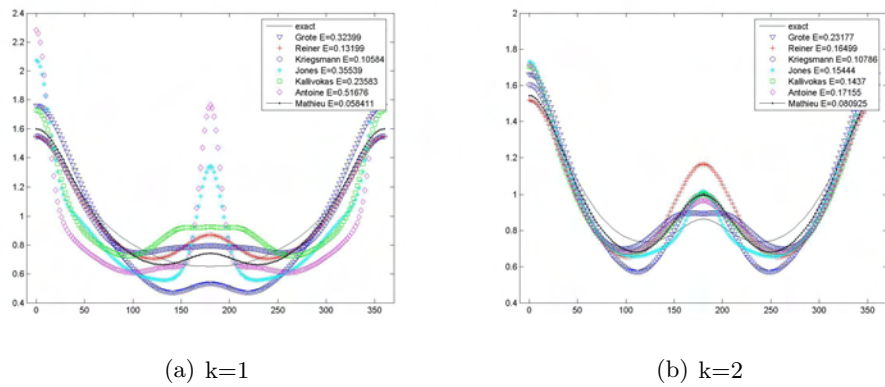


Figure 5.4: OSRC Dirichlet bc,  $k = 3, 4$ , AR=3.3 and  $\theta = 0^\circ$

Figure 5.5: OSRC Dirichlet bc,  $k = 1, 2$ , AR=2 and  $\theta = 0^\circ$ Figure 5.6: OSRC Dirichlet bc,  $k = 3, 4$ , AR=2 and  $\theta = 0^\circ$ Figure 5.7: OSRC Dirichlet bc,  $k = 1, 2$ , AR=1.4 and  $\theta = 0^\circ$

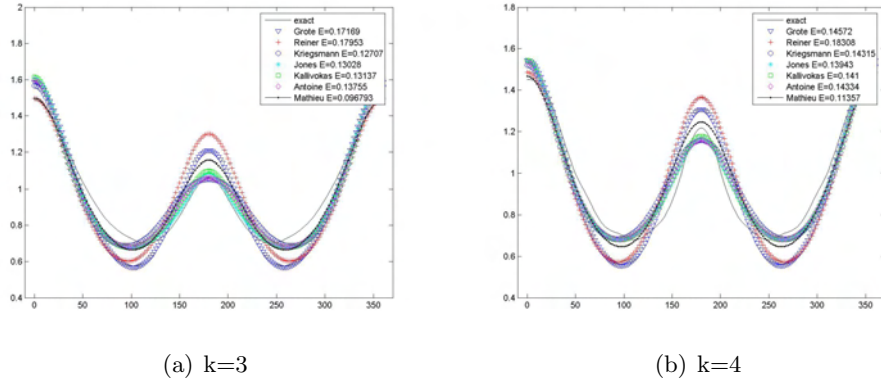


Figure 5.8: OSRC Dirichlet bc,  $k = 3, 4$ ,  $AR=1.4$  and  $\theta = 0^\circ$

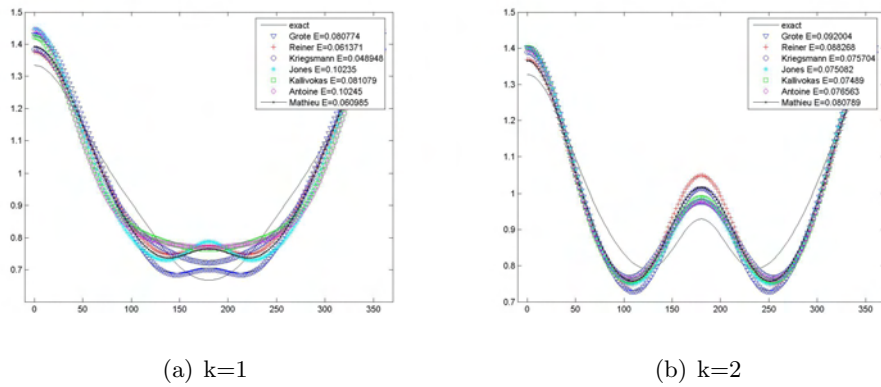


Figure 5.9: OSRC Dirichlet bc,  $k = 1, 2$ ,  $AR=1.1$  and  $\theta = 0^\circ$

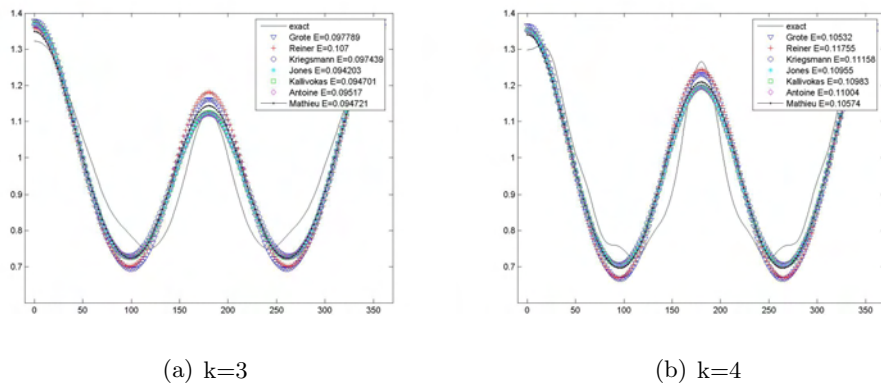


Figure 5.10: OSRC Dirichlet bc,  $k = 3, 4$ ,  $AR=1.1$  and  $\theta = 0^\circ$

(a) Aspect ratio = 10

	$k = 1$	$k = 2$	$k = 3$	$k = 4$
Grote	1.698167	1.682620	1.663030	1.643526
Reiner	0.477691	0.621664	0.684807	0.712769
Kriegsmann	0.871846	0.859938	0.830644	0.800266
Jones	1.663419	1.679475	1.691250	1.701557
Kallivokas	1.049311	1.133602	1.187688	1.231029
Antoine	1.682464	1.660473	1.648922	1.640055
Mathieu	0.073203	0.164564	0.270321	0.417518

(b) Aspect ratio = 3.3

	$k = 1$	$k = 2$	$k = 3$	$k = 4$
Grote	1.625111	1.418146	1.217227	1.037886
Reiner	0.346708	0.437734	0.468637	0.473207
Kriegsmann	0.533451	0.410173	0.354216	0.331366
Jones	1.724184	1.740937	1.724938	1.677681
Kallivokas	1.235455	1.375885	1.427826	1.421557
Antoine	1.657684	1.615694	1.576186	1.524033
Mathieu	0.061860	0.114928	0.164027	0.229203

(c) Aspect ratio = 2

	$k = 1$	$k = 2$	$k = 3$	$k = 4$
Grote	1.118339	0.690395	0.471381	0.346887
Reiner	0.228771	0.282275	0.298277	0.296918
Kriegsmann	0.243895	0.192966	0.190528	0.198767
Jones	1.416620	0.635669	0.320338	0.238883
Kallivokas	0.868737	0.450220	0.280967	0.233479
Antoine	1.447359	0.854357	0.390827	0.262040
Mathieu	0.057951	0.089575	0.113563	0.142629

(d) Aspect ratio = 1.4

	$k = 1$	$k = 2$	$k = 3$	$k = 4$
Grote	0.323988	0.231774	0.171692	0.145721
Reiner	0.131994	0.164993	0.179526	0.183079
Kriegsmann	0.105842	0.107858	0.127070	0.143147
Jones	0.355388	0.154439	0.130277	0.139428
Kallivokas	0.235829	0.143702	0.131366	0.140997
Antoine	0.516761	0.171546	0.137548	0.143342
Mathieu	0.058411	0.080925	0.096793	0.113574

(e) Aspect ratio = 1.1

	$k = 1$	$k = 2$	$k = 3$	$k = 4$
Grote	0.080774	0.092004	0.097789	0.105320
Reiner	0.061371	0.088268	0.107000	0.117554
Kriegsmann	0.048948	0.075704	0.097439	0.111576
Jones	0.102350	0.075082	0.094203	0.109552
Kallivokas	0.081079	0.074890	0.094701	0.109835
Antoine	0.102452	0.076563	0.095170	0.110041
Mathieu	0.060985	0.080789	0.094721	0.105738

Table 5.1: OSRC Dirichlet boundary condition ( $\theta = 0^\circ$ )  $L_2$  error

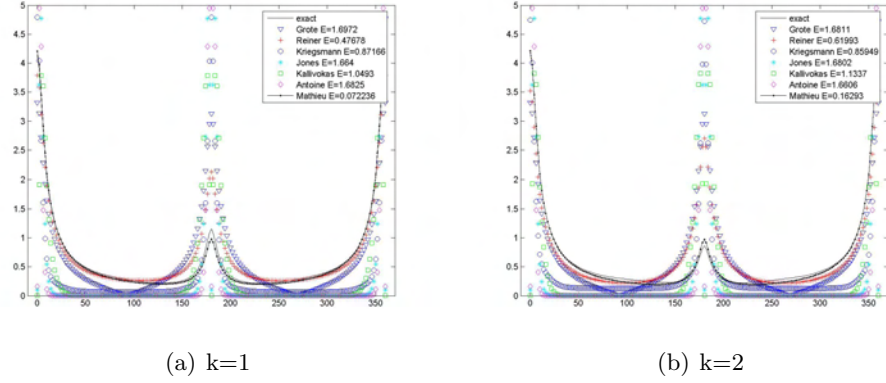
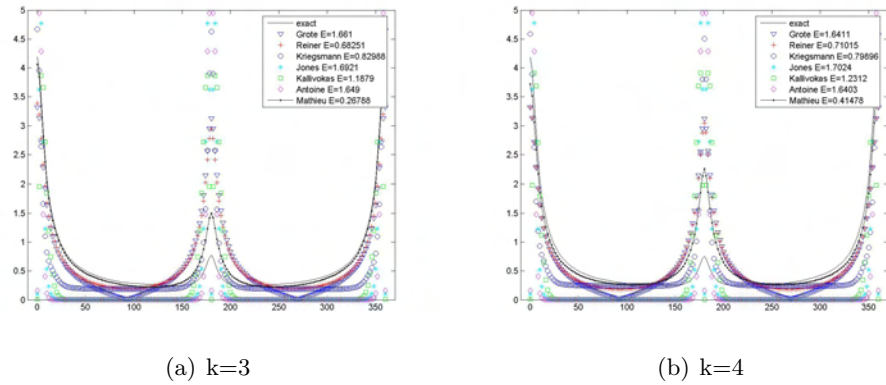
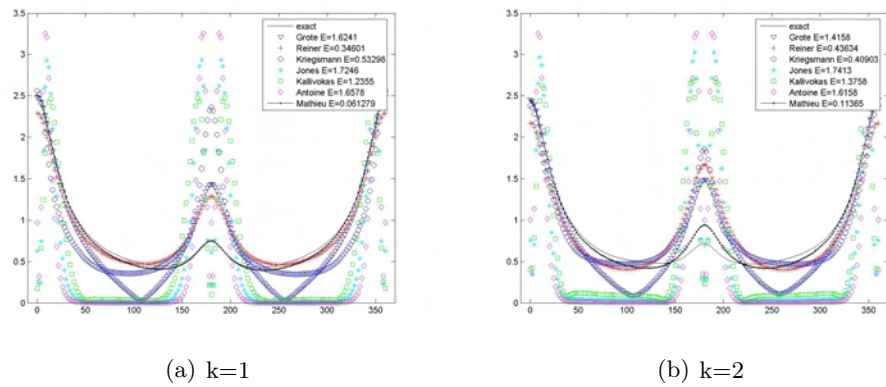
We found that there is no standard method that is consistently superior over the other standard methods. For example, in Figures 5.1 and 5.2 on page 50 ( Table 5.0(a) on page 54) Reiner's method yielded the best results among the standard methods, while in Figures 5.3 and 5.4 on page 51 ( Table 5.0(b) on page 54) Kriegsmann's OSRC is the best for  $k > 1$ . Another example is that the Grote method is the worst in Figure 5.1 , but achieves in Figure 5.10 on page 53 the best result for  $k = 4$ .

Furthermore, we find that the new method, based on Mathieu functions, is significantly better than the other standard methods. This is expected for low and intermediate frequencies, because this corresponds to the results that for lower wave numbers around a circle, the modal expansion in Hankel functions is the best [22]. When the wave number is increasing, mainly for the middle aspect ratio, most standard methods yield better results than for low frequencies. For example, see Figures 5.5 and 5.6 on pages 52, 52 ( Table 5.0(c) on page 54) for Antoine method results. The situation is different for our new method and Reiner's method; when  $k$  is increasing, these approximations consistently depart from the exact solution and become similar to other methods.

We can also learn from these results that when the aspect ratio decreases, then with most standard methods, better results are achieved. For example, see the result of Grote's method for  $AR = 10$  Figures 5.1 and 5.2 on page 50 that becomes increasingly better when the ellipse approaches a circle; see for example Figures 5.7 and 5.8 on page 52 or Figures 5.9 and 5.10 on page 53 .

For an incident angle  $\theta = 5$  similar results are observed. In Figures 5.11 and 5.12 on page 56 we consider  $k = 1, 2, 3, 4$  and an aspect ratio of 10. In Figures 5.13 and 5.14 on page 56 we consider the same wave numbers but with an aspect ratio of 3.3. In Figures 5.15 and 5.16 on page 57 the aspect ratio is 2, in Figures 5.17 and 5.18 on page 58 the aspect ratio 1.4 and in Figures 5.19 and 5.20 on page 58 , it is 1.1 . The  $L_2$  errors can be found in the legend and in Table 5.2 on page 59 .

Observing the Table 5.2 on page 59 one can find improvement in the results from all methods with aspect ratios from 10 to 1.1. Note also that the improvement for increasing wave numbers is similar to the case of an incident angle of 0; take Kallivokas's method in Figures 5.15 and 5.16 on page 57 for example. There is still no consistent superior among the standard methods; note Kriegsmann versus Reiner for the aspect ratio of 1.4 Figures 5.17 and 5.18 on page 58 and 3.3 with  $k > 1$  Figures 5.15 and 5.16 on page 57 . The method based on Mathieu functions is once again superior.

Figure 5.11: OSRC Dirichlet bc,  $k = 1, 2$ , AR=10 and  $\theta = 5^\circ$ Figure 5.12: OSRC Dirichlet bc,  $k = 3, 4$ , AR=10 and  $\theta = 5^\circ$ Figure 5.13: OSRC Dirichlet bc,  $k = 1, 2$ , AR=3.3 and  $\theta = 5^\circ$

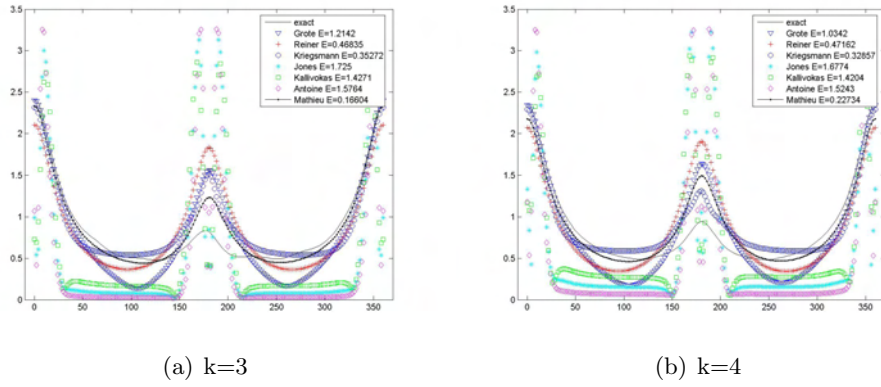


Figure 5.14: OSRC Dirichlet bc,  $k = 3, 4$ , AR=3.3 and  $\theta = 5^\circ$

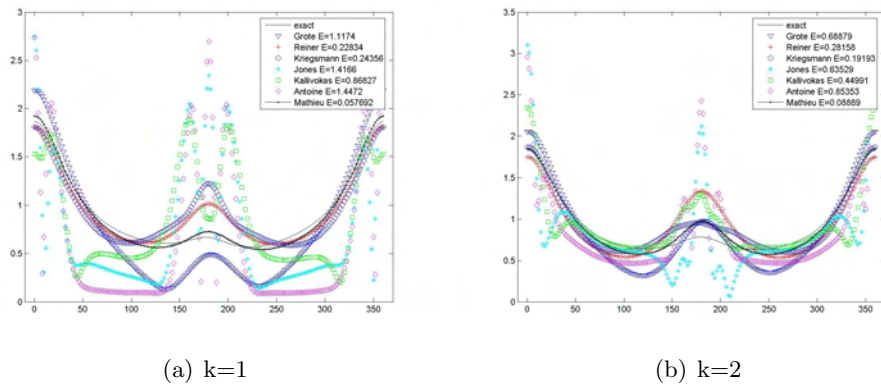


Figure 5.15: OSRC Dirichlet bc,  $k = 1, 2$ , AR=2 and  $\theta = 5^\circ$

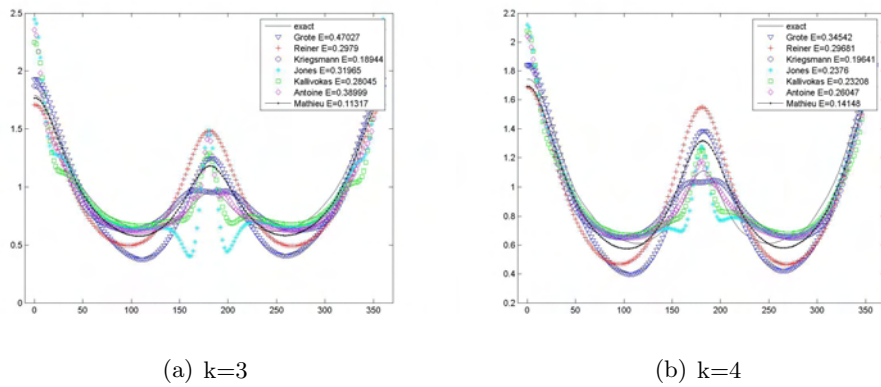
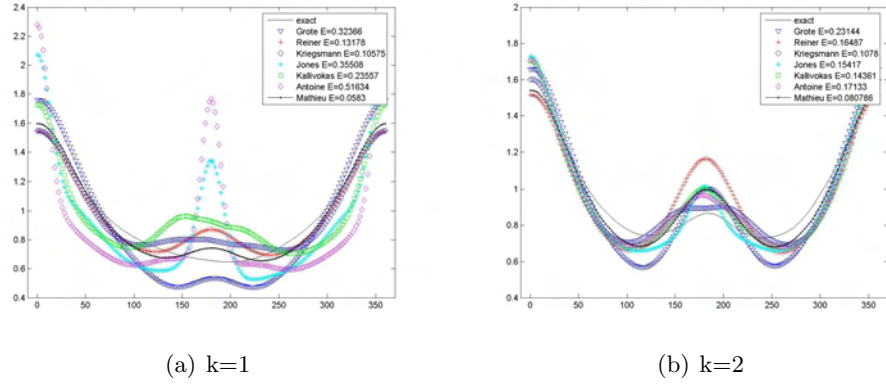
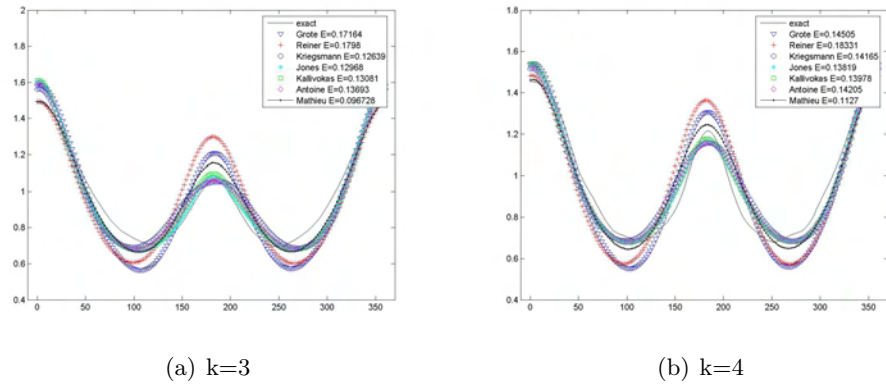
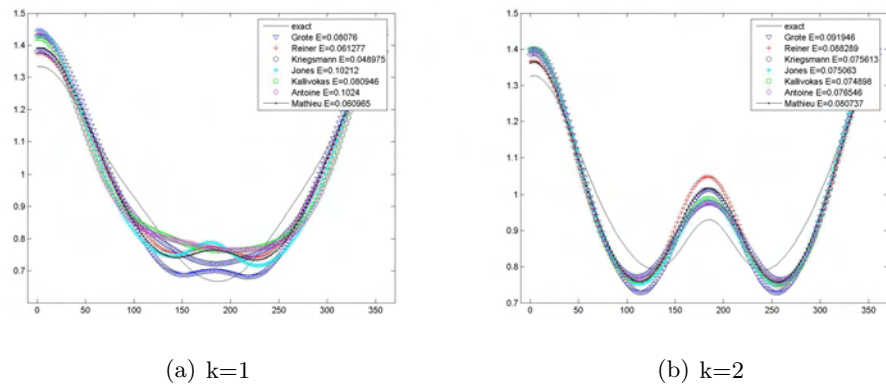


Figure 5.16: OSRC Dirichlet bc,  $k = 3, 4$ , AR=2 and  $\theta = 5^\circ$

Figure 5.17: OSRC Dirichlet bc,  $k = 1, 2$ ,  $AR=1.4$  and  $\theta = 5^\circ$ Figure 5.18: OSRC Dirichlet bc,  $k = 3, 4$ ,  $AR=1.4$  and  $\theta = 5^\circ$ Figure 5.19: OSRC Dirichlet bc,  $k = 1, 2$ ,  $AR=1.1$  and  $\theta = 5^\circ$

(a) Aspect ratio = 10

	$k = 1$	$k = 2$	$k = 3$	$k = 4$
Grote	1.697209	1.681055	1.660974	1.641059
Reiner	0.476777	0.619929	0.682511	0.710153
Kriegsmann	0.871659	0.859494	0.829879	0.798958
Jones	1.663996	1.680240	1.692110	1.702447
Kallivokas	1.049335	1.133721	1.187891	1.231155
Antoine	1.682520	1.660554	1.649023	1.640290
Mathieu	0.072236	0.162932	0.267880	0.414783

(b) Aspect ratio = 3.3

	$k = 1$	$k = 2$	$k = 3$	$k = 4$
Grote	1.624136	1.415842	1.214211	1.034188
Reiner	0.346009	0.436344	0.468350	0.471617
Kriegsmann	0.532979	0.409034	0.352717	0.328566
Jones	1.724585	1.741294	1.724998	1.677418
Kallivokas	1.235542	1.375849	1.427071	1.420351
Antoine	1.657765	1.615836	1.576444	1.524254
Mathieu	0.061279	0.113654	0.166036	0.227337

(c) Aspect ratio = 2

	$k = 1$	$k = 2$	$k = 3$	$k = 4$
Grote	1.117424	0.688787	0.470269	0.345422
Reiner	0.228344	0.281582	0.297896	0.296812
Kriegsmann	0.243565	0.191926	0.189439	0.196409
Jones	1.416575	0.635285	0.319649	0.237599
Kallivokas	0.868273	0.449911	0.280453	0.232078
Antoine	1.447234	0.853531	0.389988	0.260473
Mathieu	0.057692	0.088890	0.113169	0.141481

(d) Aspect ratio = 1.4

	$k = 1$	$k = 2$	$k = 3$	$k = 4$
Grote	0.323662	0.231437	0.171638	0.145046
Reiner	0.131779	0.164875	0.179795	0.183308
Kriegsmann	0.105746	0.107805	0.126390	0.141648
Jones	0.355084	0.154171	0.129682	0.138190
Kallivokas	0.235568	0.143613	0.130812	0.139777
Antoine	0.516343	0.171332	0.136929	0.142046
Mathieu	0.058300	0.080786	0.096728	0.112699

(e) Aspect ratio = 1.1

	$k = 1$	$k = 2$	$k = 3$	$k = 4$
Grote	0.080760	0.091946	0.097762	0.105115
Reiner	0.061277	0.088289	0.107099	0.117618
Kriegsmann	0.048975	0.075613	0.097248	0.111198
Jones	0.102116	0.075063	0.094061	0.109211
Kallivokas	0.080946	0.074898	0.094559	0.109493
Antoine	0.102402	0.076546	0.095018	0.109694
Mathieu	0.060965	0.080737	0.094683	0.105527

Table 5.2: OSRC Dirichlet boundary condition ( $\theta = 5^\circ$ )  $L_2$  error

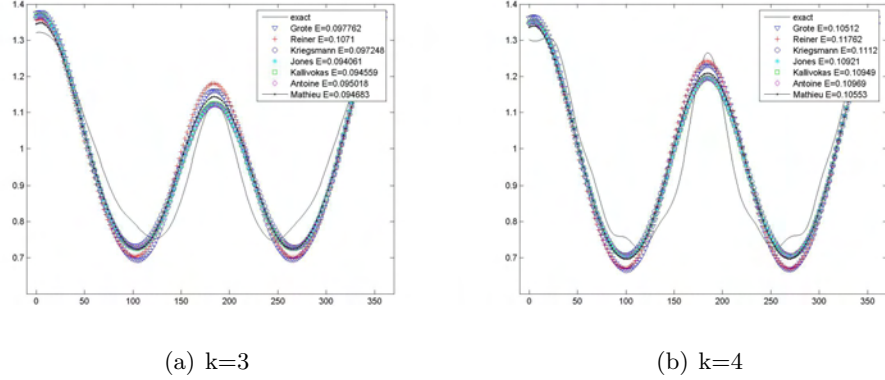


Figure 5.20: OSRC Dirichlet bc,  $k = 3, 4$ , AR=1.1 and  $\theta = 5^\circ$

### 5.1.2 Neumann Condition

We continue with the Neumann problem, once again starting from an incident angle  $\theta = 0$ . In Figures 5.21 and 5.22 on page 61 the same methods are compared with the exact solution for wave numbers  $k = 0.5, 1, 2, 4$  and an aspect ratio of 3.3. The  $L_2$  error between the approximate solutions and the exact solution is again in the legend and in the table Table 5.3 on page 64. In Figures 5.23 and 5.24 on page 61 we consider the same  $k$ 's but an aspect ratio 2, in Figures 5.25 and 5.26 on page 62 the aspect ratio is 1.4 and in Figures 5.27 and 5.28 on page 63 the aspect ratio is 1.1.

One can see the improvement with decreasing aspect ratio; see Kallivokas's method, for example, from Figure 5.21 on page 61 to Figure 5.28 on page 63. But now the results with the high aspect ratio are much worse, and this is the reason why an aspect ratio of 10 is not presented here.

The situation with increasing wave numbers is not consistent in the case of the Neumann condition. For example, the Jones and Grote methods become better for increasing wave numbers in Figures 5.25 and 5.26 on page 62, but both become worse for increasing  $k$  with aspect ratio 1.1 [see Figures 5.27 and 5.28 on page 63].

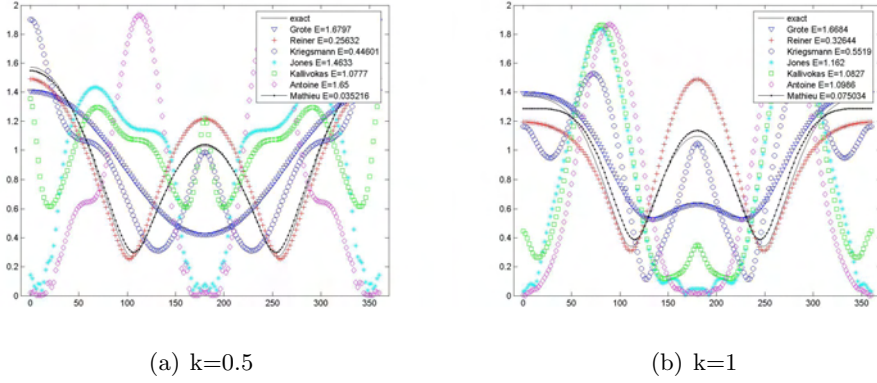


Figure 5.21: OSRC Neumann bc  $k = 0.5, 1$ ,  $AR=3.3$  and  $\theta = 0^\circ$

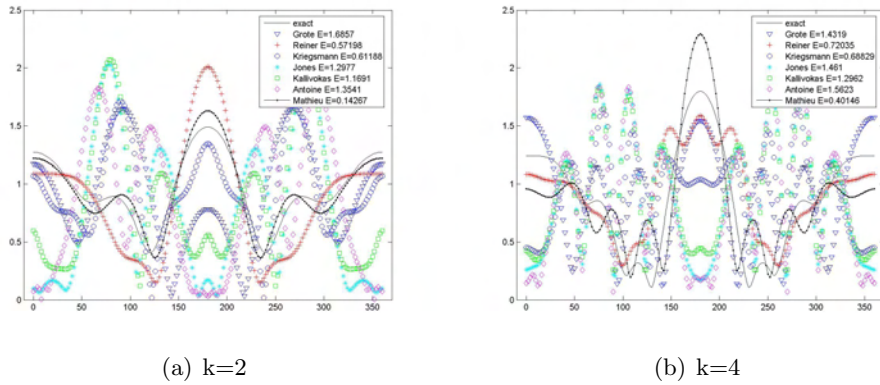


Figure 5.22: OSRC Neumann bc  $k = 2, 4$ ,  $AR=3.3$  and  $\theta = 0^\circ$

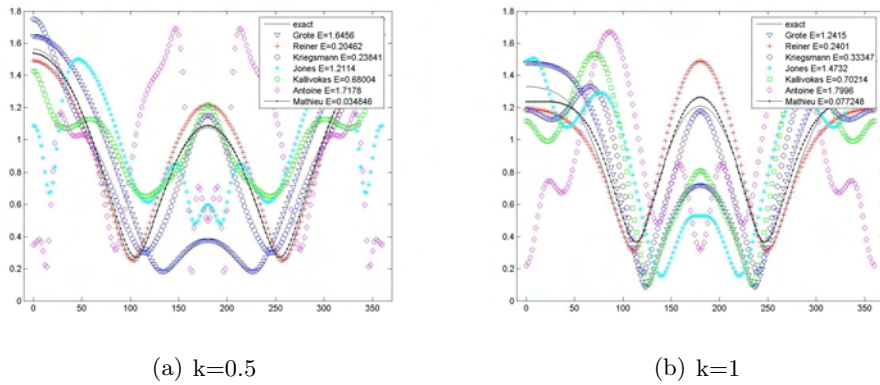
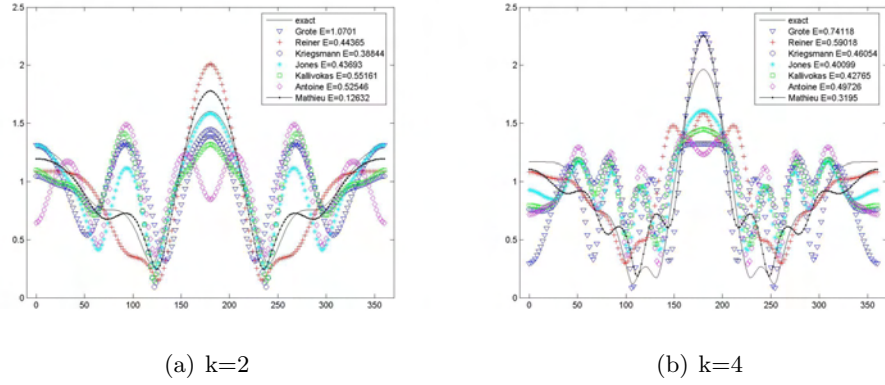
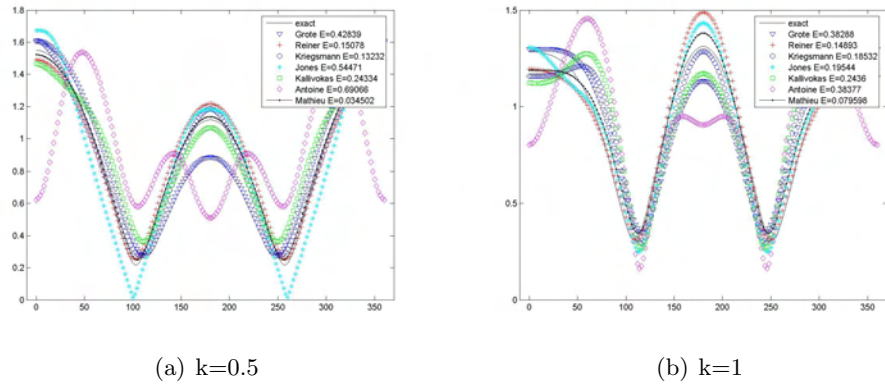
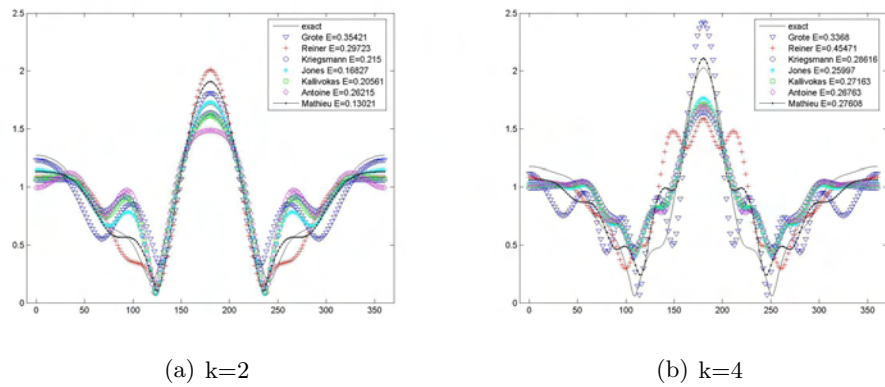


Figure 5.23: OSRC Neumann bc  $k = 0.5, 1$ ,  $AR=2$  and  $\theta = 0^\circ$

Figure 5.24: OSRC Neumann bc  $k = 2, 4$ ,  $AR=2$  and  $\theta = 0^\circ$ Figure 5.25: OSRC Neumann bc  $k = 0.5, 1$ ,  $AR=1.4$  and  $\theta = 0^\circ$ Figure 5.26: OSRC Neumann bc  $k = 2, 4$ ,  $AR=1.4$  and  $\theta = 0^\circ$

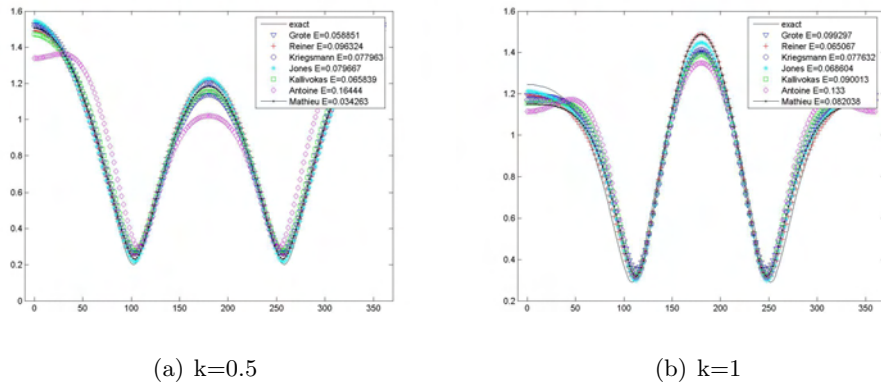


Figure 5.27: OSRC Neumann bc  $k = 0.5, 1$ ,  $AR=1.1$  and  $\theta = 0^\circ$

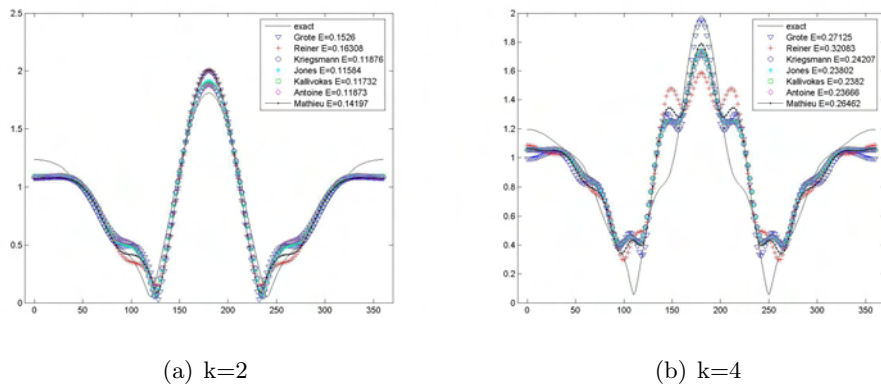


Figure 5.28: OSRC Neumann bc  $k = 2, 4$ ,  $AR=1.1$  and  $\theta = 0^\circ$

(a) Aspect ratio = 3.3

	$k = 0.5$	$k = 1$	$k = 2$	$k = 4$
Grote	1.679674	1.668416	1.685739	1.431850
Reiner	0.256319	0.326444	0.571977	0.720348
Kriegsmann	0.446008	0.551897	0.611881	0.688292
Jones	1.463312	1.162046	1.297723	1.460995
Kallivokas	1.077718	1.082665	1.169074	1.296184
Antoine	1.649973	1.098637	1.354081	1.562304
Mathieu	0.035216	0.075034	0.142668	0.401460

(b) Aspect ratio = 2

	$k = 0.5$	$k = 1$	$k = 2$	$k = 4$
Grote	1.645635	1.241495	1.070095	0.741185
Reiner	0.204618	0.240101	0.443649	0.590184
Kriegsmann	0.238405	0.333474	0.388437	0.460539
Jones	1.211410	1.473217	0.436932	0.400990
Kallivokas	0.680037	0.702142	0.551608	0.427651
Antoine	1.717771	1.799634	0.525463	0.497256
Mathieu	0.034846	0.077248	0.126324	0.319496

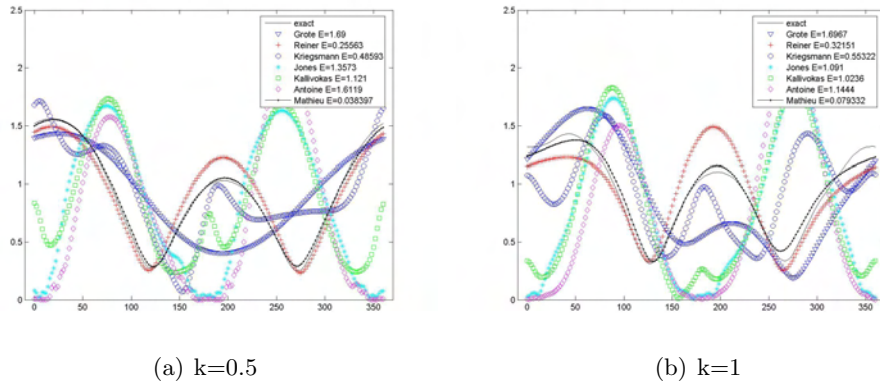
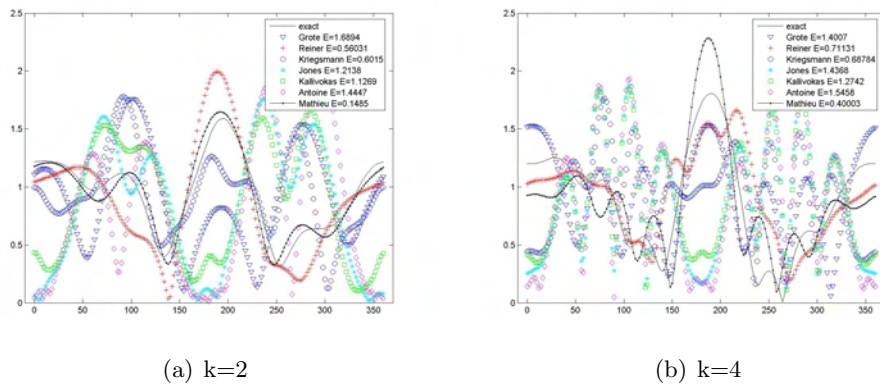
(c) Aspect ratio = 1.4

	$k = 0.5$	$k = 1$	$k = 2$	$k = 4$
Grote	0.428385	0.382879	0.354214	0.336801
Reiner	0.150778	0.148930	0.297230	0.454710
Kriegsmann	0.132319	0.185319	0.215000	0.286164
Jones	0.544712	0.195435	0.168271	0.259969
Kallivokas	0.243344	0.243601	0.205610	0.271627
Antoine	0.690659	0.383769	0.262147	0.267628
Mathieu	0.034502	0.079598	0.130213	0.276079

(d) Aspect ratio = 1.1

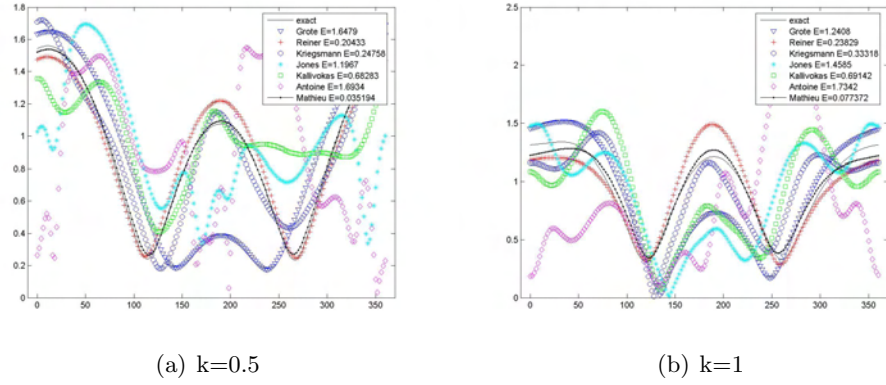
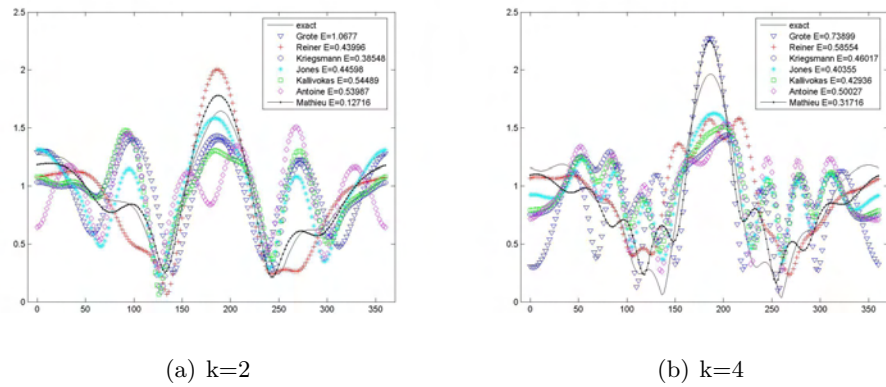
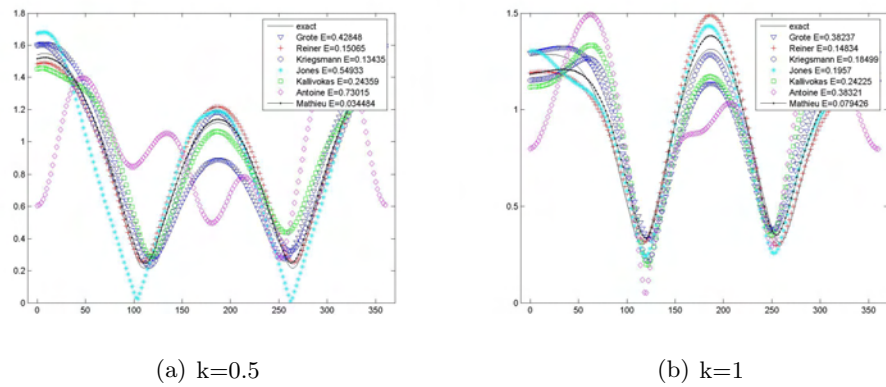
	$k = 0.5$	$k = 1$	$k = 2$	$k = 4$
Grote	0.058851	0.099297	0.152597	0.271251
Reiner	0.096324	0.065067	0.163079	0.320830
Kriegsmann	0.077963	0.077632	0.118763	0.242074
Jones	0.079667	0.068604	0.115839	0.238024
Kallivokas	0.065839	0.090013	0.117317	0.238205
Antoine	0.164443	0.133003	0.118730	0.236663
Mathieu	0.034263	0.082038	0.141973	0.264621

Table 5.3: OSRC Neumann boundary condition ( $\theta = 0^\circ$ )  $L_2$  error

Figure 5.29: OSRC Neumann bc  $k = 0.5, 1$ ,  $AR=3.3$  and  $\theta = 5^\circ$ Figure 5.30: OSRC Neumann bc  $k = 2, 4$ ,  $AR=3.3$  and  $\theta = 5^\circ$ 

Again, when incident angle  $\theta = 5$  is considered, similar results are again observed. In Figures 5.29 and 5.30 on page 65 we consider wave numbers  $k = 0.5, 1, 2, 4$  with aspect ratio 3.3 and in Figures 5.31 and 5.32 on page 66 the same wave numbers but with aspect ratio 1.4; in Figures 5.33 and 5.34 on page 66 the aspect ratio is 1.4 and in Figures 5.35 and 5.36 on page 67 the same  $k$ s using an aspect ratio of 1.1. The  $L_2$  errors is again in the legend and in Table 5.4 on page 68.

The results are worse again for high aspect ratios [see Figures 5.29 and 5.30 on page 65 for aspect ratio 3.3] and improve when the aspect ratio is decreased [see Figures 5.33 and 5.34 on page 66]. We note again the inconsistency of behavior for changes in wave number [see Jones method in Figures 5.29 and 5.30 on page 65 (aspect ratio 3.3) and Figures 5.33 and 5.34 on page 66 (aspect ratio 1.4)]. The new method is still superior there.

Figure 5.31: OSRC Neumann bc  $k = 0.5, 1$ ,  $AR=2$  and  $\theta = 5^\circ$ Figure 5.32: OSRC Neumann bc  $k = 2, 4$ ,  $AR=2$  and  $\theta = 5^\circ$ Figure 5.33: OSRC Neumann bc  $k = 0.5, 1$ ,  $AR=1.4$  and  $\theta = 5^\circ$

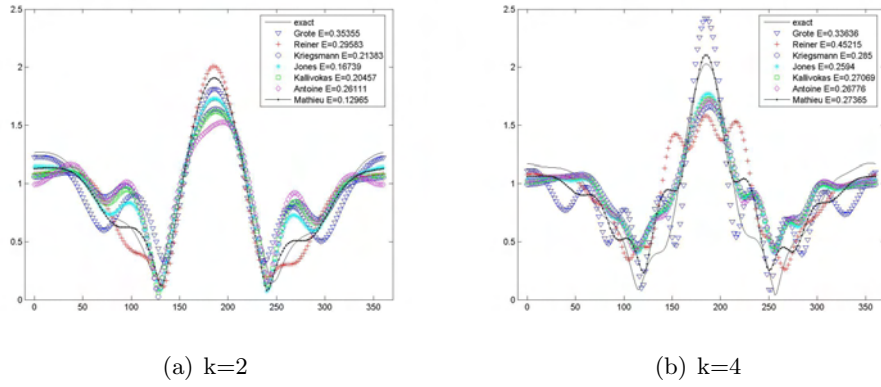


Figure 5.34: OSRC Neumann bc  $k = 2, 4$ ,  $AR=1.4$  and  $\theta = 5^\circ$

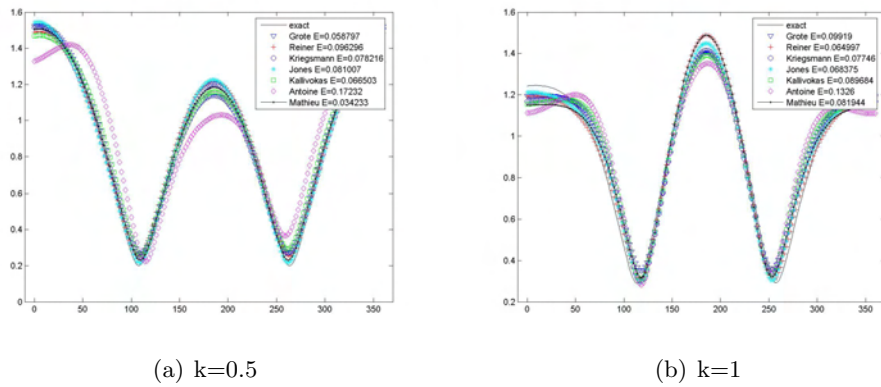


Figure 5.35: OSRC Neumann bc  $k = 0.5, 1$ ,  $AR=1.1$  and  $\theta = 5^\circ$

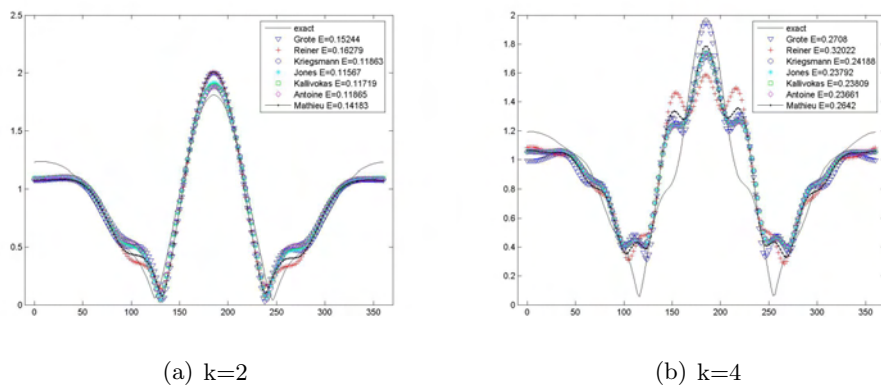


Figure 5.36: OSRC Neumann bc  $k = 2, 4$ ,  $AR=1.1$  and  $\theta = 5^\circ$

(a) Aspect ratio = 3.3

	$k = 0.5$	$k = 1$	$k = 2$	$k = 4$
Grote	1.689982	1.696687	1.689380	1.400735
Reiner	0.255631	0.321508	0.560313	0.711307
Kriegsmann	0.485934	0.553221	0.601497	0.687845
Jones	1.357314	1.091030	1.213791	1.436839
Kallivokas	1.121044	1.023555	1.126920	1.274206
Antoine	1.611918	1.144413	1.444736	1.545802
Mathieu	0.038397	0.079332	0.148502	0.400030

(b) Aspect ratio = 2

	$k = 0.5$	$k = 1$	$k = 2$	$k = 4$
Grote	1.647913	1.240791	1.067731	0.738991
Reiner	0.204326	0.238295	0.439958	0.585539
Kriegsmann	0.247582	0.333181	0.385482	0.460173
Jones	1.196725	1.458536	0.445982	0.403548
Kallivokas	0.682831	0.691423	0.544894	0.429358
Antoine	1.693432	1.734234	0.539865	0.500273
Mathieu	0.035194	0.077372	0.127163	0.317161

(c) Aspect ratio = 1.4

	$k = 0.5$	$k = 1$	$k = 2$	$k = 4$
Grote	0.428483	0.382369	0.353545	0.336355
Reiner	0.150650	0.148337	0.295833	0.452151
Kriegsmann	0.134345	0.184993	0.213831	0.284995
Jones	0.549332	0.195701	0.167390	0.259404
Kallivokas	0.243586	0.242249	0.204569	0.270691
Antoine	0.730155	0.383206	0.261114	0.267760
Mathieu	0.034484	0.079426	0.129645	0.273647

(d) Aspect ratio = 1.1

	$k = 0.5$	$k = 1$	$k = 2$	$k = 4$
Grote	0.058797	0.099190	0.152444	0.270802
Reiner	0.096296	0.064997	0.162788	0.320225
Kriegsmann	0.078216	0.077460	0.118627	0.241878
Jones	0.081007	0.068375	0.115674	0.237922
Kallivokas	0.066503	0.089684	0.117187	0.238086
Antoine	0.172322	0.132598	0.118651	0.236614
Mathieu	0.034233	0.081944	0.141827	0.264203

Table 5.4: OSRC Neumann boundary condition ( $\theta = 5^\circ$ )  $L_2$  error

At the end of this subsection, we once again draw attention to the fact that for the high aspect ratio and low frequencies the new method based on Mathieu functions is clearly and significantly better than the standard methods for OSRC with Neumann conditions. But it is worth noting that as the ellipse becomes more circular for large wave numbers we can observe that some standard methods overtake the new one [see Jones's method in Figures 5.25 and 5.26 on page 62 ], which did not happen with the Dirichlet condition.

## 5.2 Absorbing Boundary Condition

In this section we consider the same absorbing boundary conditions but exterior to the ellipse. Both the scatterer and the outer artificial surface are concentric ellipses. As before, the next two subsections present the results for both Dirichlet and Neumann conditions on an elliptical scatterer.

### 5.2.1 Dirichlet condition

We begin with a Dirichlet boundary condition and incident angle  $\theta = 0$ . We also check the dependence of these ABCs on the place of the truncation of infinity, that is on the distance between the artificial ellipse and the scatterer. The exterior ellipse is defined by its major axis  $a_{ext}$ . As was explained in Section 1.1, to define the ellipse we need a pair from the set  $a, b, f, c$ ; we have the focal distance of the scatterer, thus we use  $(a_{ext}, f)$ .

In Figures 5.37 and 5.38 on page 70 we compare the methods described in Chapter 2 with the exact solution for various values of the wave number ( $k = 0.5, 1, 2, 4$ ), an aspect ratio of 10 and an artificial boundary defined by  $a_{ext} = 1.1$ . The  $L_2$  error between the approximate solutions exterior to the ellipse and the exact normal derivative is given in the legend. The errors for  $a_{ext} = 1.1$  are also given in Table 5.5 on page 72. In Figures 5.39 and 5.40 on page 71 we consider the same  $ks$  and  $a_{ext}$  but using aspect ratio 2 and in Figures 5.41 and 5.42 on page 71 the aspect ratio is 1.4.

In Figures 5.43 and 5.44 on page 73 we consider  $a_{ext} = 1.5$  with the same wave numbers and an aspect ratio of 10 while in Figures 5.45 and 5.46 on page 74 the aspect ratio is 2 and Figures 5.47 and 5.48 on page 74 the aspect ratio is 1.4. The error is given in Table 5.6 on page 75 and in the legend.

In Figures 5.49 and 5.50 on page 76 we consider  $a_{ext} = 2$  with the same wave numbers and an aspect ratio of 10, in Figures 5.51 and 5.52 on page 76 the aspect

ratio is 2 and in Figures 5.53 and 5.54 on page 77 the aspect ratio is 1.4. The error is given in the legend and in Table 5.7 on page 78 for  $a_{ext} = 2$ .

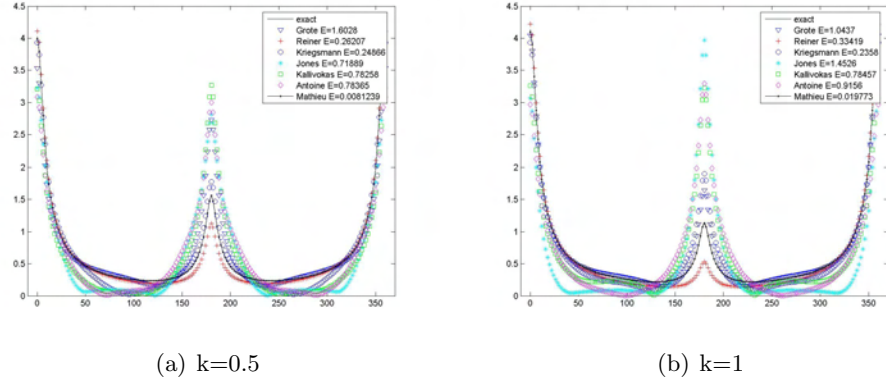


Figure 5.37: ABC Dirichlet bc,  $a_{ext} = 1.1$   $k = 0.5, 1$ , AR=10 and  $\theta = 0^\circ$

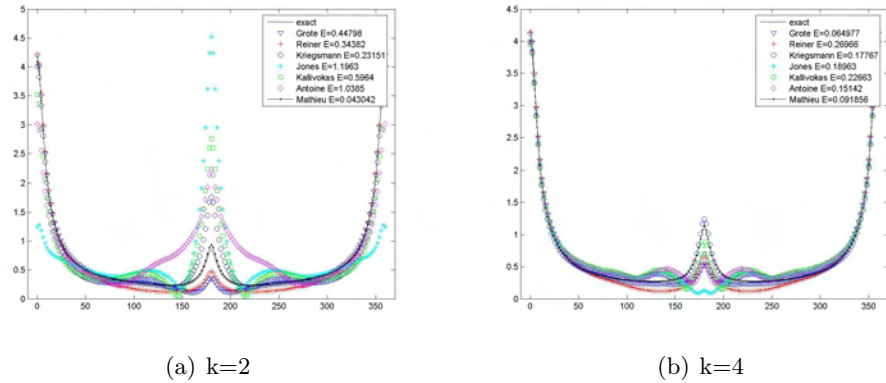


Figure 5.38: ABC Dirichlet bc,  $a_{ext} = 1.1$   $k = 2, 4$ , AR=10 and  $\theta = 0^\circ$

One can see that when the artificial ellipse is far away from the scatterer the approximations become closer to an exact solution, this also explains the poor results that were observed for some methods with an OSRC. This is extremely noticeable for Grote's method, which was in most cases the worst for an OSRC but became superior over standard methods when the artificial ellipse was defined by  $a_{ext} = 2$  and the corresponding focal distance.

By moving the position of the artificial surface the best results, amongst those presented here, are observed for  $a_{ext} = 2$ , but the general behavior is independent of the artificial surface placement. Thus there is again improvement with a decreasing aspect ratio [for example, see Kriegsmann's method from Figure 5.37 on page 70 to Figure 5.42 on page 72 or from Figure 5.49 on page 76 to Figure 5.54 on page 77].

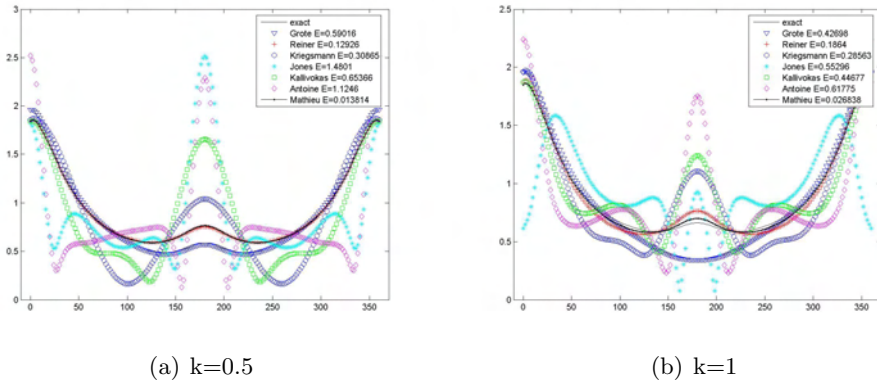


Figure 5.39: ABC Dirichlet bc,  $a_{ext} = 1.1$   $k = 0.5, 1$ , AR=2 and  $\theta = 0^\circ$

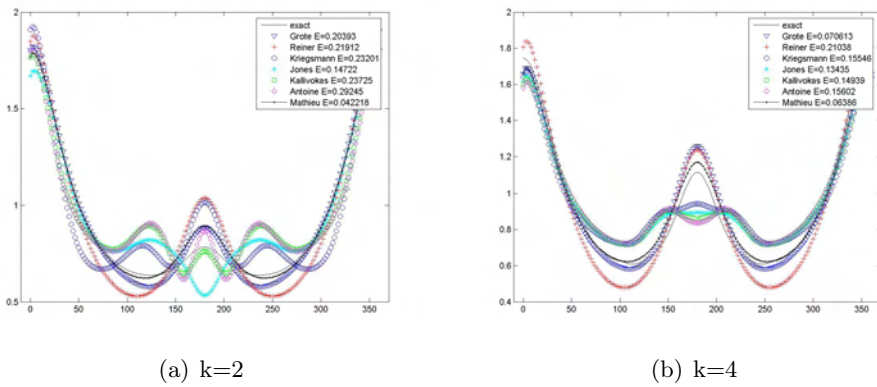


Figure 5.40: ABC Dirichlet bc,  $a_{ext} = 1.1$   $k = 2, 4$ , AR=2 and  $\theta = 0^\circ$

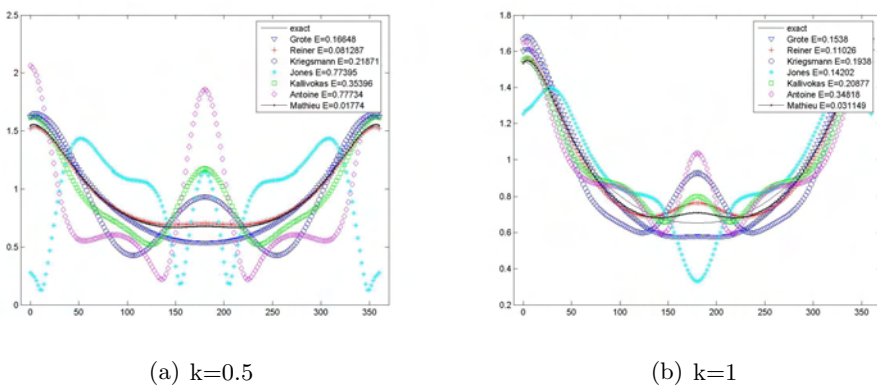
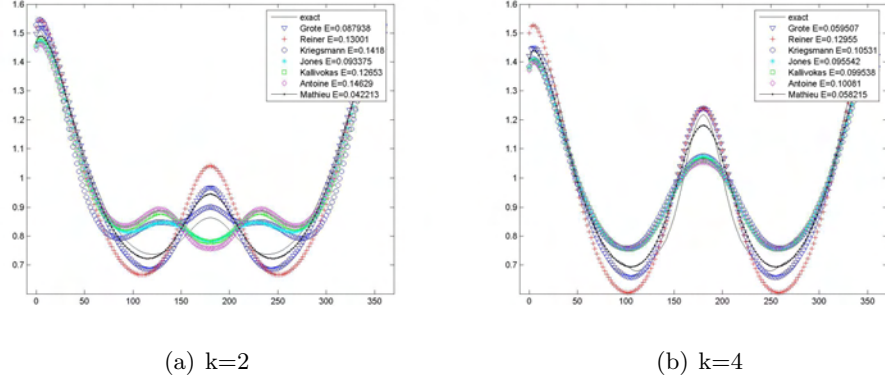


Figure 5.41: ABC Dirichlet bc,  $a_{ext} = 1.1$   $k = 0.5, 1$ , AR=1.4 and  $\theta = 0^\circ$

Figure 5.42: ABC Dirichlet bc,  $a_{ext} = 1.1$   $k = 2, 4$ ,  $AR=1.4$  and  $\theta = 0^\circ$ 

(a) Aspect ratio = 10

	$k = 0.5$	$k = 1$	$k = 2$	$k = 4$
Grote	1.602766	1.043694	0.447977	0.064977
Reiner	0.262065	0.334186	0.343818	0.269657
Kriegsmann	0.248657	0.235803	0.231507	0.177675
Jones	0.718894	1.452600	1.196275	0.189632
Kallivokas	0.782580	0.784567	0.596403	0.226631
Antoine	0.783649	0.915603	1.038527	0.151423
Mathieu	0.008124	0.019773	0.043042	0.091856

(b) Aspect ratio = 2

	$k = 0.5$	$k = 1$	$k = 2$	$k = 4$
Grote	0.590158	0.426978	0.203929	0.070613
Reiner	0.129262	0.186399	0.219118	0.210384
Kriegsmann	0.308651	0.285626	0.232009	0.155462
Jones	1.480104	0.552963	0.147219	0.134352
Kallivokas	0.653657	0.446765	0.237245	0.149388
Antoine	1.124634	0.617750	0.292450	0.156024
Mathieu	0.013814	0.026838	0.042218	0.063860

(c) Aspect ratio = 1.4

	$k = 0.5$	$k = 1$	$k = 2$	$k = 4$
Grote	0.166482	0.153803	0.087938	0.059507
Reiner	0.081287	0.110260	0.130011	0.129553
Kriegsmann	0.218715	0.193799	0.141799	0.105311
Jones	0.773949	0.142019	0.093375	0.095542
Kallivokas	0.353962	0.208765	0.126528	0.099538
Antoine	0.777344	0.348181	0.146288	0.100812
Mathieu	0.017740	0.031149	0.042213	0.058215

Table 5.5: ABC Dirichlet boundary condition ( $\theta = 0^\circ$ ,  $a_{ext} = 1.1$ )  $L_2$  error

Increasing the wave number is accompanied by consistent improvement of results for all methods [see the Jones's method in Figures 5.51 and 5.52 on page 76 , for example].

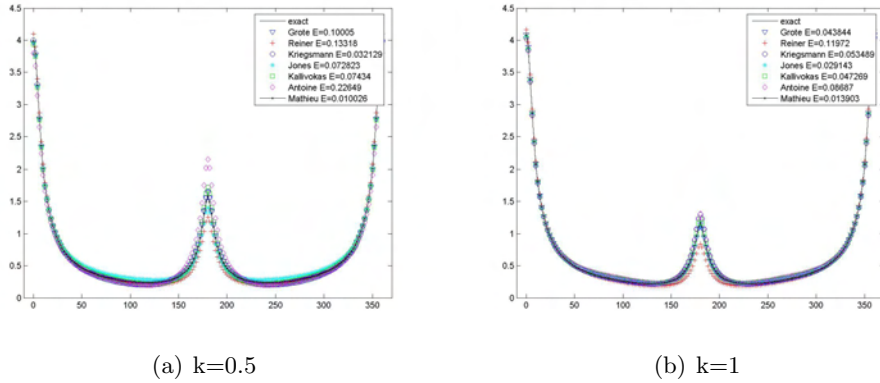


Figure 5.43: ABC Dirichlet bc,  $a_{ext} = 1.5$   $k = 0.5, 1$ , AR=10 and  $\theta = 0^\circ$

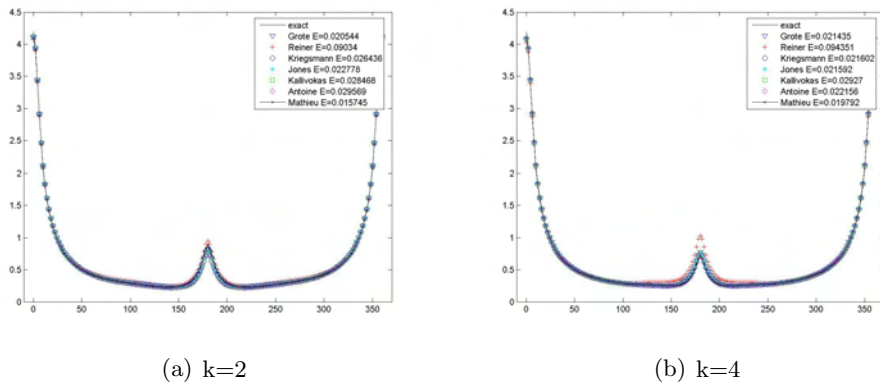
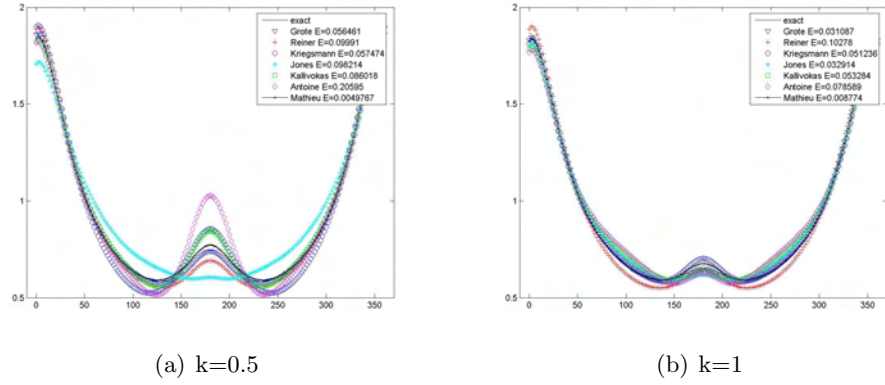
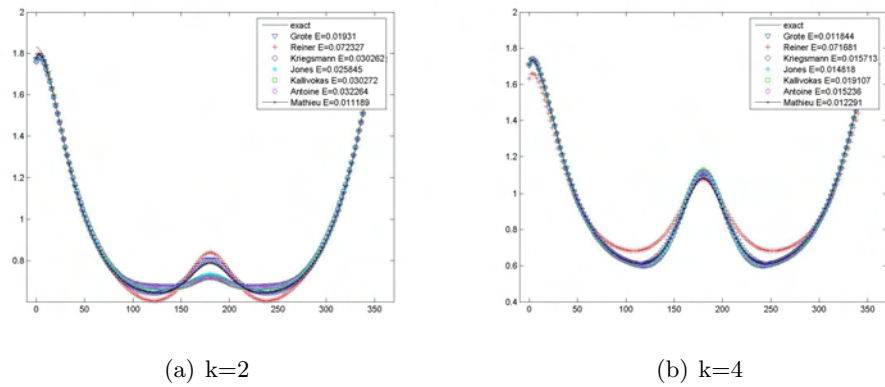
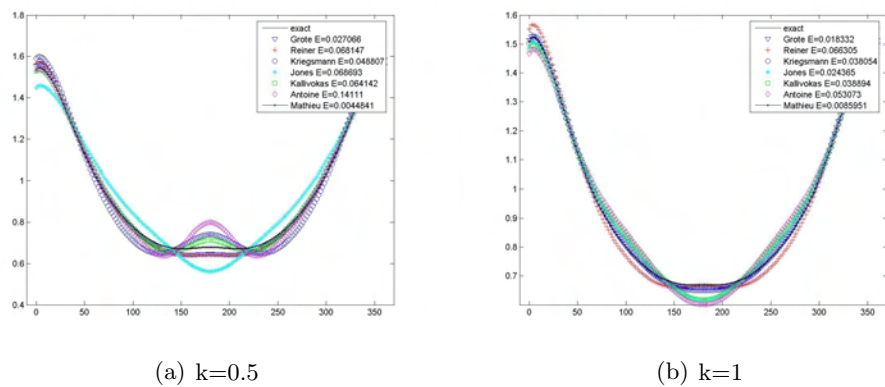
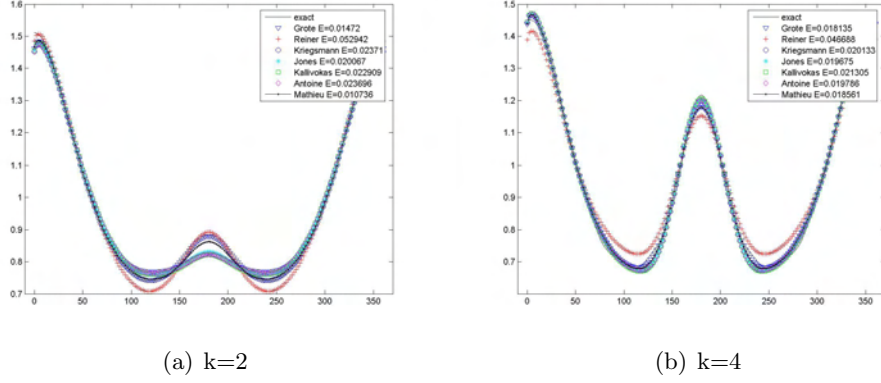


Figure 5.44: ABC Dirichlet bc,  $a_{ext} = 1.5$   $k = 2, 4$ , AR=10 and  $\theta = 0^\circ$

There is still no superior ABC between the standard methods. For  $a_{ext} = 1.1$  Kriegsmann's method is best for aspect ratio 10 and  $k < 4$  and Antoine's method is the best for  $k = 4$ , while Reinter's method is best for aspect ratio of 2 for  $k = 0.5, 1$  and Jones's method is the best for  $k = 2, 4$ . For  $a_{ext} = 1.5$  Kriegsmann's method is best for aspect ratio 10 for  $k = 0.5$  and Grote's method is superior for the remaining frequencies and for aspect ratio of 2. Similarly, with  $a_{ext} = 2$  we could not find a superior ABC among standard methods. We note that the new method is clearly superior.

The same situation is observed when the incident angle is  $\theta = 5$ . In Figures 5.55 and 5.56 on page 79 we compare the methods described in Chapter 2 with

Figure 5.45: ABC Dirichlet bc,  $a_{ext} = 1.5$   $k = 0.5, 1$ , AR=2 and  $\theta = 0^\circ$ Figure 5.46: ABC Dirichlet bc,  $a_{ext} = 1.5$   $k = 2, 4$ , AR=2 and  $\theta = 0^\circ$ Figure 5.47: ABC Dirichlet bc,  $a_{ext} = 1.5$   $k = 0.5, 1$ , AR=1.4 and  $\theta = 0^\circ$

Figure 5.48: ABC Dirichlet bc,  $a_{ext} = 1.5$   $k = 2, 4$ , AR=1.4 and  $\theta = 0^\circ$ 

(a) Aspect ratio = 10

	$k = 0.5$	$k = 1$	$k = 2$	$k = 4$
Grote	0.100053	0.043844	0.020544	0.021435
Reiner	0.133182	0.119718	0.090340	0.094351
Kriegsmann	0.032129	0.053489	0.026436	0.021602
Jones	0.072823	0.029143	0.022778	0.021592
Kallivokas	0.074340	0.047269	0.028468	0.029270
Antoine	0.226489	0.086870	0.029569	0.022156
Mathieu	0.010026	0.013903	0.015745	0.019792

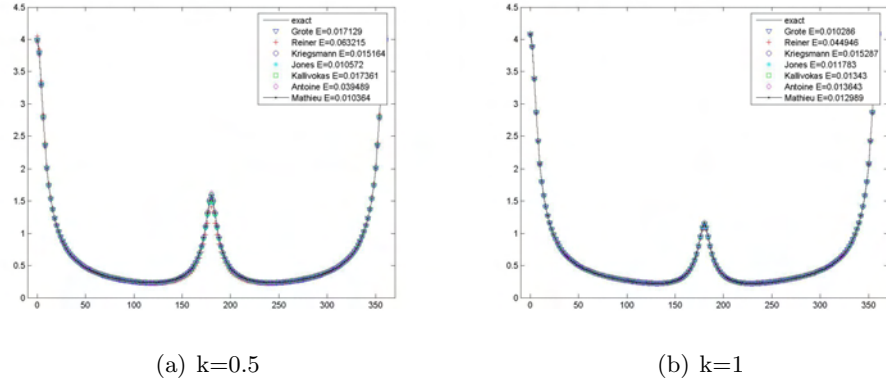
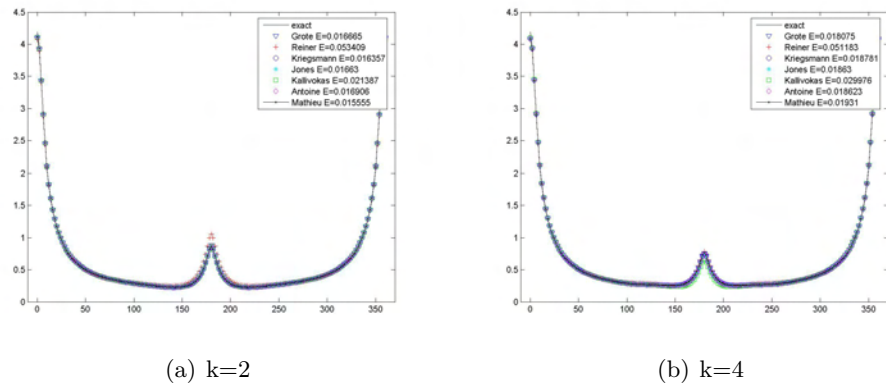
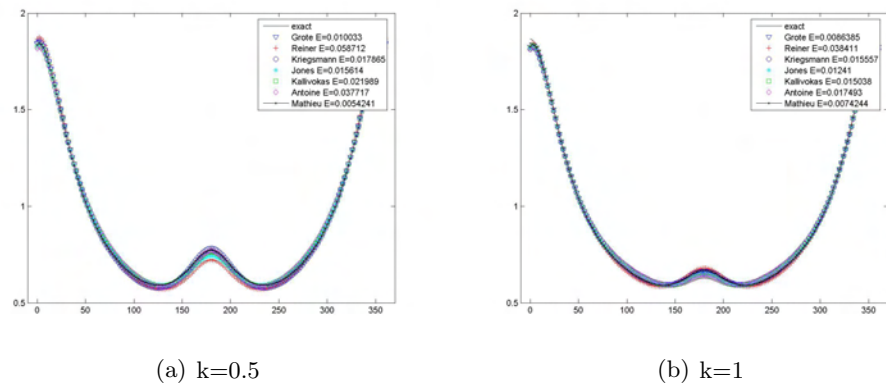
(b) Aspect ratio = 2

	$k = 0.5$	$k = 1$	$k = 2$	$k = 4$
Grote	0.056461	0.031087	0.019310	0.011844
Reiner	0.099910	0.102782	0.072327	0.071681
Kriegsmann	0.057474	0.051236	0.030262	0.015713
Jones	0.098214	0.032914	0.025845	0.014818
Kallivokas	0.086018	0.053284	0.030272	0.019107
Antoine	0.205954	0.078589	0.032264	0.015236
Mathieu	0.004977	0.008774	0.011189	0.012291

(c) Aspect ratio = 1.4

	$k = 0.5$	$k = 1$	$k = 2$	$k = 4$
Grote	0.027066	0.018332	0.014720	0.018135
Reiner	0.068147	0.066305	0.052942	0.046688
Kriegsmann	0.048807	0.038054	0.023710	0.020133
Jones	0.068693	0.024365	0.020067	0.019675
Kallivokas	0.064142	0.038894	0.022909	0.021305
Antoine	0.141115	0.053073	0.023696	0.019786
Mathieu	0.004484	0.008595	0.010736	0.018561

Table 5.6: ABC Dirichlet boundary condition ( $\theta = 0^\circ$ ,  $a_{ext} = 1.5$ )  $L_2$  error

Figure 5.49: ABC Dirichlet bc,  $a_{ext} = 2$   $k = 0.5, 1$ , AR=10 and  $\theta = 0^\circ$ Figure 5.50: ABC Dirichlet bc,  $a_{ext} = 2$   $k = 2, 4$ , AR=10 and  $\theta = 0^\circ$ Figure 5.51: ABC Dirichlet bc,  $a_{ext} = 2$   $k = 0.5, 1$ , AR=2 and  $\theta = 0^\circ$

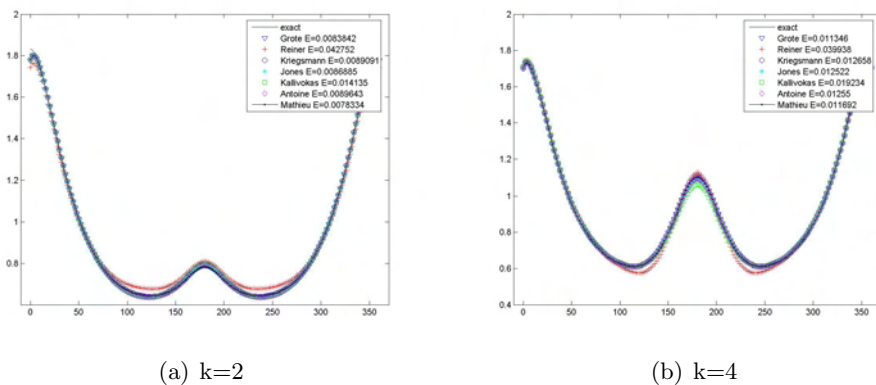


Figure 5.52: ABC Dirichlet bc,  $a_{ext} = 2$   $k = 2, 4$ , AR=2 and  $\theta = 0^\circ$

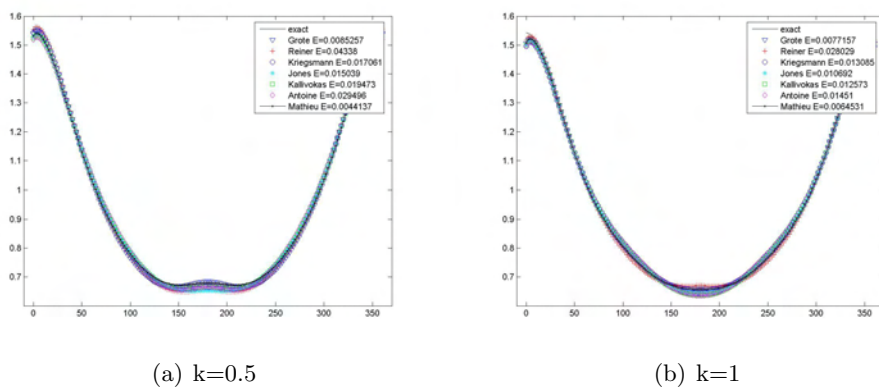


Figure 5.53: ABC Dirichlet bc,  $a_{ext} = 2$   $k = 0.5, 1$ , AR=1.4 and  $\theta = 0^\circ$

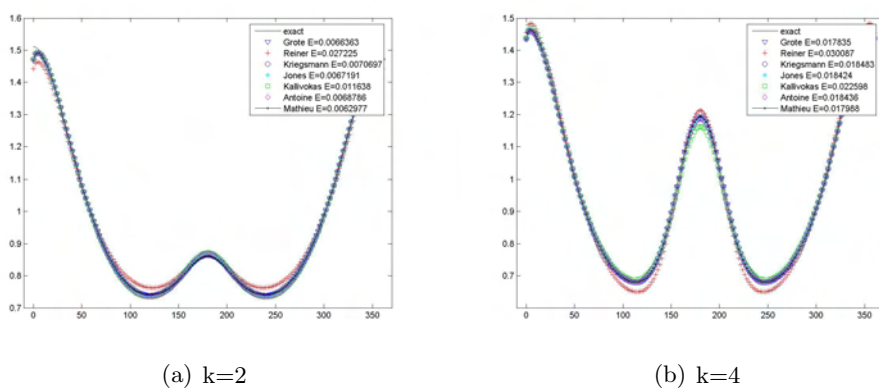


Figure 5.54: ABC Dirichlet bc,  $a_{ext} = 2$   $k = 2, 4$ , AR=1.4 and  $\theta = 0^\circ$

(a) Aspect ratio = 10

	$k = 0.5$	$k = 1$	$k = 2$	$k = 4$
Grote	0.017129	0.010286	0.016665	0.018075
Reiner	0.063215	0.044946	0.053409	0.051183
Kriegsmann	0.015164	0.015287	0.016357	0.018781
Jones	0.010572	0.011783	0.016630	0.018630
Kallivokas	0.017361	0.013430	0.021387	0.029976
Antoine	0.039489	0.013643	0.016906	0.018623
Mathieu	0.010364	0.012989	0.015555	0.019310

(b) Aspect ratio = 2

	$k = 0.5$	$k = 1$	$k = 2$	$k = 4$
Grote	0.010033	0.008638	0.008384	0.011346
Reiner	0.058712	0.038411	0.042752	0.039938
Kriegsmann	0.017865	0.015557	0.008909	0.012658
Jones	0.015614	0.012410	0.008688	0.012522
Kallivokas	0.021989	0.015038	0.014135	0.019234
Antoine	0.037717	0.017493	0.008964	0.012550
Mathieu	0.005424	0.007424	0.007833	0.011692

(c) Aspect ratio = 1.4

	$k = 0.5$	$k = 1$	$k = 2$	$k = 4$
Grote	0.008526	0.007716	0.006636	0.017835
Reiner	0.043380	0.028029	0.027225	0.030087
Kriegsmann	0.017061	0.013085	0.007070	0.018483
Jones	0.015039	0.010692	0.006719	0.018424
Kallivokas	0.019473	0.012573	0.011638	0.022598
Antoine	0.029496	0.014510	0.006879	0.018436
Mathieu	0.004414	0.006453	0.006298	0.017988

Table 5.7: ABC Dirichlet boundary condition ( $\theta = 0^\circ$ ,  $a_{ext} = 2$ )  $L_2$  error

the exact solution for various values of wave number ( $k = 0.5, 1, 2, 4$ ), aspect ratio of 10 and an artificial boundary defined by  $a_{ext} = 1.1$ . The  $L_2$  error between the approximate solutions exterior to the ellipse and the exact normal derivative is given in the legend. The errors for  $a_{ext} = 1.1$  are also given in Table 5.8 on page 81. In Figures 5.57 and 5.58 on page 80 we consider the same  $k$ s and  $a_{ext}$  but aspect ratio 2 and in Figures 5.59 and 5.60 on page 80 the aspect ratio is 1.4.

In Figures 5.61 and 5.62 on page 82 we consider  $a_{ext} = 1.5$  with the same wave numbers and an aspect ratio of 10. In Figures 5.63 and 5.64 on page 82 the aspect ratio is 2 and Figures 5.65 and 5.66 on page 83 the aspect ratio is 1.4. The error is given in Table 5.9 on page 84 and in the legend. In Figures 5.67 and 5.68 on page 85 we consider  $a_{ext} = 2$  with the same wave numbers and an aspect ratio of 10, in Figures 5.69 and 5.70 on page 86 the aspect ratio is 2 and in Figures 5.71 and 5.72 on page 86 the aspect ratio is 1.4. The error is given in the legend and in Table 5.10 on page 87 for  $a_{ext} = 2$ .

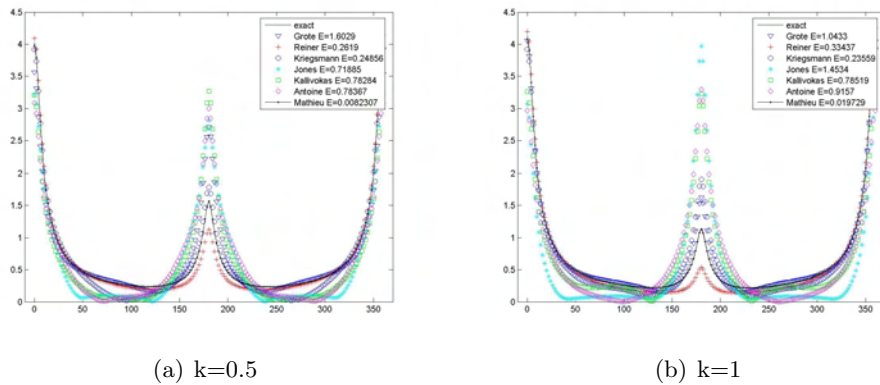


Figure 5.55: ABC Dirichlet bc  $a_{ext} = 1.1$   $k = 0.5, 1$ , AR=10 and  $\theta = 5^\circ$

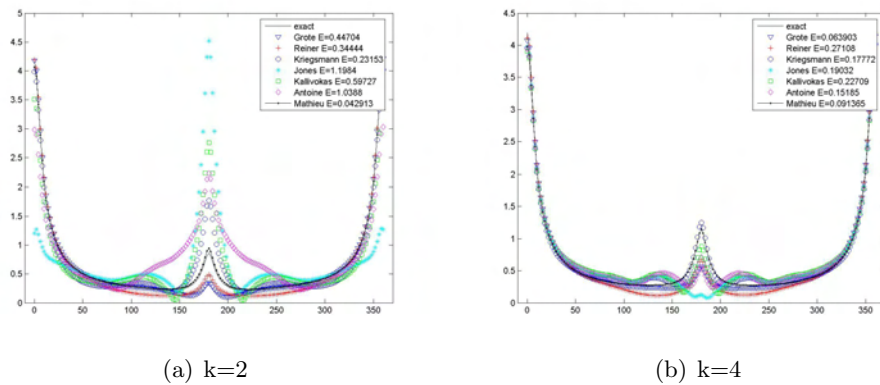
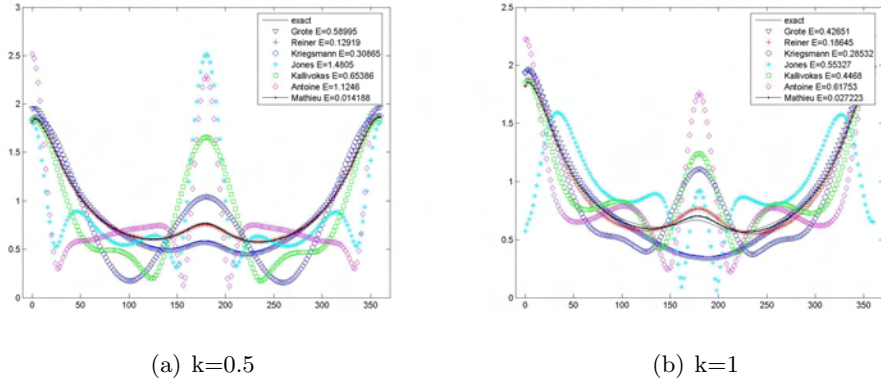
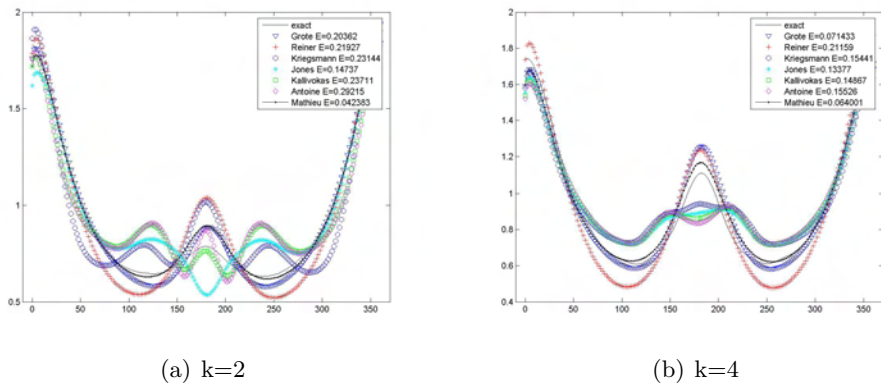
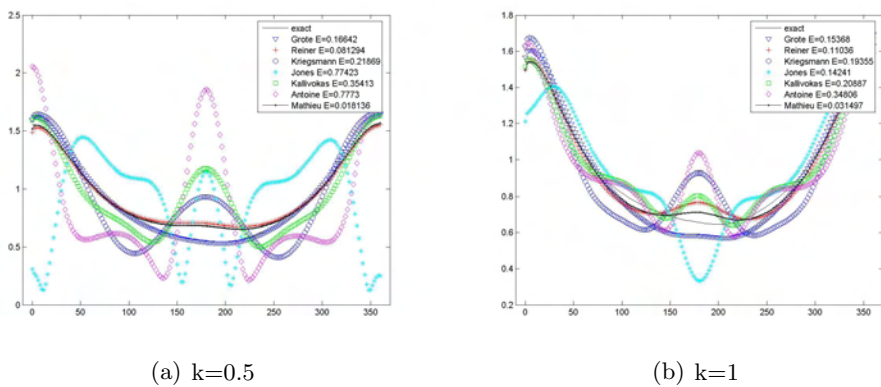
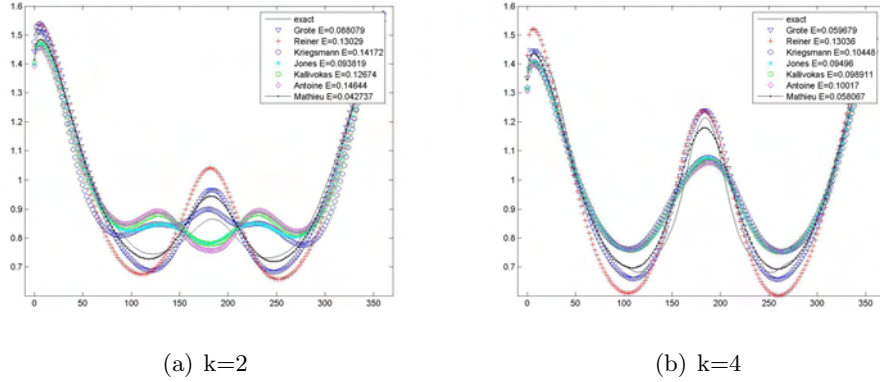


Figure 5.56: ABC Dirichlet bc  $a_{ext} = 1.1$   $k = 2, 4$ , AR=10 and  $\theta = 5^\circ$

Figure 5.57: ABC Dirichlet bc  $a_{ext} = 1.1$   $k = 0.5, 1$ , AR=2 and  $\theta = 5^\circ$ Figure 5.58: ABC Dirichlet bc  $a_{ext} = 1.1$   $k = 2, 4$ , AR=2 and  $\theta = 5^\circ$ Figure 5.59: ABC Dirichlet bc  $a_{ext} = 1.1$   $k = 0.5, 1$ , AR=1.4 and  $\theta = 5^\circ$

Figure 5.60: ABC Dirichlet bc  $a_{ext} = 1.1$   $k = 2, 4$ , AR=1.4 and  $\theta = 5^\circ$ 

(a) Aspect ratio = 10

	$k = 0.5$	$k = 1$	$k = 2$	$k = 4$
Grote	1.602877	1.043340	0.447045	0.063903
Reiner	0.261898	0.334365	0.344443	0.271083
Kriegsmann	0.248556	0.235589	0.231533	0.177722
Jones	0.718851	1.453364	1.198436	0.190317
Kallivokas	0.782845	0.785195	0.597266	0.227087
Antoine	0.783672	0.915696	1.038844	0.151852
Mathieu	0.008231	0.019729	0.042913	0.091365

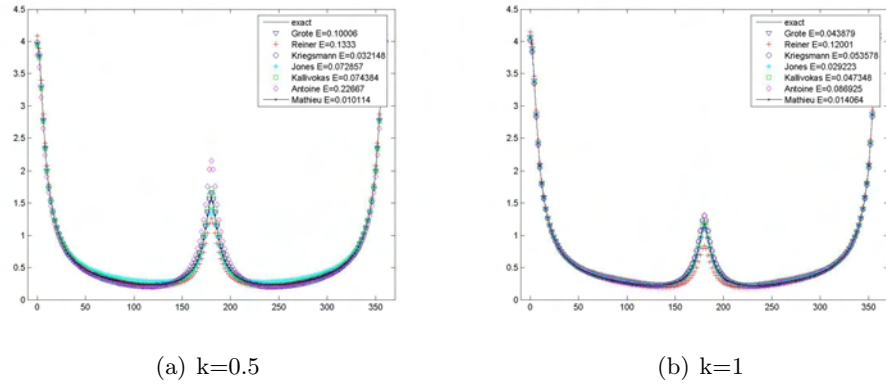
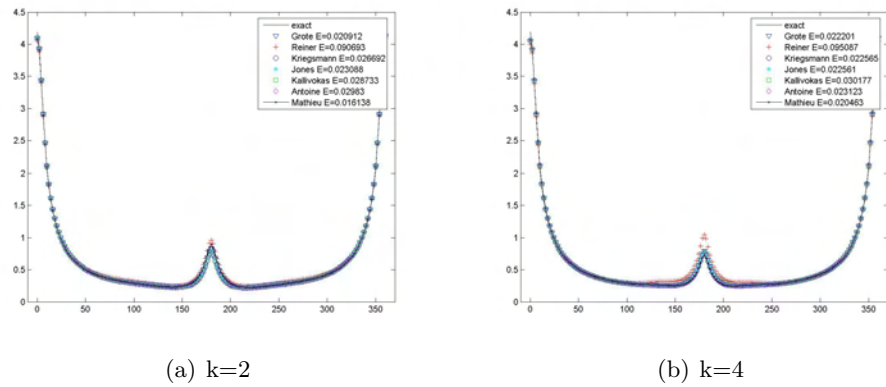
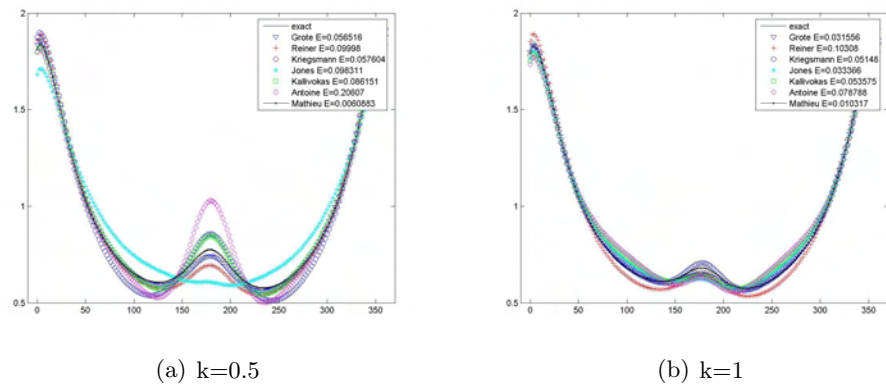
(b) Aspect ratio = 2

	$k = 0.5$	$k = 1$	$k = 2$	$k = 4$
Grote	0.589947	0.426506	0.203620	0.071433
Reiner	0.129191	0.186450	0.219266	0.211594
Kriegsmann	0.308654	0.285315	0.231441	0.154407
Jones	1.480492	0.553271	0.147374	0.133770
Kallivokas	0.653856	0.446802	0.237106	0.148673
Antoine	1.124643	0.617530	0.292152	0.155260
Mathieu	0.014188	0.027223	0.042383	0.064001

(c) Aspect ratio = 1.4

	$k = 0.5$	$k = 1$	$k = 2$	$k = 4$
Grote	0.166419	0.153676	0.088079	0.059679
Reiner	0.081294	0.110357	0.130287	0.130362
Kriegsmann	0.218688	0.193552	0.141721	0.104482
Jones	0.774228	0.142406	0.093819	0.094960
Kallivokas	0.354127	0.208866	0.126743	0.098911
Antoine	0.777298	0.348062	0.146437	0.100175
Mathieu	0.018136	0.031497	0.042737	0.058067

Table 5.8: ABC Dirichlet boundary condition ( $\theta = 5^\circ$ ,  $a_{ext} = 1.1$ )  $L_2$  error

Figure 5.61: ABC Dirichlet bc  $a_{ext} = 1.5$   $k = 0.5, 1$ , AR=10 and  $\theta = 5^\circ$ Figure 5.62: ABC Dirichlet bc  $a_{ext} = 1.5$   $k = 2, 4$ , AR=10 and  $\theta = 5^\circ$ Figure 5.63: ABC Dirichlet bc  $a_{ext} = 1.5$   $k = 0.5, 1$ , AR=2 and  $\theta = 5^\circ$

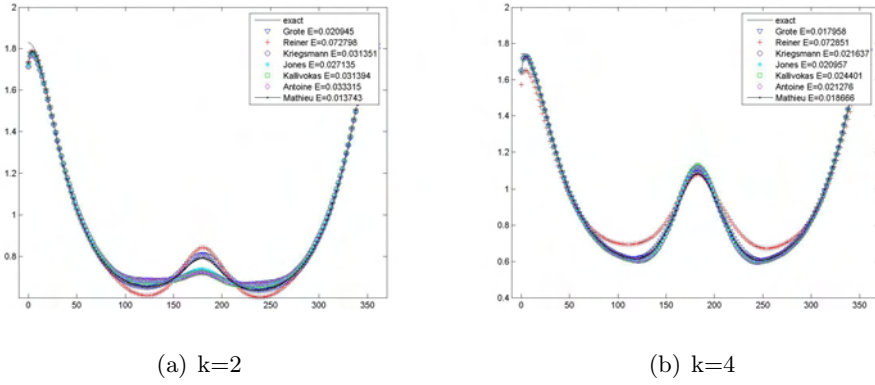


Figure 5.64: ABC Dirichlet bc  $a_{ext} = 1.5$   $k = 2, 4$ , AR=2 and  $\theta = 5^\circ$

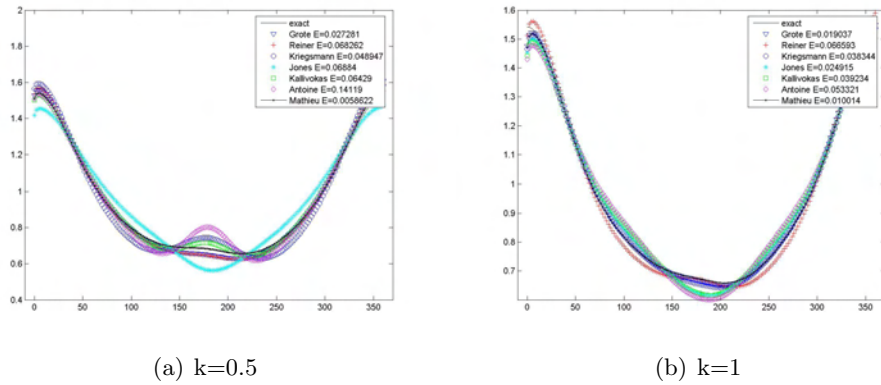


Figure 5.65: ABC Dirichlet bc  $a_{ext} = 1.5$   $k = 0.5, 1$ , AR=1.4 and  $\theta = 5^\circ$

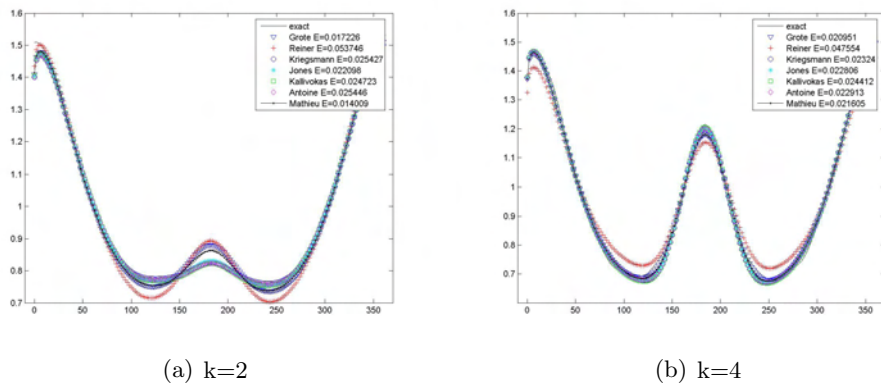


Figure 5.66: ABC Dirichlet bc  $a_{ext} = 1.5$   $k = 2, 4$ , AR=1.4 and  $\theta = 5^\circ$

(a) Aspect ratio = 10

	$k = 0.5$	$k = 1$	$k = 2$	$k = 4$
Grote	0.100058	0.043879	0.020912	0.022201
Reiner	0.133300	0.120011	0.090693	0.095087
Kriegsmann	0.032148	0.053578	0.026692	0.022565
Jones	0.072857	0.029223	0.023088	0.022561
Kallivokas	0.074384	0.047348	0.028733	0.030177
Antoine	0.226672	0.086925	0.029830	0.023123
Mathieu	0.010114	0.014064	0.016138	0.020463

(b) Aspect ratio = 2

	$k = 0.5$	$k = 1$	$k = 2$	$k = 4$
Grote	0.056516	0.031556	0.020945	0.017958
Reiner	0.099980	0.103080	0.072798	0.072851
Kriegsmann	0.057604	0.051480	0.031351	0.021637
Jones	0.098311	0.033366	0.027135	0.020957
Kallivokas	0.086151	0.053575	0.031394	0.024401
Antoine	0.206072	0.078788	0.033315	0.021276
Mathieu	0.006088	0.010317	0.013743	0.018666

(c) Aspect ratio = 1.4

	$k = 0.5$	$k = 1$	$k = 2$	$k = 4$
Grote	0.027281	0.019037	0.017226	0.020951
Reiner	0.068262	0.066593	0.053746	0.047554
Kriegsmann	0.048947	0.038344	0.025427	0.023240
Jones	0.068840	0.024915	0.022098	0.022806
Kallivokas	0.064290	0.039234	0.024723	0.024412
Antoine	0.141188	0.053321	0.025446	0.022913
Mathieu	0.005862	0.010014	0.014009	0.021605

Table 5.9: ABC Dirichlet boundary condition ( $\theta = 5^\circ$ ,  $a_{ext} = 1.5$ )  $L_2$  error

When the outer ellipse moves away from the scatterer the approximations become closer to the exact solution and this is still extremely noticeable on Grote's method. This means that the best choice is to be far enough from the scatterer; here  $a_{ext} = 2$ . The general behavior properties are still preserved. For an example of improvement with decreasing aspect ratio see Kallivokas's method from Figure 5.55 on page 79 to Figure 5.60 on page 81 or from Figure 5.61 on page 82 to Figure 5.66 on page 83. The effect of increasing wave numbers is again seen in the improvement of the results for all methods [see for example Antoine's method in Figures 5.63 and 5.64 on page 82 or Jones's method in Figures 5.69 and 5.70 on page 86 ].

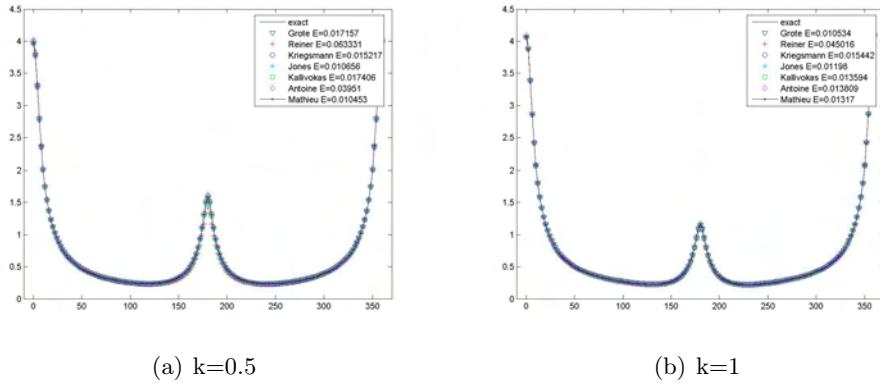


Figure 5.67: ABC Dirichlet bc  $a_{ext} = 2$   $k = 0.5, 1$ , AR=10 and  $\theta = 5^\circ$

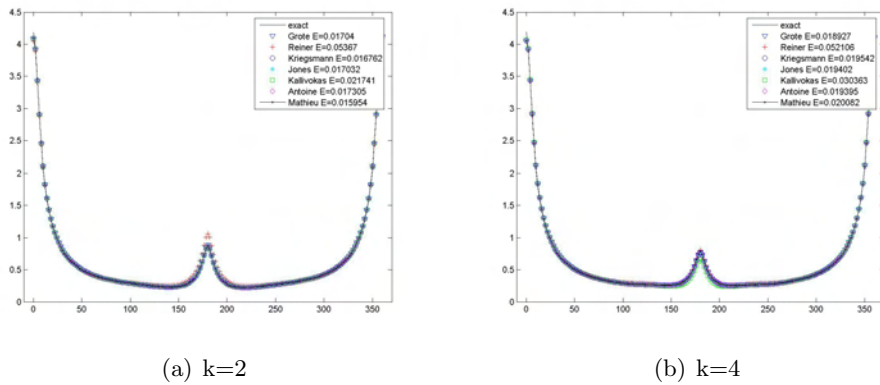
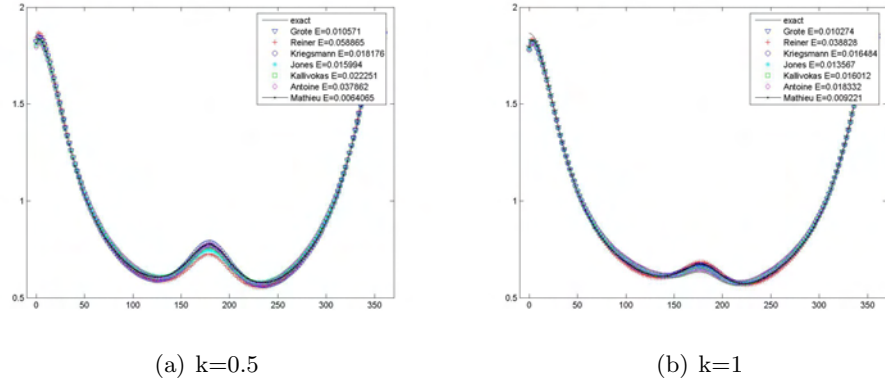
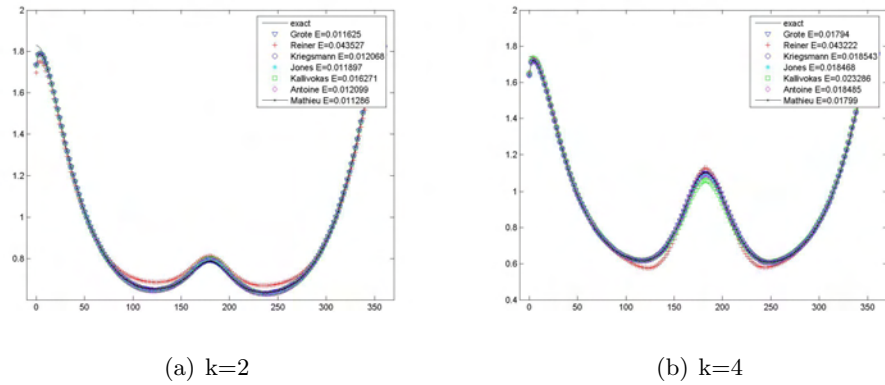
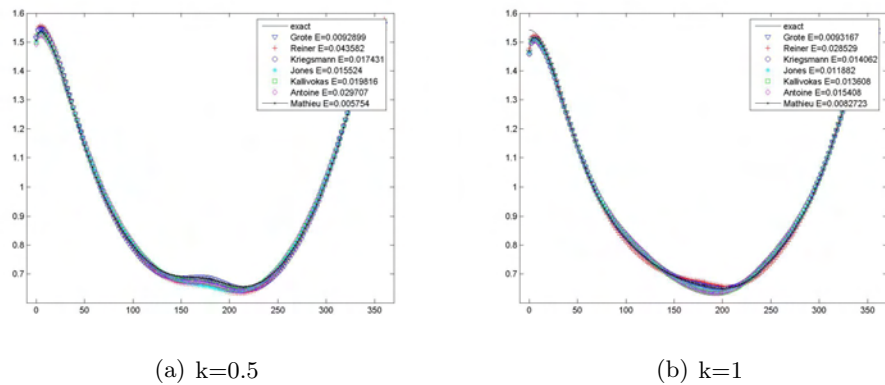
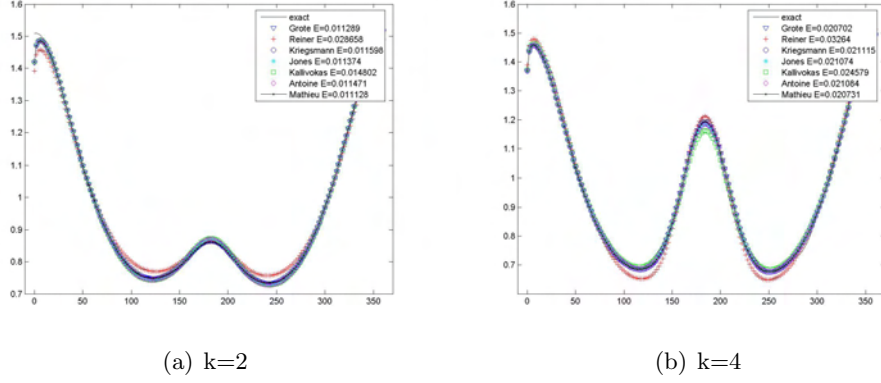


Figure 5.68: ABC Dirichlet bc  $a_{ext} = 2$   $k = 2, 4$ , AR=10 and  $\theta = 5^\circ$

Among the standard methods there is still no consistently superior ABC. With  $a_{ext} = 1.1$  and aspect ratio 10 Antoine's method again is the best for  $k = 4$  and Kriegsmann's method for the remaining frequencies. For aspect ratio 1.4 Reinter's method is the best for  $k = 0.5, 1$  and Grote's method is the best for  $k = 2, 4$ . Similarly, with the remaining  $a_{ext}$  the method with the best results of the standard

Figure 5.69: ABC Dirichlet bc  $a_{ext} = 2$   $k = 0.5, 1$ , AR=2 and  $\theta = 5^\circ$ Figure 5.70: ABC Dirichlet bc  $a_{ext} = 2$   $k = 2, 4$ , AR=2 and  $\theta = 5^\circ$ Figure 5.71: ABC Dirichlet bc  $a_{ext} = 2$   $k = 0.5, 1$ , AR=1.4 and  $\theta = 5^\circ$

Figure 5.72: ABC Dirichlet bc  $a_{ext} = 2$   $k = 2, 4$ , AR=1.4 and  $\theta = 5^\circ$ 

(a) Aspect ratio = 10

	$k = 0.5$	$k = 1$	$k = 2$	$k = 4$
Grote	0.017157	0.010534	0.017040	0.018927
Reiner	0.063331	0.045016	0.053670	0.052106
Kriegsmann	0.015217	0.015442	0.016762	0.019542
Jones	0.010656	0.011980	0.017032	0.019402
Kallivokas	0.017406	0.013594	0.021741	0.030363
Antoine	0.039510	0.013809	0.017305	0.019395
Mathieu	0.010453	0.013170	0.015954	0.020082

(b) Aspect ratio = 2

	$k = 0.5$	$k = 1$	$k = 2$	$k = 4$
Grote	0.010571	0.010274	0.011625	0.017940
Reiner	0.058865	0.038828	0.043527	0.043222
Kriegsmann	0.018176	0.016484	0.012068	0.018543
Jones	0.015994	0.013567	0.011897	0.018468
Kallivokas	0.022251	0.016012	0.016271	0.023286
Antoine	0.037862	0.018332	0.012099	0.018485
Mathieu	0.006407	0.009221	0.011286	0.017990

(c) Aspect ratio = 1.4

	$k = 0.5$	$k = 1$	$k = 2$	$k = 4$
Grote	0.009290	0.009317	0.011289	0.020702
Reiner	0.043582	0.028529	0.028658	0.032640
Kriegsmann	0.017431	0.014062	0.011598	0.021115
Jones	0.015524	0.011882	0.011374	0.021074
Kallivokas	0.019816	0.013608	0.014802	0.024579
Antoine	0.029707	0.015408	0.011471	0.021084
Mathieu	0.005754	0.008272	0.011128	0.020731

Table 5.10: ABC Dirichlet boundary condition ( $\theta = 5^\circ$ ,  $a_{ext} = 2$ )  $L_2$  error

methods varies, but the new method is consistently superior.

### 5.2.2 Neumann Condition

We finish this chapter with the ABC for the Neumann boundary condition. We compare  $a_{ext} = 2$  only, and begin with  $\theta = 0$ . In Figures 5.73 and 5.74 on page 88 we compare the same methods for wave numbers ( $k = 0.5, 1, 2, 4$ ) and an aspect ratio of 10. The  $L_2$  error between the approximate solutions exterior to the ellipse and the exact normal derivative is given again in the legend and in Table 5.11 on page 91. In Figures 5.75 and 5.76 on page 89 we consider the same  $k$ s but aspect ratio 3.3, in Figures 5.79 and 5.80 on page 90 the aspect ratio is 1.4 and in Figures 5.77 and 5.78 on page 90 the aspect ratio is 1.4.

We note again the improvement for results of most methods is with decreasing aspect ratio; for example, see Reiner's method from Figure 5.73 on page 88 to Figure 5.80 on page 92. For further examples, see the corresponding figures for the methods of Kriegsmann and Kallivokas.

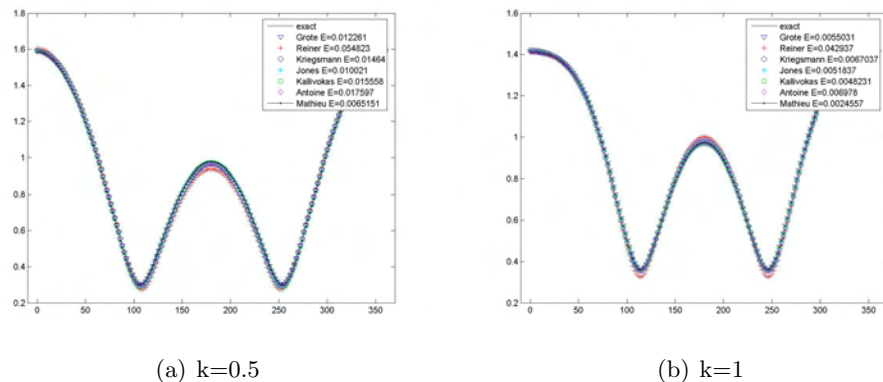


Figure 5.73: ABC Neumann bc,  $a_{ext} = 2$   $k = 0.5, 1$ , AR=10 and  $\theta = 0^\circ$

The situation with increasing wave numbers is not consistent as in the case of the OSRC Neumann. For example, Reiner's and Grote's methods for aspect ratio 10 improved from  $k = 0.5$  to  $k = 1$  but worsened for  $k = 2$  and improved again for  $k = 4$ . The behavior of Kriegsmann's method for aspect ratio 10 is similar to that of Reiner and Grote's. However, for aspect ratio 3.3 Kriegsmann's method consistently improves with increasing wave numbers, while Grote's and Reiner's methods are still not consistent.

Similarly with incident angle  $\theta = 5$ . In Figures 5.81 and 5.82 on page 92 we

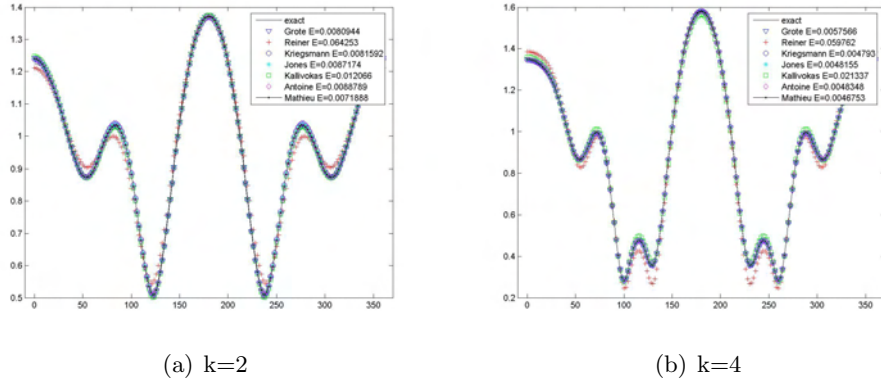


Figure 5.74: ABC Neumann bc,  $a_{ext} = 2$   $k = 2, 4$ , AR=10 and  $\theta = 0^\circ$

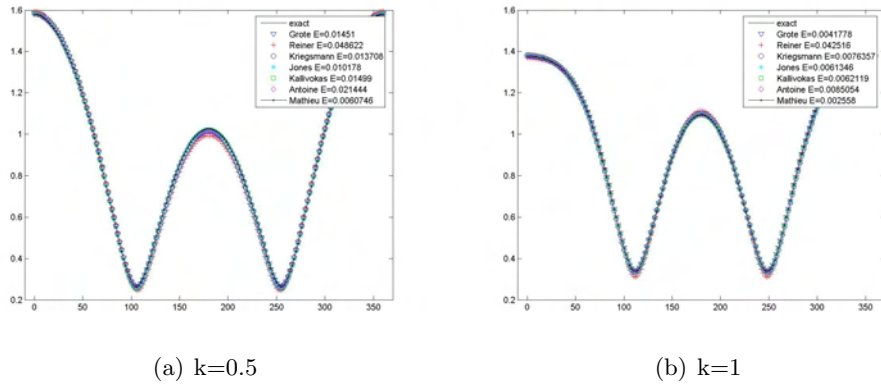


Figure 5.75: ABC Neumann bc,  $a_{ext} = 2$   $k = 0.5, 1$ , AR=3.3 and  $\theta = 0^\circ$

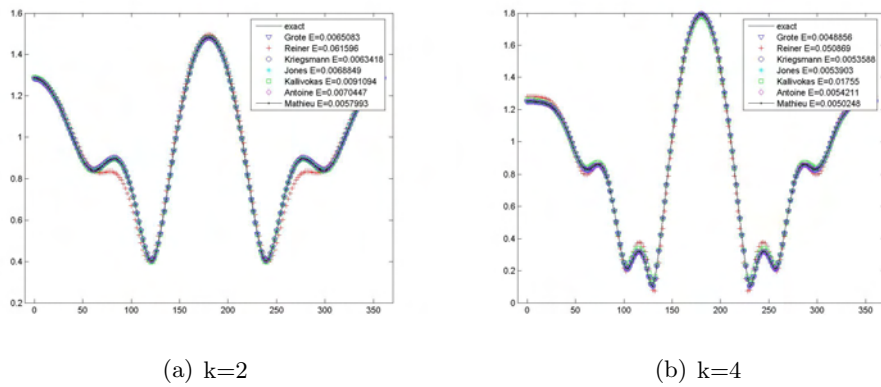
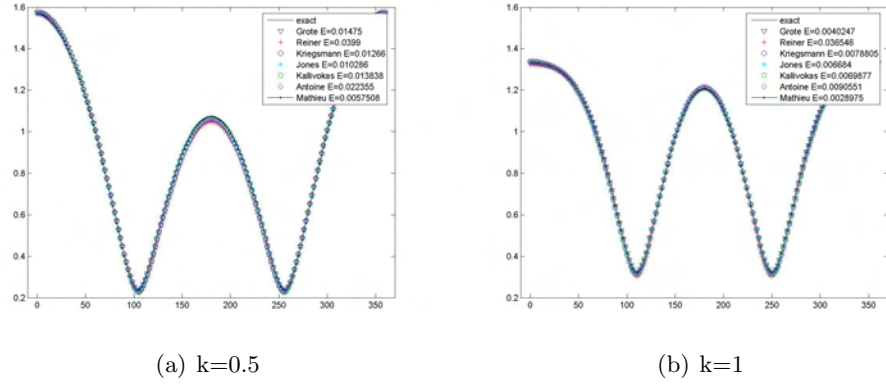
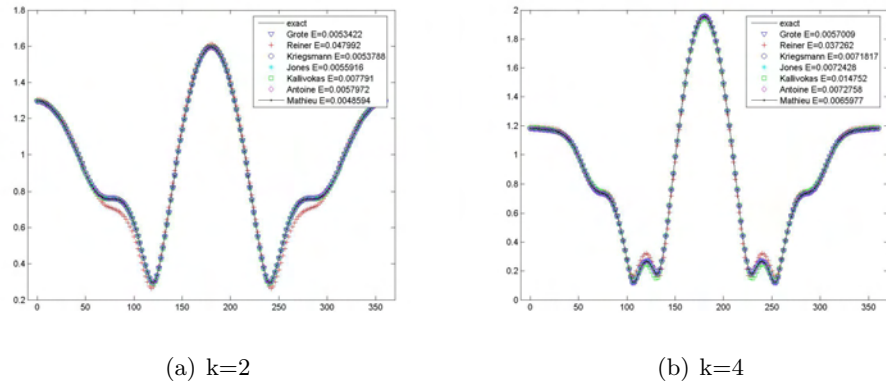
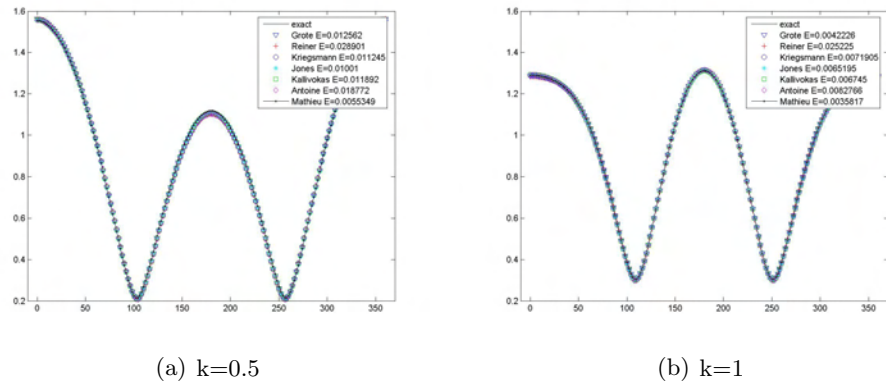


Figure 5.76: ABC Neumann bc,  $a_{ext} = 2$   $k = 2, 4$ , AR=3.3 and  $\theta = 0^\circ$

Figure 5.77: ABC Neumann bc,  $a_{ext} = 2$   $k = 0.5, 1$ , AR=2 and  $\theta = 0^\circ$ Figure 5.78: ABC Neumann bc,  $a_{ext} = 2$   $k = 2, 4$ , AR=2 and  $\theta = 0^\circ$ Figure 5.79: ABC Neumann bc,  $a_{ext} = 2$   $k = 0.5, 1$ , AR=1.4 and  $\theta = 0^\circ$

(a) Aspect ratio = 10

	$k = 0.5$	$k = 1$	$k = 2$	$k = 4$
Grote	0.012261	0.005503	0.008094	0.005757
Reiner	0.054823	0.042937	0.064253	0.059762
Kriegsmann	0.014640	0.006704	0.008159	0.004793
Jones	0.010021	0.005184	0.008717	0.004815
Kallivokas	0.015558	0.004823	0.012066	0.021337
Antoine	0.017597	0.006978	0.008879	0.004835
Mathieu	0.006515	0.002456	0.007189	0.004675

(b) Aspect ratio = 3.3

	$k = 0.5$	$k = 1$	$k = 2$	$k = 4$
Grote	0.014510	0.004178	0.006508	0.004886
Reiner	0.048622	0.042516	0.061596	0.050869
Kriegsmann	0.013708	0.007636	0.006342	0.005359
Jones	0.010178	0.006135	0.006885	0.005390
Kallivokas	0.014990	0.006212	0.009109	0.017550
Antoine	0.021444	0.008505	0.007045	0.005421
Mathieu	0.006075	0.002558	0.005799	0.005025

(c) Aspect ratio = 2

	$k = 0.5$	$k = 1$	$k = 2$	$k = 4$
Grote	0.014750	0.004025	0.005342	0.005701
Reiner	0.039900	0.036546	0.047992	0.037262
Kriegsmann	0.012660	0.007880	0.005379	0.007182
Jones	0.010286	0.006684	0.005592	0.007243
Kallivokas	0.013838	0.006988	0.007791	0.014752
Antoine	0.022355	0.009055	0.005797	0.007276
Mathieu	0.005751	0.002898	0.004859	0.006598

(d) Aspect ratio = 1.4

	$k = 0.5$	$k = 1$	$k = 2$	$k = 4$
Grote	0.012562	0.004223	0.004286	0.006747
Reiner	0.028901	0.025225	0.029459	0.023296
Kriegsmann	0.011245	0.007190	0.004646	0.008210
Jones	0.010010	0.006519	0.004638	0.008295
Kallivokas	0.011892	0.006745	0.007754	0.013740
Antoine	0.018772	0.008277	0.004800	0.008318
Mathieu	0.005535	0.003582	0.004432	0.007766

Table 5.11: ABC Neumann boundary condition ( $\theta = 0^\circ$ )  $L_2$  error

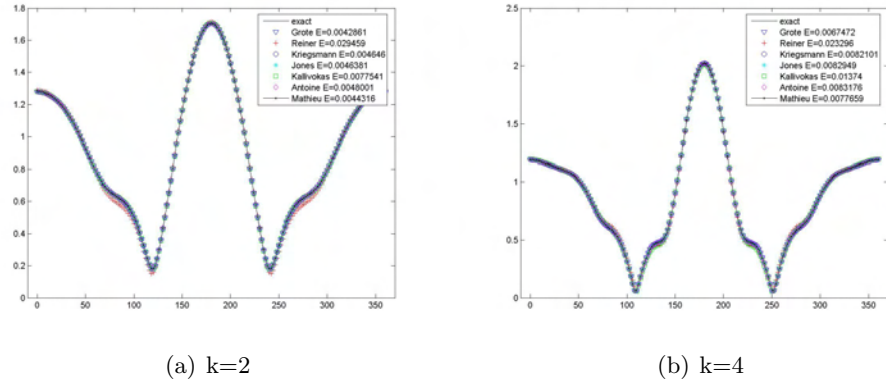


Figure 5.80: ABC Neumann bc,  $a_{ext} = 2$   $k = 2, 4$ , AR=1.4 and  $\theta = 0^\circ$

consider the same wave numbers and an aspect ratio of 10, in Figures 5.83 and 5.84 on page 93 the aspect ratio is 3.3, in Figures 5.85 and 5.86 on page 94 the aspect ratio is 3.3 and Figures 5.51 and 5.52 on page 76 the aspect ratio is 1.4. The error is given in Table 5.12 on page 95 and in the legend.

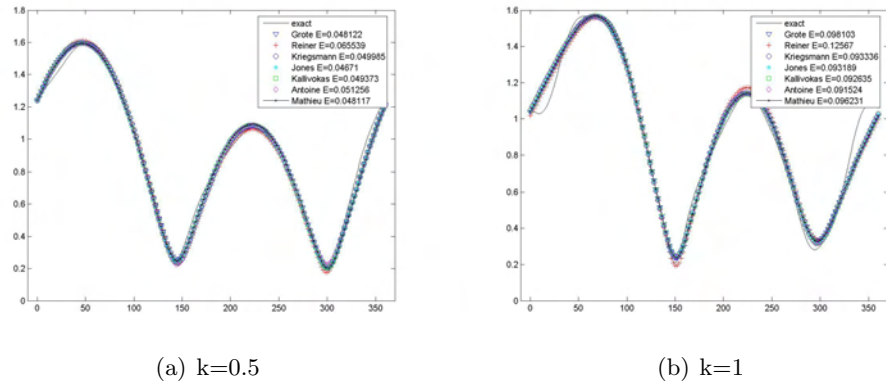


Figure 5.81: ABC Neumann bc,  $a_{ext} = 2$   $k = 0.5, 1$ , AR=10 and  $\theta = 5^\circ$

We found again an improvement in most methods when the aspect ratio decreases [for example see Antoine's method from Figure 5.81 on page 92 to Figure 5.88 on page 96]. When the wave number is increasing there is still inconsistency as before. See Kriegsmann's and Reiner's methods for aspect ratio 2 that improved from  $k = 0.5$  to  $k = 1$  but worsened for  $k = 2$  and improved again for  $k = 4$ .

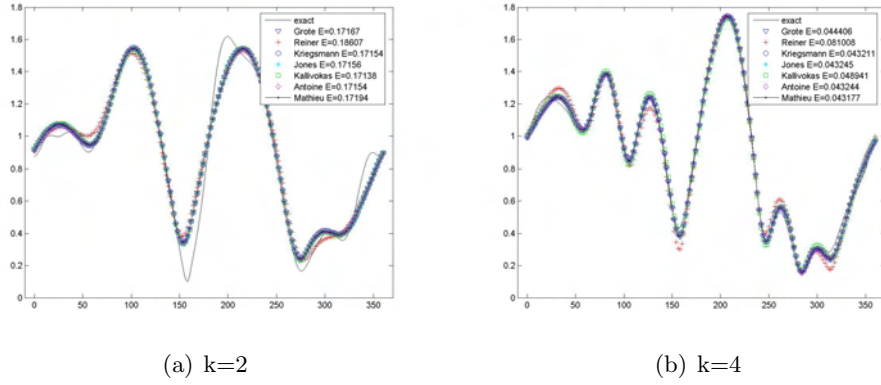


Figure 5.82: ABC Neumann bc,  $a_{ext} = 2$   $k = 2, 4$ , AR=10 and  $\theta = 5^\circ$

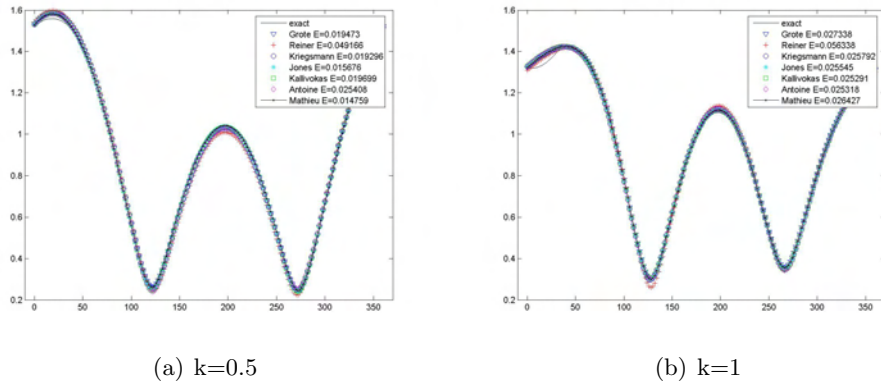


Figure 5.83: ABC Neumann bc,  $a_{ext} = 2$   $k = 0.5, 1$ , AR=3.3 and  $\theta = 5^\circ$

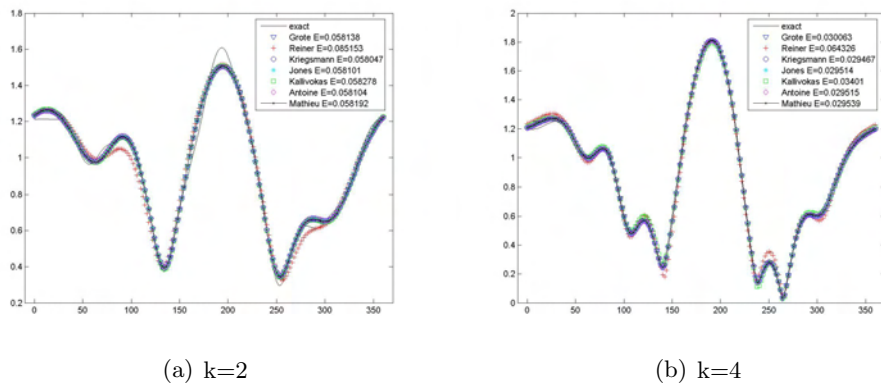
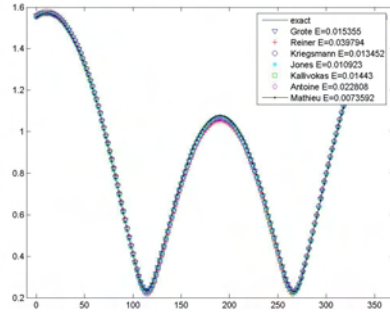
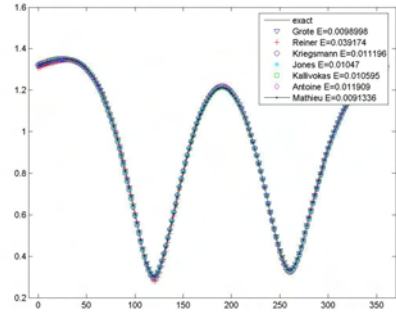


Figure 5.84: ABC Neumann bc,  $a_{ext} = 2$   $k = 2, 4$ , AR=3.3 and  $\theta = 5^\circ$

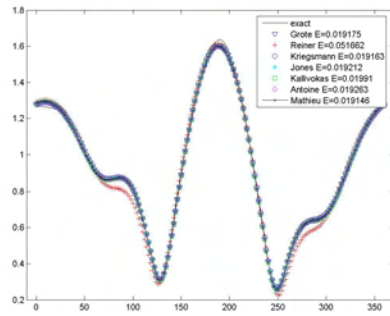


(a)  $k=0.5$

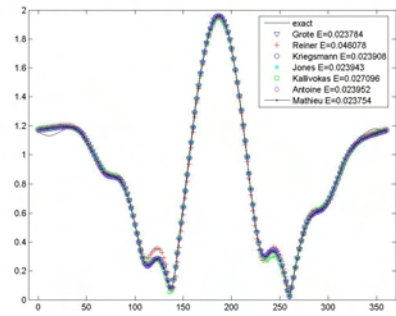


(b)  $k=1$

Figure 5.85: ABC Neumann bc,  $a_{ext} = 2$   $k = 0.5, 1$ , AR=2 and  $\theta = 5^\circ$

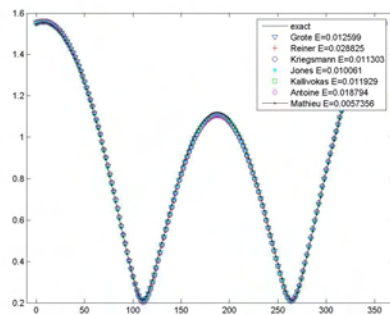


(a)  $k=2$

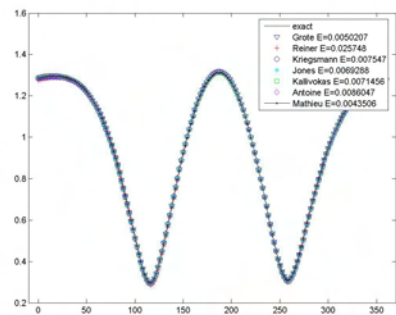


(b)  $k=4$

Figure 5.86: ABC Neumann bc,  $a_{ext} = 2$   $k = 2, 4$ , AR=2 and  $\theta = 5^\circ$



(a)  $k=0.5$



(b)  $k=1$

Figure 5.87: ABC Neumann bc,  $a_{ext} = 2$   $k = 0.5, 1$ , AR=1.4 and  $\theta = 5^\circ$

(a) Aspect ratio = 10

	$k = 0.5$	$k = 1$	$k = 2$	$k = 4$
Grote	0.048122	0.098103	0.171671	0.044406
Reiner	0.065539	0.125670	0.186071	0.081008
Kriegsmann	0.049985	0.093336	0.171538	0.043211
Jones	0.046710	0.093189	0.171562	0.043245
Kallivokas	0.049373	0.092635	0.171381	0.048941
Antoine	0.051256	0.091524	0.171537	0.043244
Mathieu	0.048117	0.096231	0.171943	0.043177

(b) Aspect ratio = 3.3

	$k = 0.5$	$k = 1$	$k = 2$	$k = 4$
Grote	0.019473	0.027338	0.058138	0.030063
Reiner	0.049166	0.056338	0.085153	0.064326
Kriegsmann	0.019296	0.025792	0.058047	0.029467
Jones	0.015676	0.025545	0.058101	0.029514
Kallivokas	0.019699	0.025291	0.058278	0.034010
Antoine	0.025408	0.025318	0.058104	0.029515
Mathieu	0.014759	0.026427	0.058192	0.029539

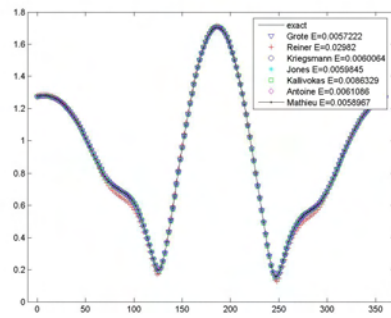
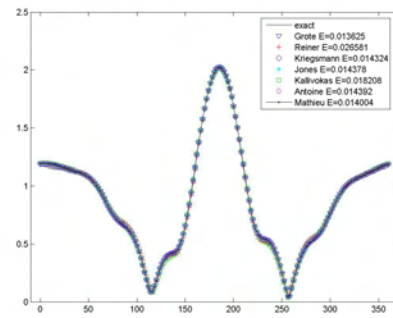
(c) Aspect ratio = 2

	$k = 0.5$	$k = 1$	$k = 2$	$k = 4$
Grote	0.015355	0.009900	0.019175	0.023784
Reiner	0.039794	0.039174	0.051662	0.046078
Kriegsmann	0.013452	0.011196	0.019163	0.023908
Jones	0.010923	0.010470	0.019212	0.023943
Kallivokas	0.014430	0.010595	0.019910	0.027096
Antoine	0.022808	0.011909	0.019263	0.023952
Mathieu	0.007359	0.009134	0.019146	0.023754

(d) Aspect ratio = 1.4

	$k = 0.5$	$k = 1$	$k = 2$	$k = 4$
Grote	0.012599	0.005021	0.005722	0.013625
Reiner	0.028825	0.025748	0.029820	0.026581
Kriegsmann	0.011303	0.007547	0.006006	0.014324
Jones	0.010061	0.006929	0.005984	0.014378
Kallivokas	0.011929	0.007146	0.008633	0.018208
Antoine	0.018794	0.008605	0.006109	0.014392
Mathieu	0.005736	0.004351	0.005897	0.014004

Table 5.12: ABC Neumann boundary condition ( $\theta = 5^\circ$ )  $L_2$  error

(a)  $k=2$ (b)  $k=4$ Figure 5.88: ABC Neumann bc,  $a_{ext} = 2$   $k = 2, 4$ , AR=1.4 and  $\theta = 5^\circ$

## Chapter 6

# Conclusion

The Helmholtz equation describes wave propagation in the frequency domain. This is important both in acoustics and electromagnetics. In particular we are interested in acoustic scattering about a soft or hard body. Since the domain is unbounded a Sommerfeld radiation condition is required to make it well-posed. For a numerical approximation we need to replace the unbounded domain by a finite domain bounded by an artificial surface. One then needs to impose a boundary condition on the artificial surface to make it both well-posed and accurate. One of the original approaches was that by Bayliss and Turkel based on matching an expansion of the solution. Their method is most appropriate for cylindrical and spherical coordinates. However, to eliminate the need for extra mesh points it would be more efficient, in many cases, to consider other shapes for the outer artificial surface. A number of generalizations have been suggested during recent years.

In this thesis we have two objectives. First to compare the accuracy of existing methods. For this purpose we investigated scattering exterior to an ellipse with an elliptically shaped artificial surface. This has the advantage that there is an explicit solution in terms of an infinite series in Mathieu functions. Thus we can compare the numerical solution with an analytical solution to compare errors between the methods. The second objective of the thesis was to construct a new absorbing boundary condition for elliptical surfaces based on an expansion in Mathieu functions. We also compare this new boundary conditions with the existing ones.

The original absorbing boundary conditions assumed that the Helmholtz equation was being solved by either a finite difference or a finite element method. Thus, the artificial surface where the absorbing boundary was imposed was some distance from the scatterer. Later, Kriegsmann et al. introduced the concept of imposing the absorbing boundary condition direction of the scatterer (OSRC = On-Surface Radiation Condition). In our comparisons we considered both OSRC methods and

finite difference schemes.

We surveyed several methods using local absorbing boundary conditions for the Helmholtz equation. We compared these methods to our new method. The comparison of these methods shows the following:

- Most of the standard methods work better for low aspect ratio  $\frac{a}{b}$  where  $a, b$  are major and minor semi-axes of the scatterer ellipse.
- For Dirichlet (hard) boundary condition on the scatterer most of the standard methods work better for high frequencies.
- For Neumann (soft) boundary condition on the scatterer none of the methods have consistent behavior for changes in wave number.
- Among the expansion type boundary conditions none is consistently much better than the simple Kriegsmann boundary condition.
- The new modal elliptical boundary condition is not significantly inferior to the optimal one and is frequently much superior, especially for lower wave numbers and when the outer boundary is close in when used as an OSRC.

# Bibliography

- [1] X. Antoine, H. Barucq, and A. Bendali. Bayliss-Turkel-like radiation conditions on surfaces of arbitrary shape. *J. Math. Anal. Appl.*, 229(1):184–211, 1999.
- [2] A. Bayliss, M. Gunzburger, and E. Turkel. Boundary Conditions for the Numerical Solution of Elliptic Equations in Exterior Regions. *SIAM Journal on Applied Mathematics*, 42(2):430–451, 1982.
- [3] A. Bayliss and E. Turkel. Radiation boundary conditions for wave-like equations. *Communications on Pure and Applied Mathematics*, 33:707–725, 1980.
- [4] J.J. Bowman, T.B.A. Senior, P.L.E. Uslenghi, et al. *Electromagnetic and acoustic scattering by simple shapes*. North-Holland, 1969.
- [5] D. Givoli and JB Keller. Non-reflecting boundary conditions for elastic waves. *Wave Motion*, 12(3):261–279, 1990.
- [6] Marcus J. Grote and Joseph B. Keller. On nonreflecting boundary conditions. *Journal of Computational Physics*, 122(2):231–243, 1995.
- [7] M.J. Grote. *Nonreflecting Boundary Conditions*. PhD thesis, Stanford university, 1995.
- [8] JC Gutierrez-Vega et al. Theory and numerical analysis of the Mathieu functions. *Tecnologico de Monterrey, Mexico report and the references given in this paper*, 2003.
- [9] E.L. Ince. Elliptic cylinder functions of second kind. *Proc. Edinburgh Math. Soc.*, 1915.
- [10] J.M. Jin, JL Volakis, and VV Liepa. A comparative study of the OSRC approach in electromagnetic scattering. *Antennas and Propagation, IEEE Transactions on*, 37(1):118–124, 1989.
- [11] DS JONES. An approximate boundary condition in acoustics. *Journal of sound and vibration*, 121(1):37–45, 1988.

- [12] D.S. Jones and G.A. Kriegsmann. Note on Surface Radiation Conditions. *SIAM Journal on Applied Mathematics*, 50(2):559–568, 1990.
- [13] L.F. Kallivokas and S. Lee. Local absorbing boundaries of elliptical shape for scalar waves. *Computer methods in applied mechanics and engineering*, 193(45-47):4979–5015, 2004.
- [14] G. Kriegsmann, A. Taflove, and K. Umashankar. A new formulation of electromagnetic wave scattering using an on-surface radiation boundary condition approach. *Antennas and Propagation, IEEE Transactions on [legacy, pre-1988]*, 35(2):153–161, 1987.
- [15] Y. Li and ZJ Cendes. Modal expansion absorbing boundary conditions for two-dimensional electromagnetic scattering. *Magnetics, IEEE Transactions on*, 29(2):1835–1838, 1993.
- [16] B. Lichtenberg, J.S. Reynolds, K.J. Webb, A.F. Peterson, and D.B. Meade. Numerical Implementation of a Conformable Two-Dimensional Radiation Boundary Condition.
- [17] E. Mathieu. Memoire sur le mouvement vibratoire d’une membrane de forme elliptique. *Jour. de Math. Pures et Appliques (Jour. de Liouville)*, 13:137–203, 1868.
- [18] D.B. Meade, A.F. Peterson, and C. Piellusch-Castle. Derivation and Comparison of Radiation Boundary Conditions for the Two-Dimensional Helmholtz Equation with Non-Circular Artificial Boundaries. *Proceedings of the Third International Conference on Mathematical and Numerical Aspects of Wave Propagation, Mandelieu-La-Napoule*, 1995.
- [19] DB Meade, W. Slade, AF Peterson, and KJ Webb. Comparison of local radiation boundary conditions for the scalar Helmholtz equation with general boundary shapes. *Antennas and Propagation, IEEE Transactions on*, 43(1):6–10, 1995.
- [20] Djellouli R. Reiner, R.C. and I. Harari. The performance of local absorbing boundary conditions for acoustic scattering from elliptical shapes. *Computer methods in applied mechanics and engineering*, 195(29-32):3622–3665, 2006.
- [21] I.A. Stegun and M. Abramowitz. *Handbook of Mathematical Functions: With Formulas, Graphs, and Mathematical Tables*. National Bureau of Standards, 1968.

- [22] E. Turkel, C. Farhat, and U. Hetmaniuk. Improved accuracy for the Helmholtz equation in unbounded domains. *Int. J. Numer. Meth. Eng.*, 59:1963–1988, 2004.
- [23] ET Whittaker and GN Watson. *A Course of Modern Analysis*, Cambridge Univ. Press, Cambridge, 1927.



## Appendix A

### A.1

$$\frac{\partial^2 \varphi}{\partial s^2} = \frac{1}{h_\xi} \frac{\partial}{\partial \varphi} \frac{1}{h_\xi} = -\frac{1}{h_\xi^3} \frac{\partial h_\xi}{\partial \varphi} = -\frac{f^2 \sin 2\varphi}{2h_\xi^4}$$

### A.2

$$\frac{\partial^2 u}{\partial s^2} = \frac{\partial u}{\partial s} \left( \frac{\partial \varphi}{\partial s} \frac{\partial u}{\partial \varphi} \right) = \frac{\partial^2 u}{\partial \varphi^2} \left( \frac{\partial \varphi}{\partial s} \right)^2 + \frac{\partial u}{\partial \varphi} \frac{\partial^2 \varphi}{\partial s^2} = \frac{1}{h_\xi^2} \frac{\partial^2 u}{\partial \varphi^2} + \frac{\partial u}{\partial \varphi} \frac{f^2 \sin(2\varphi)}{-2h_\xi^4}$$

### A.3

$$\begin{aligned} \frac{\partial}{\partial \varphi} \left( \frac{1}{2(ik - \zeta)} \frac{1}{h_\xi} \frac{\partial u}{\partial \varphi} \right) &= \left( \frac{\partial}{\partial \varphi} \frac{1}{2(ik - \zeta)} \right) \frac{1}{h_\xi} \frac{\partial u}{\partial \varphi} + \frac{1}{2(ik - \zeta)} \frac{\partial}{\partial \varphi} \left( \frac{1}{h_\xi} \frac{\partial u}{\partial \varphi} \right) \\ &= \frac{1}{2(ik - \zeta)^2} \frac{\partial \zeta}{\partial \varphi} \frac{1}{h_\xi} \frac{\partial u}{\partial \varphi} \\ &+ \frac{1}{2(ik - \zeta)} \left( \frac{-f^2 \sin(2\varphi)}{2h_\xi^3} \frac{\partial u}{\partial \varphi} + \frac{1}{h_\xi} \frac{\partial^2 u}{\partial \varphi^2} \right) \end{aligned}$$



# תקציר

בעבודה זו אנו משווים מספר תנאי שפה בולעים עבור הפתרונות הנומריים של משוואת Helmholtz בתחום חיצוני לאליפסה. כמו כן, אנו מציגים תנאי שפה חדש, המבוסס על פיתוח מודאלי (modal expansion) בפונקציית Mathieu. אנו משווים את השיטה החדשה עם שיטות אחרות בקואורדינטות אליפטיות.

משוואות אליפטיות בתחום חיצוני מחייבות הצבת תנאי שפה באינסוף, וזאת על מנת להבטיח מוצגות-היטב. אחד היישומים המעשיים הוא משוואת Helmholtz. משאבי המחשב המוגבלים מחייבים פתרון בתחום חסום (קיטוע התחום האינסופי). קיטוע האינסוף מתבצע, בדרך כלל, בעזרת תחום חיצוני מלאכותי, עליו מוחלים תנאי שפה בולעים, המיועדים לספוג החזרים לתוך התחום הפיזיקלי. בייליס וטורקל [3], ויותר מאוחר עם גנסבורגר [2], הציגו סדרה של תנאי שפה כנ"ל עבור קואורדינטות פולריות וכדוריות. תנאי שפה אלה הוכללו על ידי מספר מחברים עבור משטחים מלאכותיים שאינם מעגל או כדור.

בעבודה זו אנו משווים תנאי שפה מקומיים (הקושרים רק נקודות שכנות לנקודות השפה). לשם כך, אנו עוסקים בבעית פיזור גלים מגוף אליפטי, עבורה הפתרון המדויק ידוע. אנו מתמקדים במשוואת Helmholtz הדו-ממדית במישור התדר. אנו עוסקים הן בבעיית On Surface Radiation Conditions (OSRC) והן בבעיה החיצונית. הפתרונות מושגים בשיטת ההפרשים הסופיים.



## לאישתי ז'אנה

ברצוני להודות למנחה העבודה, פרופסור אלי טורקל, על הנחייתו המסורה ועצותיו. כמו כן, אני מודה ליעקוב אולשנסקי על שגרת Matlab לפתרון המדויק, ועל היותו מקור הידע שלי עבור פונקציות Mathieu.

כמובן, אני מודה למשפחתי על התמיכה והאהבה. בלעדיהם עבודה זו לעולם לא יכלה להתקיים (פשוטו כמשמעו)



אוניברסיטת תל-אביב  
הפקולטה למדעים מדויקים  
ע"ש ריימונד וברלי סאקלר

# השוואת תנאי שפה בולעים לפיזור גלים מסביב לגוף אליפטי

חיבור זה הוגש כחלק מהדרישות לקבלת תואר  
מוסמך אוניברסיטה M. Sc. באוניברסיטת תל-אביב

החוג למתמטיקה שימושית

על ידי

מיכאל מדבינסקי

העבודה הוכנה בהדרכתו של פרופסור אלי טורקל

